Function of A20 in the regulation of *Helicobacter pylori*-induced alternative NF-κB and caspase-8-dependent apoptotic cell death

Thesis

for the degree of

doctor rerum naturalium (Dr. rer. nat.)

approved by the Faculty of Natural Sciences of Otto von Guericke University Magdeburg

by M.Sc. Michelle Chin Chia Lim

born on 13.05.1976 in Singapore

Examiners: Prof. Dr. rer. nat. Michael Naumann

Prof. Dr. rer. nat. Lienhard Schmitz

submitted on: 17.01.2022

defended on: 06.07.2022

Publications

This work is published under the following titles:

Lim, M.C.C.***, Maubach, G.*****, Sokolova, O., Feige, M.H., Diezko, R., Buchbinder, J., Backert, S., Schlüter, D., Lavrik, I.N., and Naumann, M. (2017). Pathogen-induced ubiquitin-editing enzyme A20 bifunctionally shuts off NF-κB and caspase-8-dependent apoptotic cell death. Cell Death Differ *24*, 1621-1631. 10.1038/cdd.2017.89.

* These authors contributed equally to this work

Lim, M.C.C., Maubach, G., Birkl-Toeglhofer, A.M., Vieth, M., Haybäck, J., Naumann, M. (2021). A20 undermines alternative NF-κB activity and expression of anti-apoptotic genes in Helicobacter pylori infection. Cell Mol Life Sci, 2022 Jan 28;79(2):102. doi: 10.1007/s00018-022-04139-y.

Other Publications:

Lim, M.C.C., Maubach, G., and Naumann, M. (2018). NF-κB-regulated ubiquitin-editing enzyme A20 paves the way for infection persistency. Cell Cycle *17*, 3-4. 10.1080/15384101.2017.1387435.

Maubach, G., Feige, M.H., **Lim, M.C.C.**, and Naumann, M. (2019). NF-kappaB-inducing kinase in cancer. Biochim Biophys Acta Rev Cancer *1871*, 40-49. 10.1016/j.bbcan.2018.10.002.

Maubach, G., **Lim, M.C.C.**, Sokolova, O., Backert, S., Meyer, T.F., and Naumann, M. (2021). TIFA has dual functions in Helicobacter pylori-induced classical and alternative NF-κB pathways. EMBO Rep, e52878. 10.15252/embr.202152878.

Table of Contents

Publications II

Table of Contents III

Abbreviations VI

Zusammenfassung IX

Abstract XI

1. Introduction 1

1.1 Pathogenicity of *H. pylori* 1

1.1.2 Type IV secretion system (T4SS) 2

1.1.3 Cytotoxin-associated gene A (CagA) 3

1.2 The mammalian NF-κB family of transcription factors 5

1.2.1 The classical NF-κB pathway 6

1.2.1.1 *H. pylori*-induced classical NF-κB signalling 8

1.2.2 The alternative NF-κB pathway 10

1.2.2.1 *H. pylori*-induced alternative NF-κB signalling 11

1.3 Apoptosis 12

1.3.1 The intrinsic apoptotic pathway 14

1.3.2 The extrinsic apoptotic pathway 14

1.3.3 *H. pylori*-induced apoptosis in gastric epithelial cells 15

1.4 Regulation of inflammatory responses by A20 17

1.4.1 A20-mediated regulation of NF-κB pathways 17

1.4.2 A20-mediated regulation of apoptosis 19

2. Thesis Objectives 20

3. Results 21

3.1 Function of A20 in *H. pylori*-induced NF-κB signalling pathways in gastric epithelial cells 21

3.1.1 NF-κB regulates A20 expression in gastric carcinoma epithelial cells upon *H. pylori* infection 21

3.1.2 A20 suppresses *H. pylori*-induced activation of the classical and alternative NF-κB pathways 23

3.1.3 A20 interacts with NIK regulatory complex-bound TIFA in *H. pylori* infection 28

3.1.4 Alternative NF-κB signalling promotes the expression of anti-apoptotic genes during *H. pylori* infection 31

3.1.5 Summary 34

3.2 Function of A20 in *H. pylori*-induced caspase-8-dependent apoptotic cell death in gastric epithelial cells 35
3.2.1 *H. pylori* triggers the processing of caspases-8 and -3 leading to apoptotic cell death 35
3.2.2 A20 suppresses the processing of caspases-8 and -3 in *H. pylori* infection 36
3.2.3 A20 regulates the processing of caspase-8 in *H. pylori* infection 37
3.2.4 Cul3-mediated polyubiquitinylation of caspase-8 supports its activation leading to apoptotic cell death in *H. pylori* infection 39
3.2.5 The DUB activity of A20 counteracts efficient caspase-8 activation by removal of K63-linked polyubiquitin in *H. pylori* infection 40
3.2.6 The scaffold protein p62 promotes the interaction between A20 and caspase-8 in *H. pylori* infection 42
3.2.7 p62 supports the deubiquitinylation of caspase-8 by A20 in *H. pylori* infection 44
3.2.8 Summary 45
4. Discussion 46
5. Materials and Methods 51
5.1 Materials 51
5.1.1 General lab consumables 51
5.1.2 Materials for cell culture 51
5.1.2.1 Cell lines 52
5.1.3 Chemicals and reagents 53
5.1.4 Buffers and solutions 56
5.1.5 Antibodies 58
5.1.6 siRNAs 60
5.1.7 Instruments 61
5.2 Methods 62
5.2.1 Cell culture 62
5.2.1.1 Cultivation and maintenance of cell lines 62
5.2.1.2 Freezing and thawing of cell lines 62
5.2.1.3 Cultivation of cells for experiments 63
5.2.2 Handling of *H. pylori* strains 63
5.2.2.1 Preparation of agar plates 63
5.2.2.2 Preparation of *H. pylori* culture for infection 64
5.2.3 Transfection of siRNAs, plasmids and recombinant proteins 64
5.2.4 Preparation of total cell lysates and subcellular fractionation for SDS-PAGE and immunoblotting 65
5.2.5 Immunoprecipitation 66
5.2.6 Site-directed mutagenesis 66
5.2.7 Generation of knock-out AGS cell lines using CRISPR/Cas9 67

5.2.8 Flow cytometry 67
5.2.9 Quantitative real-time polymerase chain reaction 68
5.2.10 Densitometric analysis 68
5.2.11 Statistical analysis 68
Reference List 69
Ehrenerklärung 90

Abbreviations

Abbreviations that were used only once are not included as they have been defined in the text.

α	anti
% (v/v)	volume percent
% (w/v)	mass percent
ADP	adenosine diphosphate
ALPK1	alpha-kinase 1
ANK	ankyrin repeats
ASK1	apoptosis signal-regulating kinase 1
A. tumefaciens	*Agrobacterium tumefaciens*
BAFF-R	B-cell-activating factor receptor
BCL	B-cell lymphoma
BCL2A1	BCL 2-related protein A1
BCL2L11	Bcl-2-like protein 11
BH	B-cell lymphoma 2 homology
BIRC	baculoviral IAP repeat-containing
Cag	cytotoxin-associated gene
*cag*PAI	cytotoxin-associated gene pathogenicity island
Cas9	CRISPR-associated protein 9
CD	cluster of differentiation
CD95L	CD95 ligand
cDNA	complementary deoxyribonucleic acid
CFLAR	caspase-8 and FADD-like apoptosis regulator
cIAP	cellular inhibitor of apoptosis protein
CRISPR	clustered regularly interspaced short palindromic repeats
Cul3	cullin3
DISC	death-inducing signalling complex
DNA	deoxyribonucleic acid

EPIYA	glutamic acid-proline-isoleucine-tyrosine-alanine
FADD	Fas-associated protein with death domain
FHA	forkhead-associated
Fn14	fibroblast growth factor-inducible 14
GAPDH	glyceraldehyde-3-phosphate dehydrogenase
HDAC1	histone deacetylase 1
H. pylori	*Helicobacter pylori*
HRP	horse radish peroxidase
HTLV-I	human T-cell leukaemia virus type I
IB	immunoblot
IgG	immunoglobulin G
IL	interleukin
IκB	inhibitor of NF-κB
IKK	IκB kinase
IKKα	IκB kinase alpha
IKKβ	IκB kinase beta
IP	immunoprecipitation
K48	lysine48
K63	lysine63
LPS	lipopolysaccharide
$LT\alpha_1\beta_2$	lymphotoxin alpha1beta2
LTβR	lymphotoxin-beta receptor
M1	methionine1
MEKK3	mitogen activated protein kinase kinase kinase 3
mRNA	messenger ribonucleic acid
NEMO	NF-κB essential modulator
NF-κB	nuclear factor kappa-light-chain-enhancer of activated B cells
NIK	NF-κB-inducing kinase
NLS	nuclear localisation signal

OTU	ovarian tumour
PAMPs	pathogen-associated molecular patterns
PBS	phosphate-buffered saline
PCR	polymerase chain reaction
PVDF	polyvinylidene fluoride
RANK	receptor activator of NF-κB
RGD	arginine-glycine-aspartic acid
RHD	Rel homology domain
RIPK1	receptor-interacting serine/threonine-protein kinase 1
RNA	ribonucleic acid
RPL13A	60S ribosomal protein L13a
RT	room temperature
Scr	scrambled
SDS-PAGE	sodium dodecylsulfate polyacrylamide gel electrophoresis
siRNA	small interfering RNA
T4SS	type IV secretion system
TAD	transactivation domain
TAK1	transforming growth factor β-activated kinase 1
TBS	tris-buffered saline
TIFA	tumour necrosis factor receptor-associated factor-interacting protein with forkhead-associated domain
TNF	tumour necrosis factor
TNFAIP3	TNF alpha-induced protein 3
TNFR1	TNF receptor 1
TRADD	TNF receptor-associated protein with death domain
TRAF	TNF receptor-associated factor
TRAIL	TNF-related apoptosis-inducing ligand
VacA	vacuolating cytotoxin A
wt	wild-type
ZnF	zinc finger

Zusammenfassung

Fast die Hälfte der Weltbevölkerung ist mit dem humanpathogenen Bakterium *Helicobacter pylori*, einem Paradigma für eine hartnäckige jedoch asymptomatische Infektion, infiziert. Eine Infektion mit *H. pylori* erhöht das Risiko der Entstehung von Magenerkrankungen einschließlich des Magenkrebses. Ein Kennzeichen der Infektion mit *H. pylori*, welches das Magenepithel besiedelt, ist die gleichzeitige Aktivierung des klassischen und des alternativen '*nuclear factor kappa-light-chain-enhancer* of *activated B cells*' (NF-κB) Signalweges. Der klassische Signalweg reguliert Gene, die bei Entzündungsprozessen und dem Überleben der Zelle eine Rolle spielen, wohingegen die Funktion des alternativen Signalweges in Bezug auf die *H. pylori* Infektion ungeklärt ist. Des Weiteren aktiviert die Infektion mit *H. pylori* apoptotische Signalwege, welche zum Zelltod führen. Das Studium der obengenannten Signalwege ist bedeutend, da *in vivo* das Gleichgewicht zwischen Überleben und Tod der Zelle einen direkten Einfluss auf die Homödynamik der Magenmukosa hat. Die Homöodynamik ist eindeutig mit Art und Schwere der Erkrankung, die durch die *H. pylori* Infektion hervorgerufen wird, verknüpft. Wir berichteten, dass A20 als Zielgen des klassischen NF-κB Signalweges zur Negativregulation des alternativen NF-κB Signalweges, während der *H. pylori* Infektion von Magenepithelzellen, beiträgt. Mechanistisch bindet das *de novo* synthetisierte A20 Protein an das '*tumour necrosis factor receptor-associated factor-interacting protein with forkhead-associated domain*' (TIFA) Protein und interferiert so mit der Bindung von TIFA an den '*NF-κB-inducing kinase*' (NIK)-regulierenden Komplex. Dies führt zur Stabilisierung der '*cellular inhibitor of apoptosis protein 1*' (cIAP1) im NIK-regulierenden Komplex und zur Beendigung der Aktivierung des alternativen NF-κB Signalweges. Wir zeigten ebenfalls, dass die Aktivität des alternativen NF-κB Signalweges in Magenepithelzellen zur vermehrten Expression von antiapoptotischen Genen wie '*baculoviral IAP repeat-containing 2'* (*BIRC2*), *BIRC3* und '*B-cell lymphoma 2-related protein A1'* (*BCL2A1*) führte. Dies und die beobachtete RelB abhängige Unterdrückung des apoptotischen Zelltods während der *H. pylori* Infektion weisen auf eine Mitwirkung des alternativen NF-κB Signalweges an der Regulation des apoptotischen Zelltods hin. Andererseits ist A20 auch an der Negativregulation des Caspase-8 abhängigen apoptotischen Zelltod beteiligt. In diesem Fall wirkt die Deubiquitinylierungsaktivität des A20 Proteins der Cullin3 vermittelten Ubiquitinylierung (Lysin 63) der Caspase-8 entgegen, um deren Aktivität einzudämmen. Interessanterweise ist ein anderes NF-κB Zielgen, nämlich das p62 Protein, für die Wechselwirkung zwischen A20 und Caspase-8 essenziell.

Zusammenfassend geben diese Untersuchungen einen neuen Einblick in die Funktion des A20 Proteins hinsichtlich der Modulation des alternativen NF-κB Signalweges, als auch des Caspase-8 abhängigen apoptotischen Zelltods während der *H. pylori* Infektion.

Abstract

The human pathogen *Helicobacter pylori* infects almost half of the world's population and is a paradigm for persistent yet asymptomatic infection. Infection by *H. pylori* increases the risk for developing gastric diseases including gastric adenocarcinoma. A hallmark of infection by *H. pylori*, which colonises the human gastric epithelium, is the simultaneous activation of the classical and alternative nuclear factor kappa-light-chain-enhancer of activated B cells (NF-κB) pathways. In *H. pylori* infection, classical NF-κB signalling regulates genes involved in inflammation and cell survival, while the function of the alternative NF-κB signalling remains unclarified. Infection of gastric epithelial cells by *H. pylori* also triggers apoptotic signalling cascades leading to cell death. Studying the regulation of all the above-mentioned signalling cascades is important given that *in vivo*, the balance between cell survival and cell death has a direct impact on mucosal homeodynamics, which in turn is explicitly linked to the type and severity of disease(s) associated with *H. pylori* infection. We reported that the classical NF-κB target gene product A20 contributes to the negative regulation of alternative NF-κB activation in gastric epithelial cells infected by *H. pylori*. Mechanistically, the *de novo* synthesised A20 interacts with tumour necrosis factor receptor-associated factor-interacting protein with forkhead-associated domain (TIFA), and thereby interferes with the association of TIFA with the cellular inhibitor of apoptosis protein 1 (cIAP1) of the NF-κB-inducing kinase (NIK) regulatory complex. This leads to stabilisation of the NIK regulatory complex and the termination of alternative NF-κB activation. We also showed that alternative NF-κB activity contributes to the up-regulation of anti-apoptotic genes such as baculoviral IAP repeat-containing 2 (*BIRC2)*, *BIRC3* and B-cell lymphoma 2-related protein A1 (*BCL2A1)* in gastric epithelial cells. This and the observed RelB-dependent suppression of apoptotic cell death highlight a contributory role of the alternative NF-κB pathway towards cell survival in *H. pylori* infection. On the other hand, A20 also participates in the negative regulation of caspase-8-dependent apoptotic cell death. Herein, the deubiquitinylase activity of A20 counteracts the cullin3-mediated K63-linked ubiquitinylation of caspase-8 to curtail its activity. Interestingly, another inducible NF-κB target gene product, the scaffold protein p62, was found to ameliorate the interaction of A20 with caspase-8. In conclusion, these studies provide novel insight into the function of A20 in modulating the alternative NF-κB pathway as well as caspase-8-dependent apoptotic cell death in *H. pylori* infection.

1. Introduction

The Gram-negative bacterium *Helicobacter pylori* is one of the most successful human pathogens with a worldwide prevalence of 44 % (Zamani et al., 2018). *H. pylori* colonises the gastric mucosal epithelium and elicits host inflammatory responses leading to the recruitment of immune cells including neutrophils, dendritic cells and macrophages (Kalisperati et al., 2017). Infection of gastric epithelial cells by *H. pylori* activates the classical nuclear factor kappa-light-chain-enhancer of activated B cells (NF-κB), a critical regulator of the pro-inflammatory responses underlying the pathogenicity of *H. pylori* (Naumann et al., 2017). Infection of gastric epithelial cells by *H. pylori* also triggers activation of the alternative NF-κB (Feige et al., 2018; Mejías-Luque et al., 2016). In addition to NF-κB activation, apoptosis of gastric epithelial cells infected by *H. pylori* is also part of the host response contributing to disease progression (Alzahrani et al., 2014; Díaz et al., 2018). This knowledge prompted us to examine the molecular interplay of NF-κB and apoptotic pathways to further understand the inflammatory response towards *H.* pylori infection, which has implications for the pathogenesis of *H.* pylori-associated diseases.

1.1 Pathogenicity of *H. pylori*

The human pathogen *H. pylori*, a microaerophilic and spiral-shaped bacterium, was first discovered lining the gastric epithelium of the stomach by Warren and Marshall (1983). Infection with *H. pylori* is believed to be acquired most likely through human-to-human transmission during early childhood (Goh et al., 2011). Unless treated, *H. pylori* infection is persistent leading to chronic active gastritis, which is associated with chronic inflammation, in all infected individuals (Watari et al., 2014). Long term infection with *H. pylori*, however, often remains unrecognised because only few show clinical manifestations of this condition, although in a subgroup of infected individuals, chronic active gastritis could progress to diverse gastrointestinal complications (Burkitt et al., 2017). Not surprisingly, infection by *H. pylori* constitutes the most significant risk factor for the development of gastric cancer (Park et al., 2018), underlying the classification of *H. pylori* by the International Agency for Research on Cancer (IARC) as a class I carcinogen (Schistosomes, liver flukes and Helicobacter pylori. IARC Working Group on the Evaluation of Carcinogenic Risks to Humans. Lyon, 7-14 June 1994, 1994). The combined influence of host genetics, bacterial virulence factors and environmental factors determine the clinical outcome of a person infected with *H. pylori*. Bacterial virulence factors play significant roles in the pathogenesis of *H. pylori* because they are required for the bacterial colonisation as well as the circumvention of host immune responses, two important aspects associated with disease outcomes. These bacterial-specific factors include urease, flagella, adhesins, the type IV secretion system (T4SS),

cytotoxin-associated gene A (CagA) and vacuolating cytotoxin A (VacA) (Chang et al., 2018). Both the T4SS and CagA are described in more details in the following subsections.

1.1.2 Type IV secretion system (T4SS)

T4SSs are essentially large multiprotein complexes belonging to a family of functionally diverse translocation systems that are present in nearly all bacterial and some archaeal species (Costa et al., 2021; Makarova et al., 2016). The two main T4SS subfamilies are the conjugation and the effector translocator systems, which function in a cell-to-cell contact-dependent manner. The former allows the transfer of deoxyribonucleic acid (DNA) within and across bacterial species. The spread of antibiotic resistance genes or other virulence traits among bacterial populations for instance is largely attributed to the conjugation system (Virolle et al., 2020). The effector translocator systems, on the other hand, enable the transfer of mainly proteins, termed effectors, from bacteria to the extracellular milieu, from bacteria to bacteria and from bacteria to eukaryotic host cells (Asrat et al., 2015; Souza et al., 2015). These effectors play significant roles in the infection processes of many Gram-negative and Gram-positive bacteria including *Agrobacterium tumefaciens* (*A. tumefaciens*), *H. pylori*, *Legionella pneumophila* and *Streptococcus suis* (Gonzalez-Rivera et al., 2016). The T4SS originally defined for *A. tumefaciens*, comprising eleven VirB proteins (VirB1 to VirB11) and one VirD4 protein, is a paradigm for the T4SS superfamily.

Genes within the cytotoxin-associated gene pathogenicity island (*cag*PAI) encode the structural and functional components of *H. pylori*'s T4SS. The *cag*PAI of *H. pylori* corresponds to a 40 kilo base pairs DNA region, which was acquired via horizontal gene transfer from an unknown ancestral donor, containing approximately 32 genes (Noto and Peek, 2012). The T4SS of *H. pylori*, henceforth referred to as *cag*T4SS, comprises orthologues of all the VirB and VirD4 proteins of *A. tumefaciens* together with 5 additional proteins that have no sequence similarity to any known proteins (Fischer, 2011). As visualised by electron microscopy, the *cag*T4SS is a 41 nm multiprotein complex traversing across the inner and outer bacterial cell membranes with a needle-like structure (also referred to as a pilus) protruding out of the outer bacterial surface membrane (Frick-Cheng et al., 2016). Specifically, the *cag*T4SS consists of a bacterial inner membrane complex made up of CagE, CagW and CagV, and a core complex (Figure 1). The core complex is composed of Cagδ, CagM and CagX, which is covered by a sheath of CagY proteins, and a ring of CagT proteins that surrounds the base of the outgrowing *cag*T4SS (Rohde et al., 2003). The CagI, CagL and CagH proteins contribute to the formation of the pilus as mutant *H. pylori* strains lacking any one of these components showed either no pilus formation (for Δ*cagI* and Δ*cagL* strains) or altered pilus dimensions (for Δ*cagH* strain) (Shaffer et al., 2011).

Several components of the *cag*T4SS have been found to interact with integrin molecules on host cells (more details in section 1.1.4), implying a direct interplay between *cag*T4SS and host signalling events.

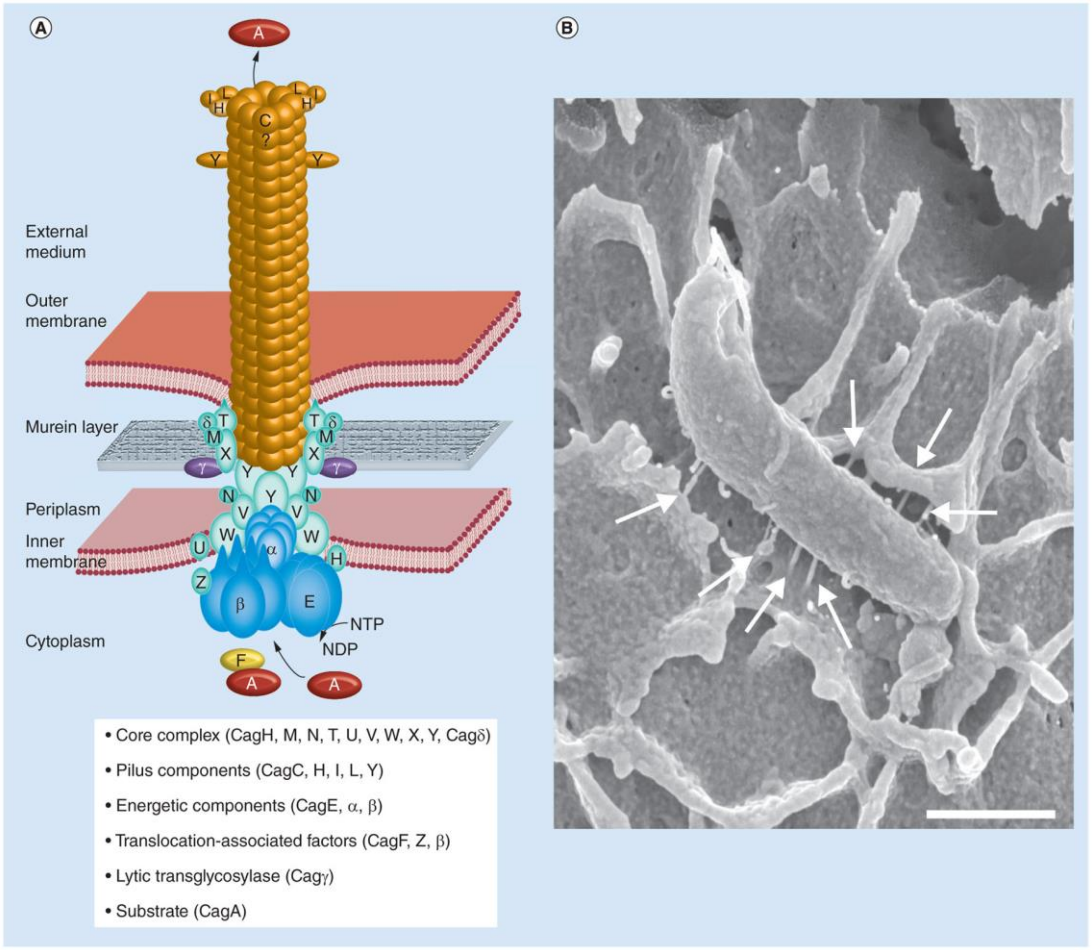

Figure 1. A model of *H. pylori*'s *cag*T4SS.
(A) The *cag* nomenclature is used to describe components of *H. pylori*'s *cag*T4SS, which are depicted in different colours corresponding to their subcellular localisation.
(B) Scanning electron microscopy reveals the attachment of a *H. pylori* bacterium to human gastric epithelial cells (AGS cell line). The *cag*T4SS pili (arrows) connect the bacterium to the host cell membrane.
This figure is a re-print from Backert and colleagues (2015) with permission of Future Medicine Ltd.

1.1.3 Cytotoxin-associated gene A (CagA)

The *cagA* gene located within the *cag*PAI region of *H. pylori*'s genome encodes CagA. CagA is the only effector protein known to be translocated through the *cag*T4SS (Kwok et al., 2007). Here, an arginine-rich secretion signal sequence located at the carboxyl (C)-terminal region of CagA (Hohlfeld et al., 2006) as well as the amino (N)-terminal domain (Schindele et al., 2016) is required for its recognition by the *cag*T4SS. Moreover, recently, Lettl and colleagues (2021) showed that the unfolding of CagA itself is a prerequisite for its transport through the *cag*T4SS.

The *cag*T4SS-dependent translocation of CagA into the host cell occurs in several ways. One way is by the binding of CagA either directly to the transmembrane receptor integrin $\alpha_5\beta_1$, which is present at focal adhesions, via a binding site mapped to its N-terminus (Kaplan-Türköz et al., 2012) or indirectly through its interaction with CagL, CagY and CagI, components of the *cag*T4SS pilus. CagL contains an arginine-glycine-aspartic acid (RGD) motif that recognises integrin $\alpha_5\beta_1$ and immunogold labelling revealed that once this initial contact is established, CagA appears at the tip of the pilus (Kwok et al., 2007). Interestingly, CagL has also been described to bind to integrin $\alpha_v\beta_6$ to promote CagA translocation (Buß et al., 2019). The C-terminal part of CagY and intact CagI also bind to integrin $\alpha_5\beta_1$ but in a RGD-independent manner (Jiménez-Soto et al., 2009). A recent study, however, suggests that interaction of *cag*T4SS with cell surface carcinoembryonic antigen-related cell adhesion molecules are essential for CagA translocation (Zhao et al., 2018). Pilus-exposed CagA can also be translocated by binding through its arginine-X-arginine motif to host membrane phosphatidylserine, which is a phospholipid usually found in the inner membrane leaflet but becomes aberrantly exposed to the outer membrane leaflet upon contact with *H. pylori* (Murata-Kamiya et al., 2010).

Alternatively, CagA can also be delivered into the host cytoplasm in a *cag*T4SS-independent manner. *H. pylori* secretes outer membrane vesicles containing CagA (Mullaney et al., 2009), which are taken up by the gastric epithelial cells via clathrin-dependent and clathrin-independent endocytic pathways (Olofsson et al., 2014).

The binding of CagL or CagA to host integrin $\alpha_5\beta_1$ triggers a cascade of signalling events leading to the activation of various host tyrosine kinases belonging to the Src and Abelson (Abl) families, which phosphorylate CagA (Backert and Tegtmeyer, 2017). The phosphorylation of CagA occurs at one or two specific glutamic acid-proline-isoleucine-tyrosine-alanine (EPIYA) sequence motifs, which are present in multiple numbers in the C-terminal polymorphic region (Higashi et al., 2005). Depending on the geographic region, the *cagA* gene exhibits polymorphisms in the sequence flanking the EPIYA motif. Four distinct EPIYA segments termed EPIYA-A, -B, -C and -D have been identified, each of which is conserved in the flanking sequence of EPIYA (Hatakeyama, 2008; Xia et al., 2009a). Variations of the *cagA* gene also occur within the EPIYA motif giving rise to alternative motifs including EPIYT, ESIYT, ESIYA and GSIYD (Zhang et al., 2015), which in turn result in CagA molecules that differ in their affinities to host interaction partners.

CagA interacts with host proteins either in its phosphorylated or non-phosphorylated form, whereby phosphorylated CagA molecules interact with the Src homology 2 (SH2) domains of host proteins (Backert and Tegtmeyer, 2017). As many as 20 host interaction partners of CagA have been identified to date, therefore CagA has impact on a multitude of host signalling

cascades and interferes with cellular effects including cell polarity, cell-to-cell junctions, pro-inflammatory and anti-apoptotic responses (Takahashi-Kanemitsu et al., 2020).

1.2 The mammalian NF-κB family of transcription factors

The mammalian NF-κB family of transcription factors comprises RelA, RelB, c-Rel, NF-κB1 (p50, processed from precursor protein p105) and NF-κB2 (p52, processed from precursor protein p100). NF-κB transcription factors bind as either homo- or heterodimers to the κB (enhancer) consensus sequence found in the promoter of target genes involved in diverse biological processes such as innate and adaptive immune responses, inflammation, and cell survival. All NF-κB proteins contain a highly conserved Rel homology domain (RHD), which harbours sequences required for dimerisation, binding to DNA and interaction with proteins of the inhibitor of NF-κB (IκB) family (Zhang et al., 2017) (Figure 2). The nuclear localisation signal (NLS) of NF-κB proteins is located adjacent to the RHD. The RelA, RelB and c-Rel transcription factors contain a C-terminal transactivation domain (TAD) for the activation of target gene expression. The p50 and p52 transcription factors, on the other hand, have a long ankyrin repeats (ANKR)-containing region and a death domain instead of the TAD. Consequently, p50 and p52 homodimers repress gene transcription, whereas the formation of p50 and p52 heterodimers with RelA, RelB, c-Rel, or other TAD-containing proteins activate gene transcription (Hayden and Ghosh, 2012).

In general, two branches of NF-κB-activating pathways exist in cells: the classical and the alternative pathways. The classical NF-κB signalling pathway generates primarily active RelA- or c-Rel-containing heterodimers, while the alternative NF-κB signalling pathway generates mostly heterodimers composed of RelB and p52. Although both pathways are triggered under diverse physiological settings (more details in sections 1.2.1 and 1.2.2), they are interconnected through several crosstalk mechanisms, for instance the transcriptional control of alternative NF-κB monomers by classical RelA and the functional overlap of NF-κB1 and NF-κB2 in the formation of classical and alternative NF-κB dimers (Shih et al., 2011).

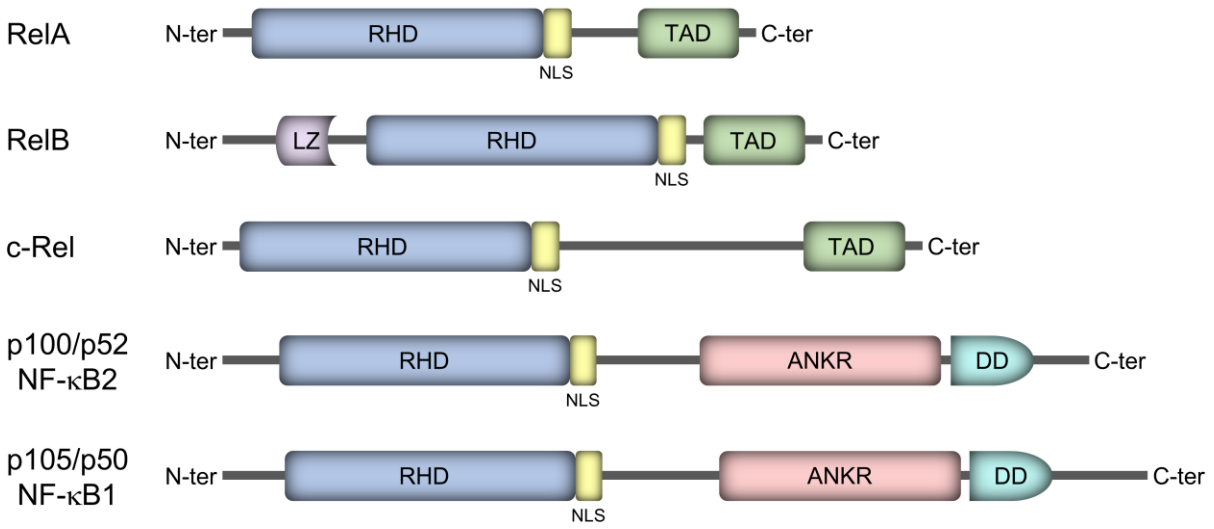

Figure 2. Members of the mammalian NF-κB protein family.
Representations of the domain structures of the mammalian NF-κB family members are based on information derived from Zhang *et al*., 2017. The abbreviations used are: N-ter, N terminal; C-ter, C terminal; RHD, Rel homology domain; TAD, transactivation domain; LZ, leucine-zipper; ANKR, ankyrin repeats-containing region; DD, death domain; and NLS, nuclear localisation signal.

1.2.1 The classical NF-κB pathway

The classical NF-κB pathway can be activated by a variety of pro-inflammatory stimuli such as cytokines, for e.g., interleukin-1β (IL-1β), IL-8 or tumour necrosis factor (TNF); pathogen-associated molecular patterns (PAMPs), for e.g., bacterial flagellin, DNA or ribonucleic acid (RNA); or damage-associated molecular patterns (DAMPs), for e.g., intracellular molecules like heat-shock proteins, high-mobility group protein 1 or S-100 proteins (Taniguchi and Karin, 2018). These ligands bind to their cognate receptors, leading to the recruitment of adaptor proteins and proximal kinases to initiate a signalling cascade that activates classical NF-κB (Figure 3).

In unstimulated cells, NF-κB dimers are latent because of their interaction with IκBs, which masks the NLS of the NF-κB dimers. This event in combination with the effect of the nuclear export signal of IκBs ensure that these complexes of NF-κB dimers and IκBs are sequestered in the cytoplasm (Hayden and Ghosh, 2012). Activation of classical NF-κB leads to the phosphorylation of IκB by the IκB kinase (IKK) complex comprising the catalytic subunits IKKα and IKKβ, and the regulatory subunit NF-κB essential modulator (NEMO). Phosphorylated IκB becomes lysine48 (K48)-linked ubiquitinylated by the S-phase kinase-associated protein 1-cullin1-F-box beta-transducin repeat-containing protein ($SCF^{\beta-TRCP}$) ubiquitin ligase complex and targeted to degradation by the 26S proteasome. The freed NF-κB dimers are transported into the nucleus to regulate gene transcription.

Ubiquitinylation of various signalling molecules plays a significant role during extracellular stimuli-mediated classical NF-κB activation. Herein, the linkages of ubiquitin involved include

K48-, K63- and methionine1 (M1)-linked (linear) polyubiquitin chains (Hu and Sun, 2016). Importantly, unanchored (non-substrate-conjugated) K63-linked polyubiquitin chains have also been proposed to engage in classical NF-κB activation (Xia et al., 2009b).

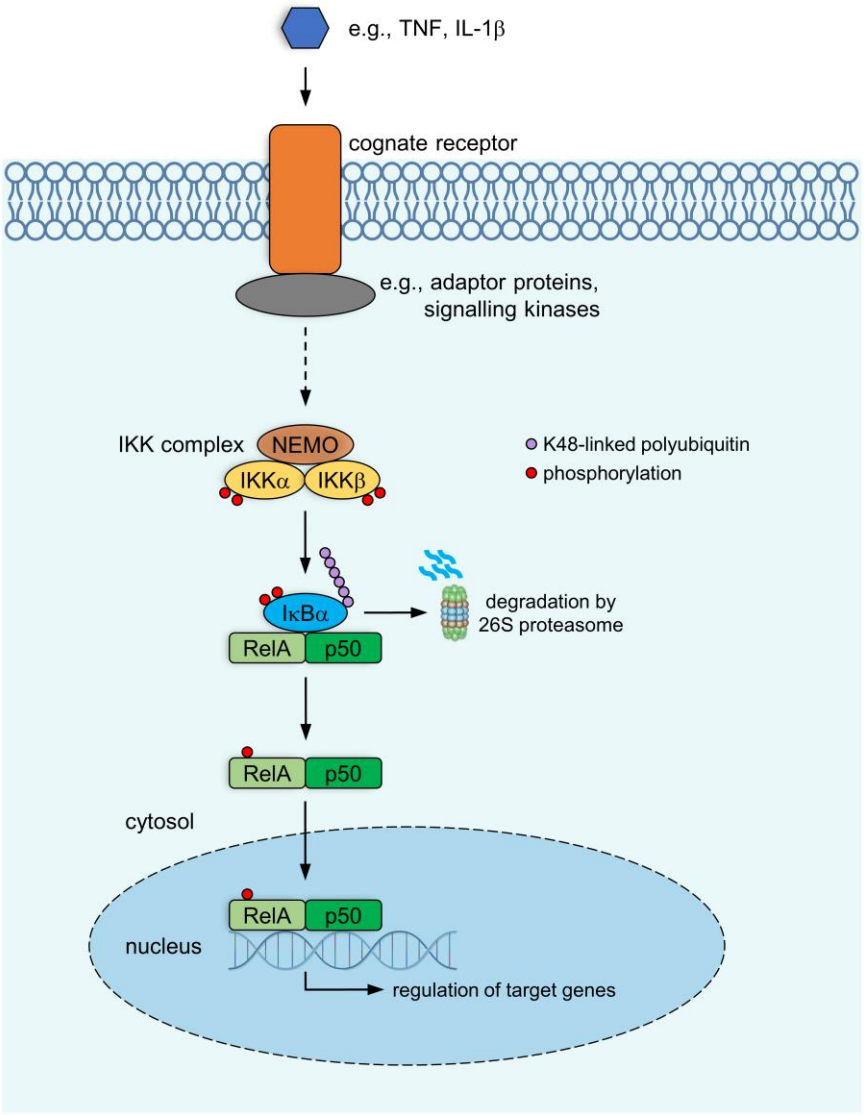

Figure 3. Classical NF-κB pathway.
Extracellular pro-inflammatory stimuli such as TNF and IL-1β engage their cognate receptors on the plasma membrane and trigger the signalling cascade leading to activation of classical NF-κB. Activation of the prototypical classical NF-κB heterodimer RelA/p50 regulates the expression of target genes.

1.2.1.1 *H. pylori*-induced classical NF-κB signalling

Over two decades ago, initial studies emerged showing the activation of classical NF-κB in response to *H. pylori* infection in the antral mucosa, the main site of infection, of *H. pylori*-positive patients *in vivo* and in *H. pylori*-infected gastric epithelial cells *in vitro* (Isomoto et al., 2000; Keates et al., 1997). Further studies revealed that *H. pylori*-induced classical NF-κB is *cag*T4SS-dependent and CagA-independent (Schweitzer et al., 2010; Sokolova et al., 2013). The lipopolysaccharide (LPS) of *H. pylori* was found to induce only weak NF-κB activation (Shimoyama et al., 2011), which could be accounted for by its low endotoxic activity (Chmiela et al., 2014). *H. pylori*'s flagellin does not activate NF-κB because it is able to evade recognition by toll-like receptor 5 due to specific acquired mutations in the FlaA protein (Andersen-Nissen et al., 2005).

Recently, the adenosine diphosphate (ADP)-L-*glycero*-β-D-*manno*-heptose (ADP-heptose), an intermediate metabolite produced in the synthesis pathway of bacterial LPS, has been shown to be the predominant PAMP inducing NF-κB in *H. pylori* infection (Pfannkuch et al., 2019), although the mechanism through which ADP-heptose enters the host cytosol is still unclear (Figure 4). In the cytosol, ADP-heptose binds to its pattern recognition receptor alpha-kinase 1 (ALPK1) (Zhou et al., 2018). ALPK1, either directly or indirectly, causes the phosphorylation of dimeric tumour necrosis factor receptor-associated factor (TRAF)-interacting protein with forkhead-associated (FHA) domain-containing protein A (TIFA) at threonine residue 9 (pT9) (Zimmermann et al., 2017). The intermolecular FHA-pT9 binding between the TIFA dimers leads to self-oligomerisation (Weng et al., 2015) and subsequent formation of large complexes (TIFAsomes) that encompass, among others, components of the classical NF-κB pathway (Zimmermann et al., 2017). As shown by our group, TRAF6 is also involved in *H. pylori*-mediated classical NF-κB activation as it is responsible for catalysing the K63-linked ubiquitinylation of transforming growth factor β-activated kinase 1 (TAK1), which together with mitogen activated protein kinase kinase kinase 3 (MEKK3) synergistically activate the IKK complex (Sokolova et al., 2014). Thereafter, the activated IKK complex phosphorylates IκBα, leading to its proteasomal degradation and the subsequent nuclear translocation of the classical RelA/p50 heterodimer.

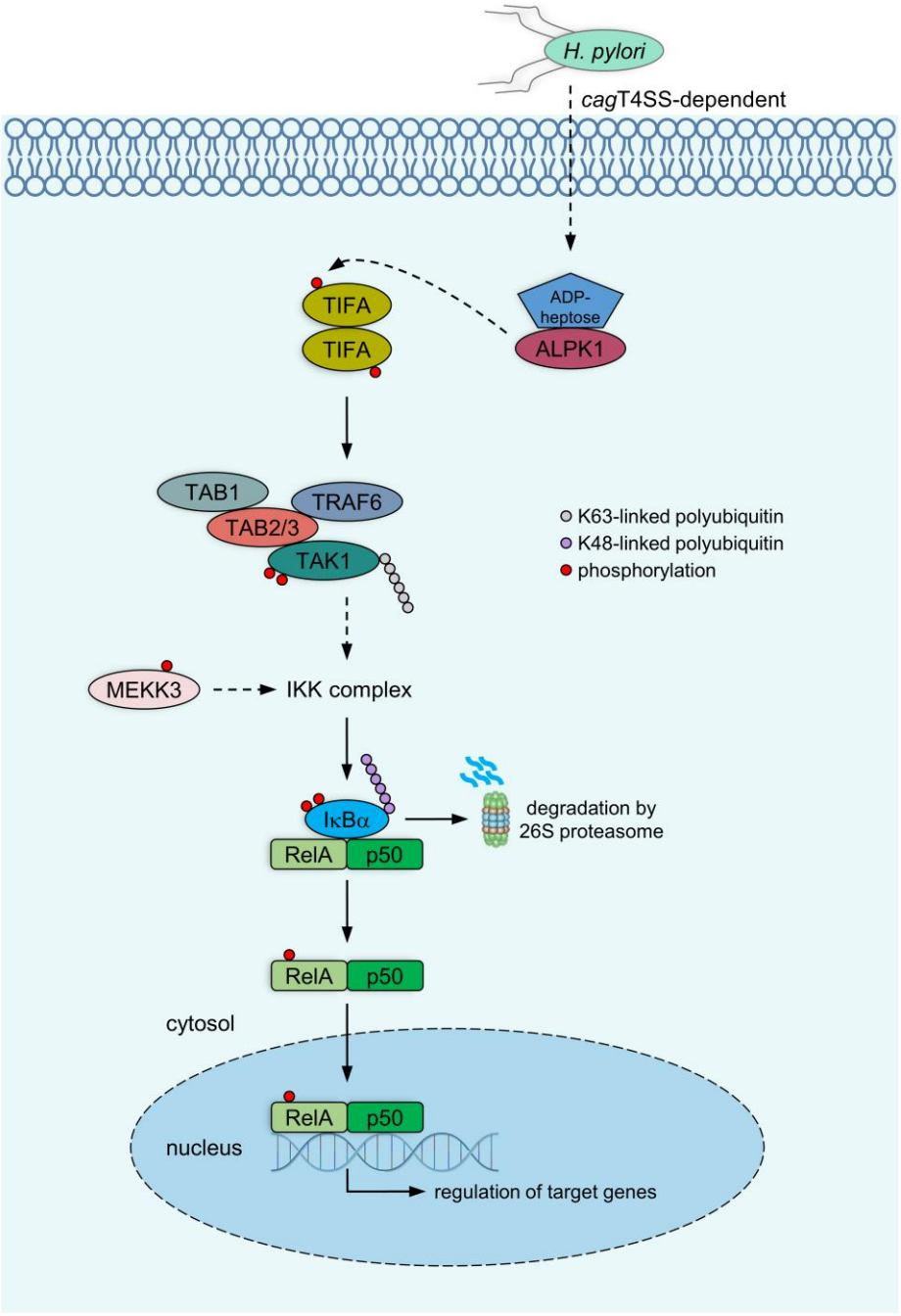

Figure 4. *H. pylori*-mediated classical NF-κB signalling pathway in gastric epithelial cells.
Infection of gastric epithelial cells by *H. pylori* leads to the release of ADP-heptose into the cytosol. The interaction of ADP-heptose with its cytosolic receptor ALPK1 induces the phosphorylation of dimeric TIFA. Subsequent oligomerisation of phosphorylated TIFA and complex formation with host factors trigger the signalling cascade leading to classical NF-κB activation.

1.2.2 The alternative NF-κB pathway

Activation of the alternative NF-κB pathway is commonly associated with developmental signalling and occurs upon stimulation of a subset of receptors belonging to the TNF receptor superfamily by their cognate ligands (Figure 5). These receptors include lymphotoxin-β receptor (LTβR), fibroblast growth factor-inducible 14 (Fn14), receptor activator of NF-κB (RANK), cluster of differentiation 40 (CD40) and B-cell-activating factor receptor (BAFF-R) (Sun, 2017).

The NF-κB-inducing kinase (NIK) plays a pivotal role in the activation of the alternative NF-κB pathway. NIK is essential not only for the phosphorylation and thereby activation of IKKα, but also for promoting the binding of IKKα to p100 (Xiao et al., 2004). The ensuing IKKα-mediated phosphorylation of p100 is the prerequisite for its proteolytic processing to p52 and the subsequent nuclear translocation of p52-containing dimers, predominantly the RelB/p52 heterodimers (Sun, 2017).

In the cytosol of resting cells, NIK is bound to a NIK regulatory complex consisting of TRAF3, TRAF2 and cellular inhibitor of apoptosis protein 1 (cIAP1) or cIAP2 (cIAP1/2). Specifically, the interaction of TRAF3 with TRAF2 enables the TRAF2-bound cIAP1/2 to catalyse the ligation of K48-linked polyubiquitin to NIK, which is bound to TRAF3, ensuring the constant degradation of NIK by the 26S proteasome (Zarnegar et al., 2008). Activation of alternative NF-κB leads to the recruitment of the NIK regulatory complex via TRAF2 and TRAF3 to the cytoplasmic region of the receptor. This results in the TRAF2-dependent K63-linked ubiquitinylation of cIAP1/2, an event which re-directs the E3 ligase activity of cIAP1/2 from NIK towards TRAF3, as shown for CD40 and BAFF-R stimulations (Vallabhapurapu et al., 2008). The K48-linked ubiquitinylated TRAF3 is subsequently degraded by the 26S proteasome, liberating NIK thus leading to its accumulation in the cytosol. This is generally accepted as a common mechanism downstream of different receptors to activate alternative NF-κB signalling. In the case of LTβR stimulation, however, it has also been postulated that recruitment of the NIK regulatory complex to the receptor causes the displacement of cIAP1/2 and NIK, thereupon TRAF2 catalyses the K48-linked ubiquitinylation of TRAF3 (Sanjo et al., 2010).

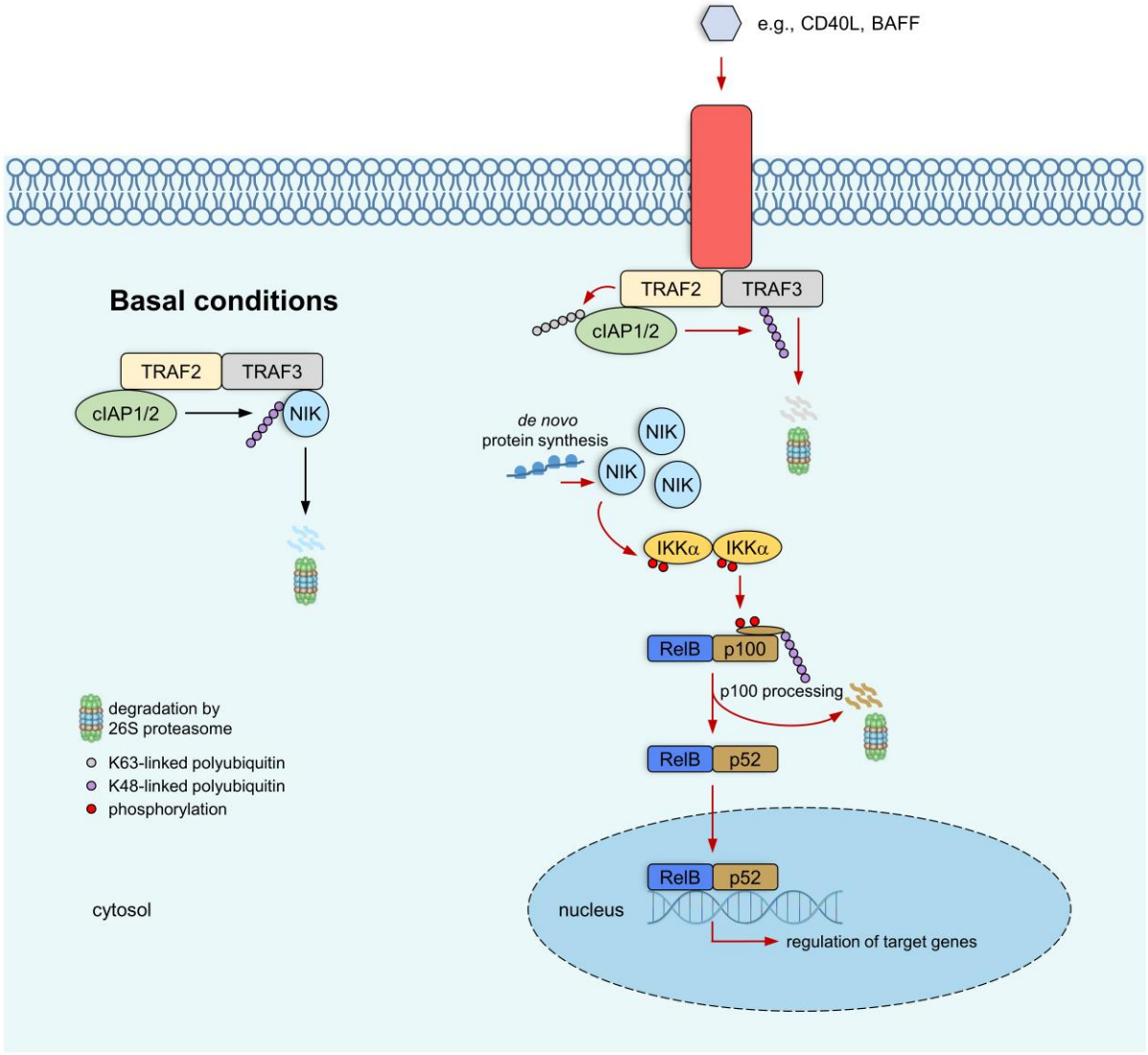

Figure 5. Alternative NF-κB pathway.
Engagement of a subset of receptors belonging to the TNF receptor superfamily by their cognate ligands including CD40 ligand (CD40L) and BAFF perturbs the NIK regulatory complex comprising NIK, TRAF3, TRAF2 and cIAP1/2, resulting in the release of NIK. Subsequent accumulation of NIK in the cytosol triggers the signalling pathway leading to alternative NF-κB (predominantly RelB/p52) activation.

1.2.2.1 *H. pylori*-induced alternative NF-κB signalling

Ohmae and colleagues (2005) observed that infection by *H. pylori* activates the alternative NF-κB pathway in B lymphocytes *in vitro*, providing the first line of evidence linking *H. pylori* infection to alternative NF-κB activation. The activation of alternative NF-κB signalling is likely to have pathophysiological consequences as p52 (alternative NF-κB) was detected in the B lymphocytes in *H. pylori*-infected gastritis tissues (Ohmae et al., 2005). Supporting this concept, the C-C motif chemokine ligand 20 (CCL20), a target gene of alternative NF-κB (Sirard et al., 2009), was positively stained in the gastric epithelial cells of patients with *H. pylori*-associated gastritis (Yoshida et al., 2009). In gastric epithelial cells, it was proposed that *H. pylori*-induced up-regulation of the protein termed homologous to lymphotoxin, exhibits

inducible expression and competes with herpes simplex virus glycoprotein D for binding to herpesvirus entry mediator, a receptor expressed on T lymphocytes (LIGHT) via the classical NF-κB pathway is responsible for triggering the LTβR-mediated alternative NF-κB signalling in a secondary loop post infection (Mejías-Luque et al., 2016). Alternatively, our group proposed that *H. pylori* triggers an early (within the first hour of infection) activation of alternative NF-κB involving the LTβR, although the molecular mechanism is unclear (Feige et al., 2018). In addition, our recent work demonstrated that the ADP-heptose – ALPK1 – TIFA signalling module is crucial for the early alternative NF-κB activation observed upon infection by *H. pylori* (Maubach et al., 2021). We showed that the formation of TIFAsomes that include components of the NIK regulatory complex facilitates the proteasome-dependent transient turnover of cIAP1, resulting in the stabilisation of NIK that is essential for activation of the alternative NF-κB pathway upon *H. pylori* infection (Maubach et al., 2021).

1.3 Apoptosis

Regulated cell death is the execution of an intracellular program to remove damaged, infected or excess cells from the body. In recent years, the view on regulated cell death was broadened to include many different modes such as apoptosis, necroptosis, autophagic cell death, mitotic catastrophe and pyroptosis (Galluzzi et al., 2018). The best studied and prevalent cell death modality is apoptosis, which can be triggered by the intrinsic or extrinsic pathway (Figure 6). Both pathways are mediated by the activation of a cascade of cysteine-dependent aspartate-specific proteases known as caspases. The two groups of caspases involved in apoptosis are the 'initiator' caspases and 'effector' caspases. In general, 'initiator' and 'effector' caspases exist as monomeric and dimeric zymogens, respectively. Apoptotic stimuli trigger the interaction of specific adaptor molecules with 'initiator' caspases (caspase-2, -8, -9, or -10) forming large protein complexes that promote dimerisation-induced *trans*-activation of the 'initiator' caspases via autocatalytic cleavage. Activated 'initiator' caspases proceed to cleave and thus activate the zymogenic forms of 'effector' caspases (caspase-3, -6 or -7). Activated 'effector' caspases then cleave specific cellular substrates including poly (ADP-ribose) polymerase (PARP) and inhibitor of caspase-activated DNase (ICAD), causing biochemical and morphological changes that lead systematically to the demise of the cell (Julien and Wells, 2017).

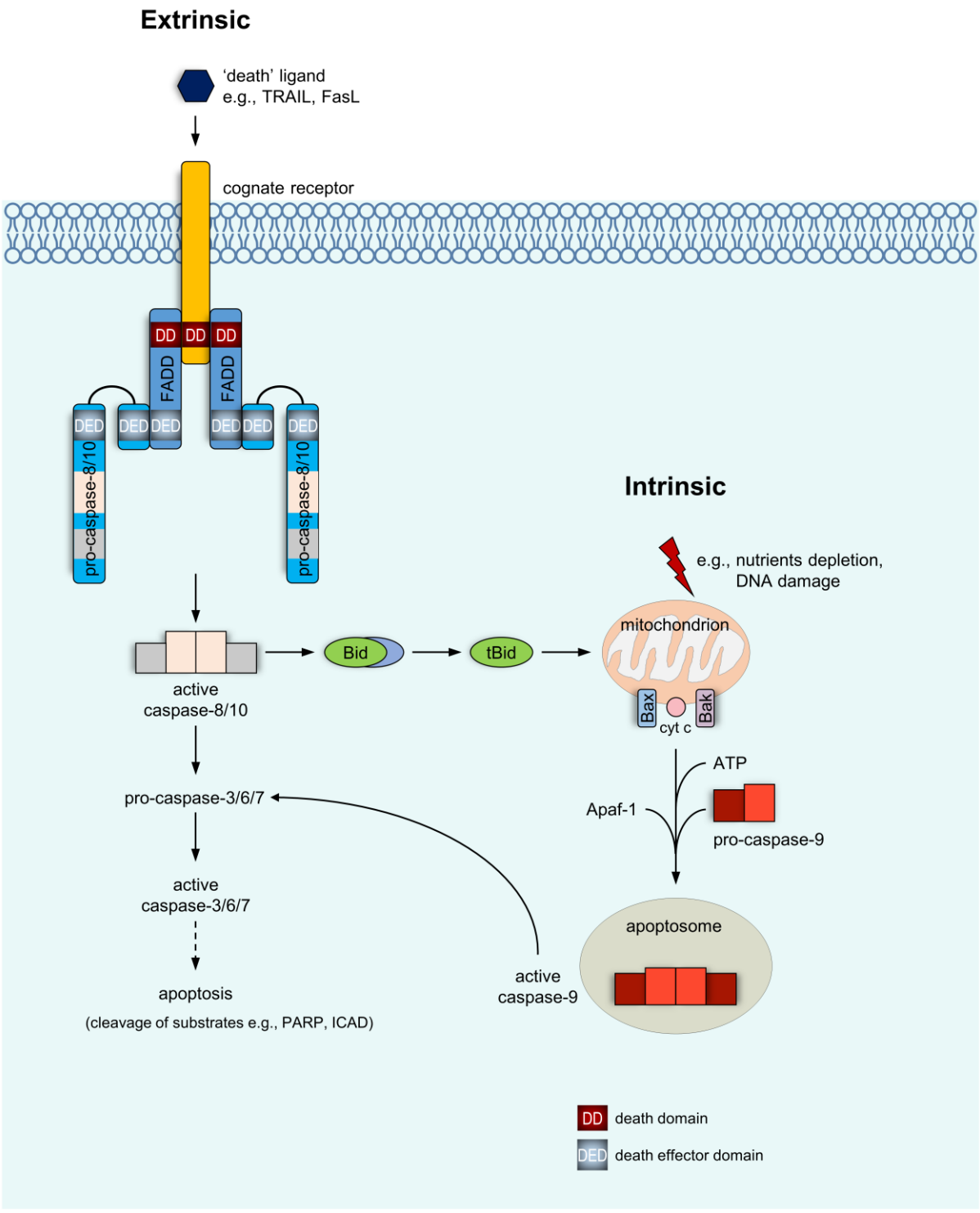

Figure 6. Extrinsic and intrinsic apoptotic signalling pathways.
The extrinsic apoptotic signalling pathway is activated when extracellular 'death' ligands bind to their cognate receptors on the plasma membrane. The intrinsic apoptotic signalling pathway is triggered in response to intracellular stressors leading to permeabilisation of the outer mitochondrial membrane and the release of cytochrome c. Both pathways involve the sequential processing and thus activation of different caspases, culminating in the cleavage of several substrates. This results in morphological and biochemical changes such as membrane blebbing and DNA fragmentation, respectively, which are typical features of an apoptotic cell.

1.3.1 The intrinsic apoptotic pathway

The intrinsic (mitochondrial) apoptotic pathway is induced in response to intracellular stress conditions such as nutrients depletion, DNA damage and oxidative stress (Figure 6). These stress conditions result in the permeabilisation of the outer mitochondrial membrane leading to the loss of mitochondrial membrane potential, the crucial step in the intrinsic apoptotic pathway. In general, the pro- and anti-apoptotic proteins belonging to the B-cell lymphoma 2 (BCL-2) family are fundamental players in this pathway, whereby the interplay between them determines the fate of the cell (Singh et al., 2019). The BCL-2 family of proteins, which are characterised by the presence of at least one of the four different BCL-2 homology domains (BH1-4, numbered in order of discovery), can be divided into three subgroups according to structure and function (Shamas-Din et al., 2013). (1) The pro-apoptotic members BCL-2-associated X protein (BAX) and BCL-2 antagonist/killer (BAK) oligomerise to form pores in the outer mitochondrial membrane to disrupt membrane integrity. (2) The BH3-only proteins, such as BCL-2-associated agonist of cell death (BAD), BH3-interacting domain death agonist (BID) and BCL-2-interacting mediator of cell death (BIM), have only one BH domain. These proteins promote apoptosis either directly by binding to the pro-apoptotic BAX or BAK proteins to activate them, or indirectly by competing for binding to the different anti-apoptotic proteins to liberate BAX and BAK. (3) The anti-apoptotic members including BCL-2, B-cell lymphoma extra large (BCL-x_L) and BCL-2-related protein A1 (BCL2A1) bind to their pro-apoptotic partners as well as some BH3-only proteins to inhibit their mechanism of action. Compromising the outer mitochondrial membrane leads to the release of cytochrome c from the mitochondrial intermembrane space to the cytoplasm. In an adenosine triphosphate (ATP)-dependent manner, cytochrome c interacts with and promotes the oligomerisation of apoptotic protease activating factor-1 (Apaf-1) to form the caspase-activating platform known as the ‘Apaf-1 apoptosome’ (Dorstyn et al., 2018). Pro-caspase-9 is recruited to the apoptosome for activation. Once activated, caspase-9 processes the zymogenic ‘effector’ caspase-3 to induce apoptotic cell death.

1.3.2 The extrinsic apoptotic pathway

The extrinsic apoptotic pathway is triggered at the plasma membrane when death receptors, which belong to the TNF superfamily, are engaged by their cognate ligands (Figure 6). These death receptors include the TNF receptor 1 (TNFR1), cluster of differentiation 95 (CD95, also known as Fas and Apo-1) and TNF-related apoptosis-inducing ligand receptor 1 (TRAIL-R1, also known as DR4). Death receptors are type I transmembrane proteins containing a defined cytoplasmic region known as the death domain. Death receptors are present as monomers or preassembled as dimers or trimers on the cell surface (O' Reilly et al., 2016). Upon interaction with their ligands, death

receptors undergo a conformational change and become activated favouring the binding of adaptor proteins, either Fas-associated protein with death domain (FADD) or TNFR-associated protein with death domain (TRADD) or both depending on the stimulus, via homotypic death domain interactions. The adaptor proteins recruit the inactive caspase-8 or -10 through homotypic interactions of their respective death effector domains (DED). Together, this macromolecular structure comprising the ligand-bound receptor complex, adaptor proteins and 'initiator' caspases is called the death-inducing signalling complex (DISC). At the DISC, caspase-8 or -10 become activated by dimerisation via their DED domains followed by interdimer (autoproteolytic) processing to further stabilize the dimer (Boatright et al., 2003; Chang et al., 2003). Upon further processing, the active or mature caspase containing two large and two small subunits (caspase-8 heterotetramer p10/p18 (Lavrik et al., 2003) or caspase-10 heterotetramer p11/p18 (Sprick et al., 2002) that is formed at the DISC is released into the cytosol to initiate apoptosis by direct proteolytic processing of zymogenic 'effector' caspase-3, -6 or -7.

Depending on cell types, two different extrinsic apoptotic pathways have been described for the prototypical CD95 ligand (CD95L)/CD95 signalling (Scaffidi et al., 1998). In type I cells, the formation of a high amount of DISC generates a high level of active caspase-8, leading to the direct processing of inactive caspase-3 as mentioned above to elicit apoptosis (Figure 6). In type II cells, however, the low level of DISC that is formed upon CD95L treatment generates only low level of active caspase-8. Therefore, to execute apoptosis in type II cells, the signalling cascade requires additional boosts, of which two ways have been described. In the first way, the mitochondria serve as an amplifier to generate more active caspase-8. Specifically, the mitochondria-specific phospholipid cardiolipin provides a platform for the targeting of caspase-8 to the mitochondrial membrane, where it oligomerises and becomes further activated (Gonzalvez et al., 2008). In the second way, a crossover from the extrinsic to the intrinsic apoptotic pathway occurs when the active caspase-8 cleaves BID (Li et al., 1998; Luo et al., 1998; Schug et al., 2011). Cleaved or truncated BID (tBID) interacts with other members of the BCL-2 family causing permeabilisation of the outer mitochondrial membrane and the subsequent release of cytochrome c (Figure 6). The processing of BID by active caspase-10 upon CD95L stimulation has also been described (Milhas et al., 2005).

1.3.3 *H. pylori*-induced apoptosis in gastric epithelial cells

H. pylori adheres to gastric epithelial cells and induces apoptosis (Jones and Sherman, 1999). This process may lead to the perturbation of gastric epithelium homeostasis and is therefore likely to contribute to the pathogenesis of *H. pylori* infection. Indeed, increased apoptotic epithelial cell death was observed in gastric mucosal biopsy specimens obtained from patients with *H. pylori*-associated gastritis. Here, the extent of apoptosis correlated with the severity of

gastritis, reaching a peak at the stage of severe gastritis, before decreasing as the condition transits to intestinal metaplasia (Scotiniotis et al., 2000). More recently, increased apoptosis of epithelial cells was also linked to *H. pylori*-associated duodenal ulcer disease (Tsukanov et al., 2015).

Induction of the extrinsic apoptotic pathway in gastric epithelial cells upon infection by *H. pylori* has been demonstrated, which was attributed to the up-regulation of CD95L, TRAIL and their respective receptors (Martin et al., 2004; Rudi et al., 1998). This fratricide phenomenon among gastric epithelial cells as well as their elimination by CD95L-expressing infiltrating lymphocytes (Wang et al., 2000) most probably account for the *H. pylori*-mediated epithelium damage frequently observed *in vivo*.

Virulence factors of *H. pylori* have been identified that contribute to the regulation of gastric epithelial cells apoptosis. VacA induces apoptosis of gastric epithelial cells in vacuolating activity-dependent and -independent manners (Kuck et al., 2001). The latter was later linked to the activation of the intrinsic apoptotic pathway (Yamasaki et al., 2006). Increased gastric epithelial cell apoptosis correlated with the colonisation with CagA-positive *H. pylori* strains (Moss et al., 2001), pointing to the involvement of CagA in this process. On the other hand, CagA has also been described to counteract the apoptosis-inducing ability of VacA (Oldani et al., 2009). The bacterial membrane-associated protein γ-glutamyl transpeptidase have been implicated in triggering the intrinsic apoptotic pathway (Shibayama et al., 2003; Valenzuela et al., 2013) or via the caspase-8/BID/BAD/caspase-3 axis (Shibayama et al., 2001). These studies collectively indicate that the host cell, when infected with *H. pylori*, can execute both extrinsic and intrinsic signalling pathways leading to apoptotic cell death.

1.4 Regulation of inflammatory responses by A20

The human A20 is encoded by the *TNFAIP3* (tumour necrosis factor alpha-induced protein 3) gene, which was first identified as a primary response gene upon TNF stimulation of human umbilical vein endothelial cells (Dixit et al., 1990). A basal expression level of A20 is observed in many cell types and this could be increased by the transcriptional up-regulation of the *TNFAIP3* gene by many agonists, including inflammatory stimuli like IL-1β and LPS that trigger classical NF-κB (Verstrepen et al., 2010). A20 is a potent negative regulator of inflammatory signalling and mutations in the *TNFAIP3* gene often correlated with increased risk for developing inflammatory disorders such as Crohn's disease, rheumatoid arthritis and atherosclerosis (Vereecke et al., 2011). The ability of A20 to restrict inflammation is commonly attributed to its involvement in the negative feedback regulation of classical NF-κB activation, which has been intensively studied over the years (Martens and van Loo, 2020). Intriguingly, evidence has recently emerged indicating the potential of A20 to limit inflammation by protecting cells from necroptosis and apoptosis (Priem et al., 2020).

1.4.1 A20-mediated regulation of NF-κB pathways

The human A20 contains an N-terminal ovarian tumour (OTU) domain (residues 1-370) and seven repeats of A20-like zinc finger (ZnF) domains near the C-terminus (Makarova et al., 2000; Opipari et al., 1990) (Figure 7). A striking feature of A20 is its ubiquitin-editing function that has only been described in the TNFR1-mediated NF-κB signalling pathway so far. To fulfil this function, it is necessary for A20 to associate with accessory proteins such as Tax1-binding protein 1 (TAX1BP1) and Itch to form the A20 ubiquitin-editing complex (Shembade and Harhaj, 2012). Upon activation of TNFR1 by TNF, FADD and TRADD are recruited as adaptor proteins to TNFR1. Subsequent binding of the receptor-interacting serine/threonine-protein kinase 1 (RIPK1) to TRADD enables the K63-linked ubiquitinylation of RIPK1 by cIAP1/2 (Bertrand et al., 2008). TAX1BP1 and Itch are essential for the interaction between A20 and its substrate RIPK1, leading to the inactivation of RIPK1 as follows. A20's deubiquitinylase (DUB) activity in the OTU domain, which is conferred by the catalytic cysteine residue 103 (C103), is targeted towards the removal of K63-linked polyubiquitin chains from RIPK1 (Wertz et al., 2004). Thereafter, A20 together with Itch mediate the subsequent polymerisation of K48-linked polyubiquitin chains to RIPK1 leading to its proteasomal degradation (Shembade et al., 2008; Wertz et al., 2004). A20 is likewise implicated in the negative regulation of T-cell receptor- and toll-like receptor-mediated NF-κB pathways by removing K63-linked polyubiquitin chains from mucosa-associated lymphoid tissue lymphoma translocation protein 1 (MALT1) and TRAF6, respectively (Boone et al., 2004; Düwel et al., 2009). Notably, the NF-κB-inhibitory function of A20 is enhanced by its phosphorylation, which is mediated by IKKβ (Hutti et al., 2007; Wertz et al., 2015).

A20 has also been shown to inhibit the classical NF-κB signalling pathway independent of its catalytic activities. One such non-catalytic mechanism of NF-κB inhibition by A20 is thought to be mediated through its ubiquitin-binding domains, namely ZnF4 for binding to K63-linked ubiquitin chains and ZnF7 for binding to K63-linked as well as linear ubiquitin chains (Martens and van Loo, 2020). The importance of these ubiquitin-binding domains in A20's NF-κB-inhibitory role is further corroborated by recent *in vivo* data (Martens et al., 2020; Razani et al., 2020). Another non-catalytic mode of action of A20 involves undermining the ubiquitinylation process of key signalling proteins in the classical NF-κB signalling pathway by antagonising the interaction between E2 ubiquitin-conjugating enzymes and specific E3 ubiquitin ligases. Specifically, in the IL-1β-mediated pathway, the inducible interaction between Ubc13 (E2 enzyme) and TRAF6 (E3 ubiquitin ligase) is disrupted upon the recruitment of A20 to TRAF6 leading to less activation of TRAF6 (Shembade et al., 2010).
A20 has been postulated to promote the activation of the LTβR-, Fn14- or RANK-mediated alternative NF-κB pathway. The enzymatic activities of A20 appear to be unnecessary for this process. Instead, A20's ZnF7 domain reportedly promotes the direct binding of A20 to cIAP1, causing dissociation of the interaction between TRAF2 and TRAF3 within the NIK regulatory complex, which results in the stabilisation of NIK (Yamaguchi et al., 2013).

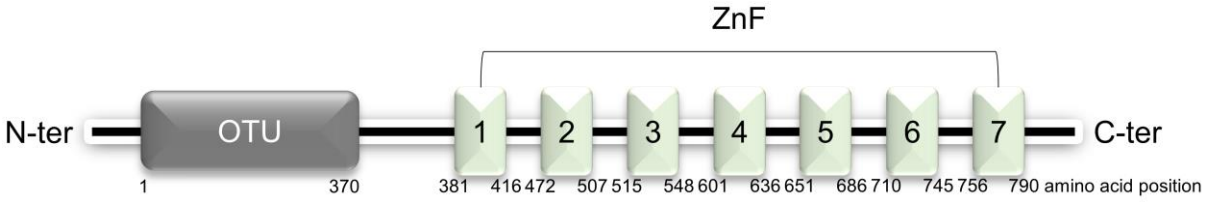

Figure 7. Domain structure of human A20.
Human A20 contains an N terminal (N-ter) ovarian tumour (OTU) domain and seven repeats of A20-like zinc finger (ZnF) domains near the C terminus (C-ter). A20 exhibits a deubiquitinylating activity, which is conferred by the catalytic cysteine residue 103 within the OTU domain. Both ZnF4 and ZnF7 domains recognise and bind polyubiquitin chains.

1.4.2 A20-mediated regulation of apoptosis

Daniel and colleagues (2004) observed that A20 inhibits caspase-8 activation in endothelial cells treated with TNF and agonistic Fas antibody. Consistent with this report, in lung cancer cell lines, A20 was identified in a tandem mass spectrometry (MS/MS) analysis of DISC-associated proteins and the interaction of A20 with caspase-8 was confirmed by co-immunoprecipitation (Jin et al., 2009). In this study, TRAIL induces the cullin3 (Cul3)-based E3 ubiquitin ligase-mediated K63-linked polyubiquitinylation of caspase-8, which promotes its full activation. Overexpression of A20 reverses this process leading to a reduction in caspase-8 activity, suggesting that the molecular basis for the anti-apoptotic function of A20 is through the deubiquitinylation of caspase-8 (Jin et al., 2009). On the other hand, in glioblastoma cell lines, TRAIL induces the K63-linked polyubiquitinylation of RIPK1 instead of caspase-8, an event suggested to be mediated by the ZnF4 domain of A20 (Bellail et al., 2012). Ubiquitinylated RIPK1 binds to the protease domain of caspase-8, blocking its dimerisation and processing to active caspase-8 (Bellail et al., 2012). In addition, A20 has been shown to counteract TNF-induced cytotoxicity indirectly by targeting apoptosis signal-regulating kinase 1 (ASK1) (Won et al., 2010). Upon TNF treatment, Won and colleagues (2010) showed that the binding of A20 to ASK1 leads to the degradation of ASK1, resulting in the suppression of the c-jun N-terminal kinase (JNK) cascade and subsequent inhibition of apoptosis.

Contrary to the negative regulation of apoptosis by A20 mentioned above, A20 has been reported to promote apoptosis indirectly by inhibiting the NF-κB-dependent expression of anti-apoptotic proteins such as BCL-X in B cells (Tavares et al., 2010) or BCL-X and BCL-2 in dendritic cells (Kool et al., 2011). A direct role of A20 in promoting apoptosis has been suggested in a recent study by Garcia-Carbonell and colleagues (2018), where they showed that transgenic mice overexpressing A20 specifically in intestinal epithelial cells displayed increased sensitivity to TNF-induced RIPK1-dependent apoptosis. The authors proposed that this function of A20 is independent of its ubiquitin-editing activities but dependent on its ZnF7 domain. A20 forms homodimers via ZnF7 domains, which bind to the linear ubiquitin chains attached to RIPK1 and promote the formation of the ‘Ripoptosome’ comprising RIPK1, FADD and caspase-8 to enhance the activation of caspase-8 (Garcia-Carbonell et al., 2018).

2. Thesis Objectives

Infection of gastric epithelial cells by *H. pylori* leads invariably to an inflammatory response, the prominent hallmark of which is activation of classical and alternative NF-κB. Infection by *H. pylori* also triggers apoptotic cell death of gastric epithelial cells. These *H. pylori*-associated events contribute significantly to the modulation of the inflammatory response that in turn is intricately linked to the pathogenesis seen in *H. pylori* infections. In view of this, determining how the *H. pylori*-triggered NF-κB response and apoptotic cell death are regulated is highly relevant for our understanding of the pathophysiology of *H. pylori*-associated diseases. The protein A20 is fascinating to study in this context because not only is it transcriptionally regulated by NF-κB, a large body of evidence also showed that its function involves regulation of NF-κB and apoptotic cell death. The objectives of this work are to investigate the function of A20 in the regulation of alternative NF-κB activation and caspase-8-dependent apoptotic cell death associated with *H. pylori* infection.

3. Results

3.1 Function of A20 in *H. pylori*-induced NF-κB signalling pathways in gastric epithelial cells

3.1.1 NF-κB regulates A20 expression in gastric carcinoma epithelial cells upon *H. pylori* infection

We first examined the kinetics of A20 expression in gastric carcinoma epithelial cells (AGS cell line) exposed to *H. pylori* infection. Immunoblot (IB) analysis revealed a significant increase in A20 expression between 2 h and 4 h followed by a gradual decrease up to 24 h in cells infected with *H. pylori* wild-type (wt) strain (Figure 8A). This was preceded by the fast (within 30 min) activation of classical NF-κB as indicated by the phosphorylation of IKKα and IKKβ, and the downstream phosphorylation of RelA (Figure 8A). Activation of classical NF-κB by *H. pylori* is dependent on its ADP-heptose, which is a metabolic precursor of LPS (Pfannkuch et al., 2019). ADP-heptose is recognised by host cytosolic ALPK1 leading to the phosphorylation at threonine residue 9 of TIFA (Zhou et al., 2018), which triggers a cascade of events leading to classical NF-κB activation (Maubach et al., 2021). Accordingly, infection by the isogenic *H. pylori* strain defective in the synthesis of LPS (ΔHP0857) had negligible effects on classical NF-κB activation and on A20 expression (Figure 8A). The same was also observed for TIFA-deficient cells infected with *H. pylori* wt strain (Figure 8A). Interestingly, we observed an early reduction in the level of endogenous TIFA in AGS cells infected with *H. pylori* wt strain but not with the isogenic ΔHP0857 strain.

Apart from NF-κB, the A20 gene promoter is also regulated by other transcription factors including CCAAT/enhancer binding protein β (C/EBPβ) and upstream stimulatory factor 1 (USF1) (Lai et al., 2013). Therefore, to demonstrate the contribution of NF-κB towards A20 gene regulation, A20 expression was examined in cells infected with *H. pylori* in the absence or presence of an IKK inhibitor. Herein, the inhibition of NF-κB signalling resulted in a suppression of A20 mRNA and protein expression (Figures 8B and 8C). Previous work from our group showed that *H. pylori* requires its T4SS but not CagA to induce NF-κB (Schweitzer et al., 2010; Sokolova et al., 2013). Consistently, A20 expression was induced by *H. pylori* P1 wt and CagA-deficient (Δ*cagA*), but not T4SS-deficient (*virB7*) isogenic strains (Figure 8D). The abundance of flagellin observed indicated moderate differences in the bacterial adherence of *H. pylori* P1 wt strain and its isogenic mutants to the AGS cells (Figure 8D). Together, our results indicate that A20 is regulated by *H. pylori*-induced NF-κB in a CagA-independent but T4SS-dependent manner.

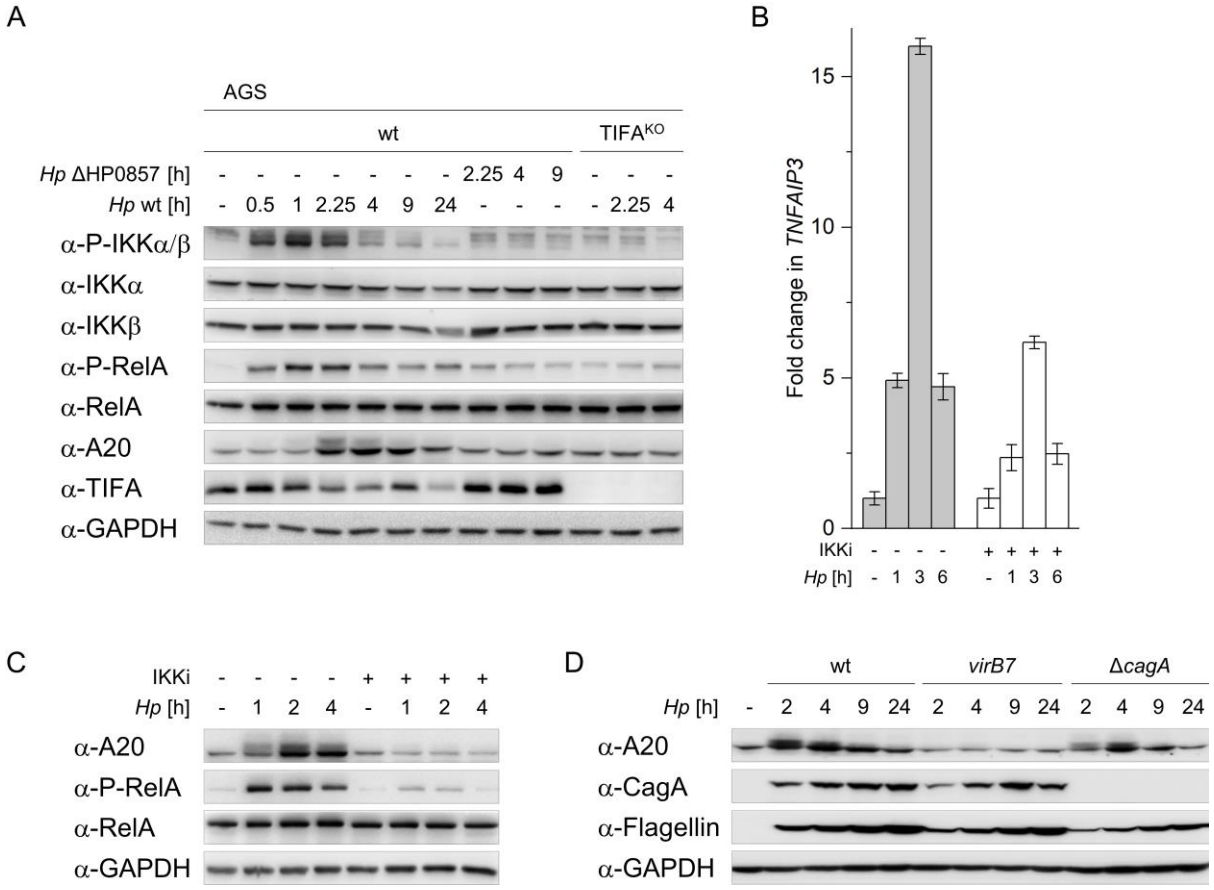

Figure 8. The expression of A20 is NF-κB-dependent in *H. pylori* infection.
(A) AGS cells were infected with *H. pylori* P1 wt or isogenic ΔHP0857 (defective in the synthesis of LPS) strains. AGS cells depleted of TIFA (TIFA^{KO}) were infected with *H. pylori* P1 wt strain.
(B) AGS cells were incubated with DMSO (vehicle) only or 10 μM IKK inhibitor VII (IKKi) for 30 min prior to infection with *H. pylori* P1 wt strain. Total RNA was isolated. Changes in the expression of the A20 transcript (*TNFAIP3*) were investigated by real-time PCR. Data shown depict the average of triplicate determinations of one experiment normalised to the *GAPDH* gene. Error bars denote means ± SD. Data shown are representative of at least two independent experiments.
(C) AGS cells were incubated with DMSO (vehicle) only or 10 μM IKK inhibitor VII (IKKi) for 30 min prior to infection with *H. pylori* P1 wt strain.
(D) AGS cells were infected with isogenic *H. pylori* P1 wt, *virB7* or Δ*cagA* strains.
Cell lysates were analysed for the indicated proteins by IB and GAPDH was used to show equivalent protein loading (A, C and D). The IBs shown in each panel are generated from the same experiment. Data are representative of at least two independent experiments.

3.1.2 A20 suppresses *H. pylori*-induced activation of the classical and alternative NF-κB pathways

Several studies have shown that A20 inhibits the classical NF-κB signalling pathway (Shembade et al., 2010; Skaug et al., 2011; Wertz et al., 2004). To explore the involvement of A20 in the regulation of *H. pylori*-induced classical NF-κB signalling pathway, A20 was depleted in AGS cells using two specific small interfering RNA (siRNA) oligonucleotides individually. Classical NF-κB activation mediated by *H. pylori* infection was more pronounced in siRNA-treated cells, as reflected by the increased phosphorylation of IκBα and RelA (Figures 9A and 9B). The difference in the band intensity of IκBα between uninfected and *H. pylori* infection for 24 h samples (Figure 9B) could be explained by an increased turnover of free IκBα in this experiment as described by Mathes and colleagues (2008), where the C-terminal proline-glutamic acid-serine-threonine (PEST) sequence is responsible for its fast degradation independent of IKK-mediated phosphorylation.

In addition, the CRISPR/Cas9 technology was utilised to generate stable A20-knockout AGS cells, which are henceforth referred to as $A20^{KO}$ cells. Control AGS cells are referred to as parental or wt AGS cells. Significantly stronger classical NF-κB activation was observed in two single cell clones of $A20^{KO}$ for TNF stimulation, indicating the successful generation of loss-of-function cell lines for A20 (Figure 9C). Similar results were also observed in the $A20^{KO}$ cells after infection by *H. pylori* (Figure 9D). To rule out that off-target effects of genome editing by the CRISPR/Cas9 technology account for the augmented *H. pylori*-induced classical NF-κB activation observed in $A20^{KO}$ cells, we performed 'rescue of phenotype' experiments by overexpressing wt A20 in these cells. The re-expression of A20 in $A20^{KO}$ cells resulted in attenuation of classical NF-κB activation compared to control $A20^{KO}$ cells (transfected with empty vector only) (Figure 9E), verifying that the effect observed is indeed due to the ablation of A20 and not an off-target effect of CRISPR/Cas9. Together, these results also indicate that A20 is involved in the negative regulation of *H. pylori*-induced classical NF-κB activation.

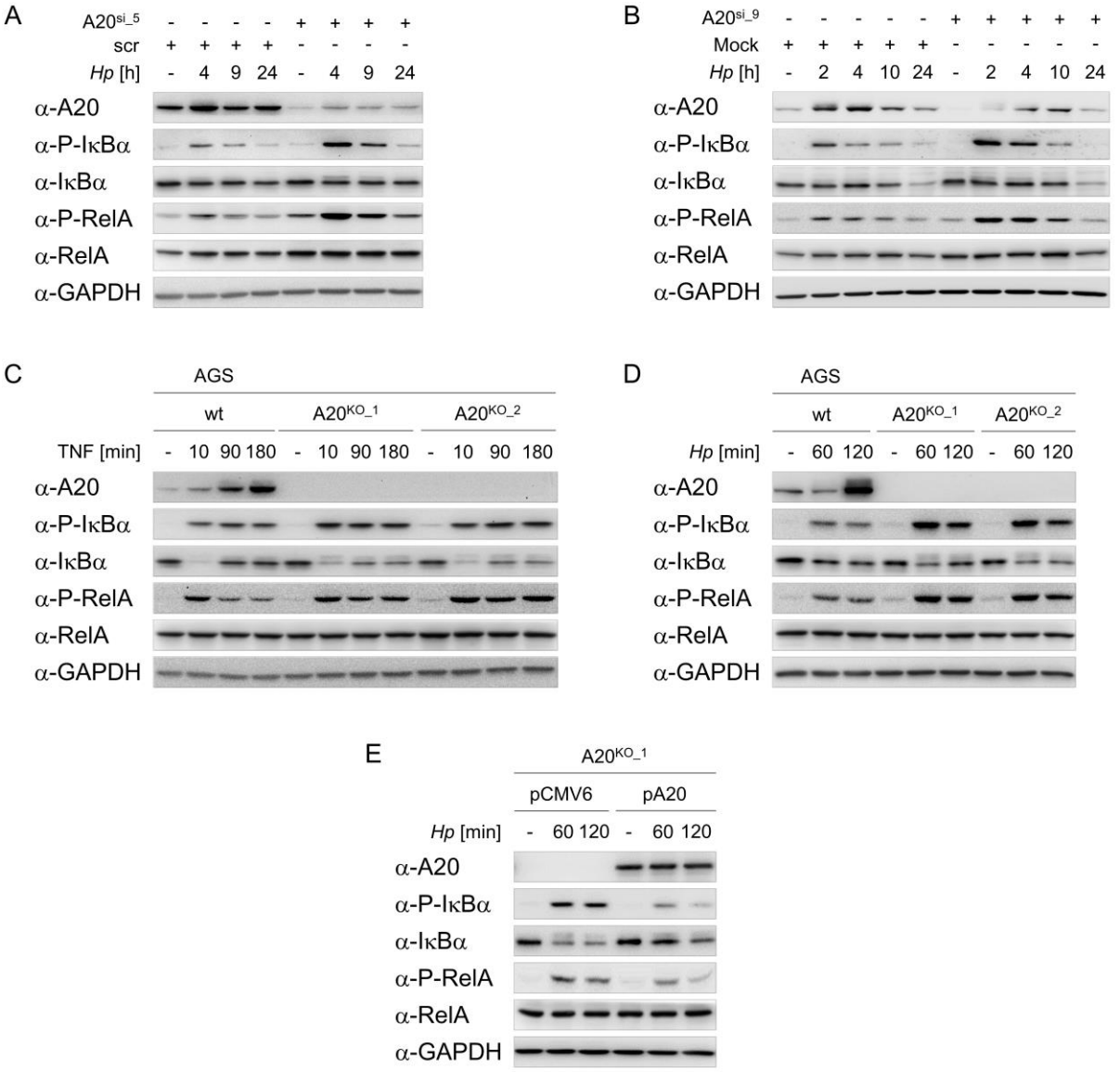

Figure 9. A20 is involved in the negative regulation of *H. pylori*-induced classical NF-κB activation.
(A) AGS cells were transfected with siRNA targeting the open reading frame of A20 ($A20^{si\_5}$) or non-target-specific scrambled (scr) siRNA for 48 h, followed by infection with *H. pylori*.
(B) AGS cells were transfected with siRNA targeting the 3'-untranslated region of A20 ($A20^{si\_9}$) or with transfection reagent only (Mock) for 48 h, followed by infection with *H. pylori*.
(C) Parental AGS cells (wt) and two different clones of A20-knockout AGS cells ($A20^{KO\_1}$ and $A20^{KO\_2}$) were stimulated with 10 ng/ml TNF.
(D) wt, $A20^{KO\_1}$ and $A20^{KO\_2}$ AGS cells were infected with *H. pylori*.
(E) $A20^{KO\_1}$ cells were transfected with either pCMV6 plasmid (as empty vector control) or plasmid containing the complete A20 coding sequence (pA20) 24 h prior to *H. pylori* infection.
The *H. pylori* P1 wt strain was used for infection (A, B, D and E). Cell lysates were analysed for the indicated proteins by IB and GAPDH was used to show equivalent protein loading (A-E). The IBs shown in each panel are generated from the same experiment. Data are representative of at least two independent experiments.

In AGS cells, exposure to *H. pylori* causes activation of the alternative NF-κB signalling pathway as shown by the transient accumulation of NIK (peaked at 2.5 h) and the inducible phosphorylation of p100 (Figure 10A), as well as the nuclear translocation of p52 and RelB (Figure 10B), which are the essential dimer-forming subunits of alternative NF-κB. The genes of both p100 and RelB are regulated by NF-κB (Bren et al., 2001; de Wit et al., 1998).

Accordingly, an increase in the expression of p100 in the total lysates (Figure 10A) and RelB in the cytosolic fraction (Figure 10B) of *H. pylori*-infected cells was also observed. The p52 protein could be generated in a co-translational manner (Heusch et al., 1999) as well as upon activation of the alternative NF-κB pathway (Xiao et al., 2001), both of which involve the proteolytic processing of its precursor, the p100 protein. This explanation accounts for the inducible increase in the cytosolic level of p52 in *H. pylori*-infected cells (Figure 10B). In comparison to *H. pylori* infection, slower kinetics of alternative NF-κB activation was observed after stimulation by lymphotoxin alpha1beta2 ($LT\alpha_1\beta_2$), a ligand that signal at the cell surface via the LTβR (Figure 10A). Of note, $LT\alpha_1\beta_2$ treatment triggered in AGS cells negligible classical NF-κB signalling, which was reflected in the absence of A20's up-regulation (Figure 10A). The activation of alternative NF-κB signalling pathway upon *H. pylori* infection was also observed in the epithelial cell lines NCI-N87 and HKC-8 (Figures 10C and 10D), thus excluding cell line-specific effects. There was no noticeable increase in the cytoplasmic level of p52 in these cells after *H. pylori* infection (Figure 10D), unlike in AGS cells (Figure 10B), probably due to its faster nuclear translocation.

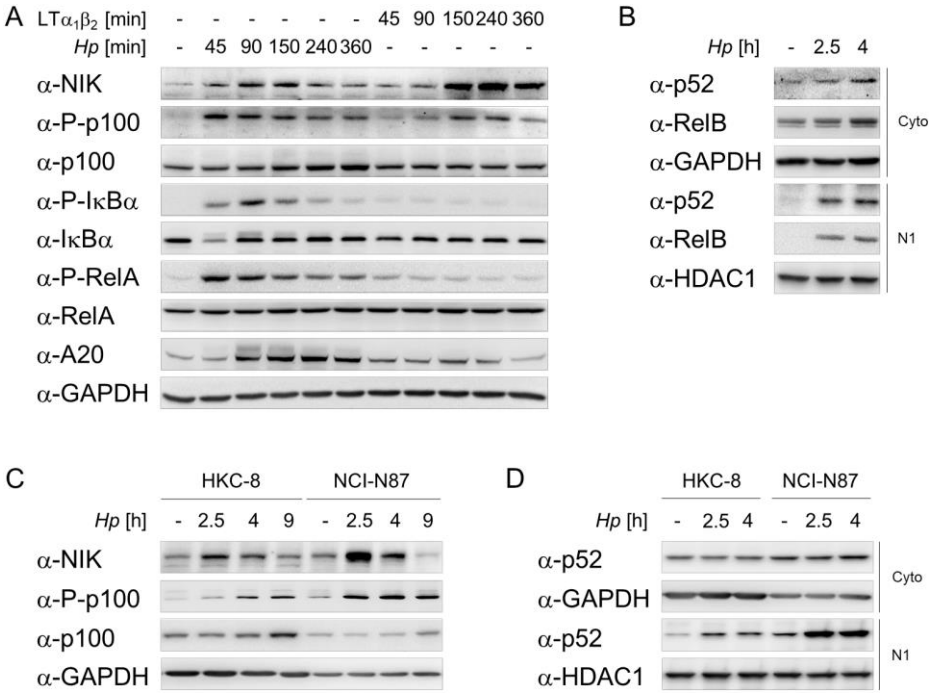

Figure 10. Infection by *H. pylori* leads to alternative NF-κB activation.
(A) AGS cells were infected with *H. pylori* or stimulated with 30 ng/ml $LT\alpha_1\beta_2$.
(B) AGS cells were infected with *H. pylori*. Cytosolic extracts (Cyto) and soluble nuclear (N1) fractions were prepared.
(C) HKC-8 and NCI-N87 cells were infected with *H. pylori*.
(D) HKC-8 and NCI-N87 cells were infected with *H. pylori*. Cyto and N1 fractions were prepared.
The *H. pylori* P1 wt strain was used for infection. Total cell lysates (A and C) or cyto and N1 fractions (B and D) were analysed for the indicated proteins by IB. GAPDH was used to show equivalent protein loading. HDAC1 was used to show equivalent protein loading in N1 fractions. The IBs shown in each panel are generated from the same experiment. Data are representative of at least two independent experiments.

To determine whether A20 plays a regulatory role in *H. pylori*-induced alternative NF-κB activation, $A20^{KO}$ AGS cells were utilised. Knockout of A20 resulted in a prominent increase in *H. pylori*-mediated activation of the alternative NF-κB signalling pathway, as indicated by the increase in the accumulation of NIK and the phosphorylation of p100 (Figure 11A). Moreover, the basal level of p100 in $A20^{KO}$ cells was also slightly higher compared to wt cells (Figure 11A). Importantly, $A20^{KO}$ cells complemented with transfected recombinant human A20 protein showed markedly diminished activation of the alternative NF-κB signalling pathway (Figure 11A). Furthermore, upon *H. pylori* infection, the cytoplasmic level of p52 and RelB, as well as their nuclear translocation in $A20^{KO}$ cells was significantly increased compared to wt cells (Figure 11B). The observed difference in the activation of alternative NF-κB in wt and $A20^{KO}$ cells was corroborated by infection with another *H. pylori* strain P12 (Figure 11C). Similarly, NCI-N87 cells depleted of A20 by siRNA transfection showed also appreciably stronger alternative NF-κB activation (Figure 11D), confirming that the effect of A20 depletion was not limited to a single cell line. On the contrary, $LT\alpha_1\beta_2$-induced alternative NF-κB activation was significantly reduced in $A20^{KO}$ cells compared to wt cells (Figure 11E). Overall, our results implied that the function of A20 in the negative regulation of alternative NF-κB activation is specific to *H. pylori* infection.

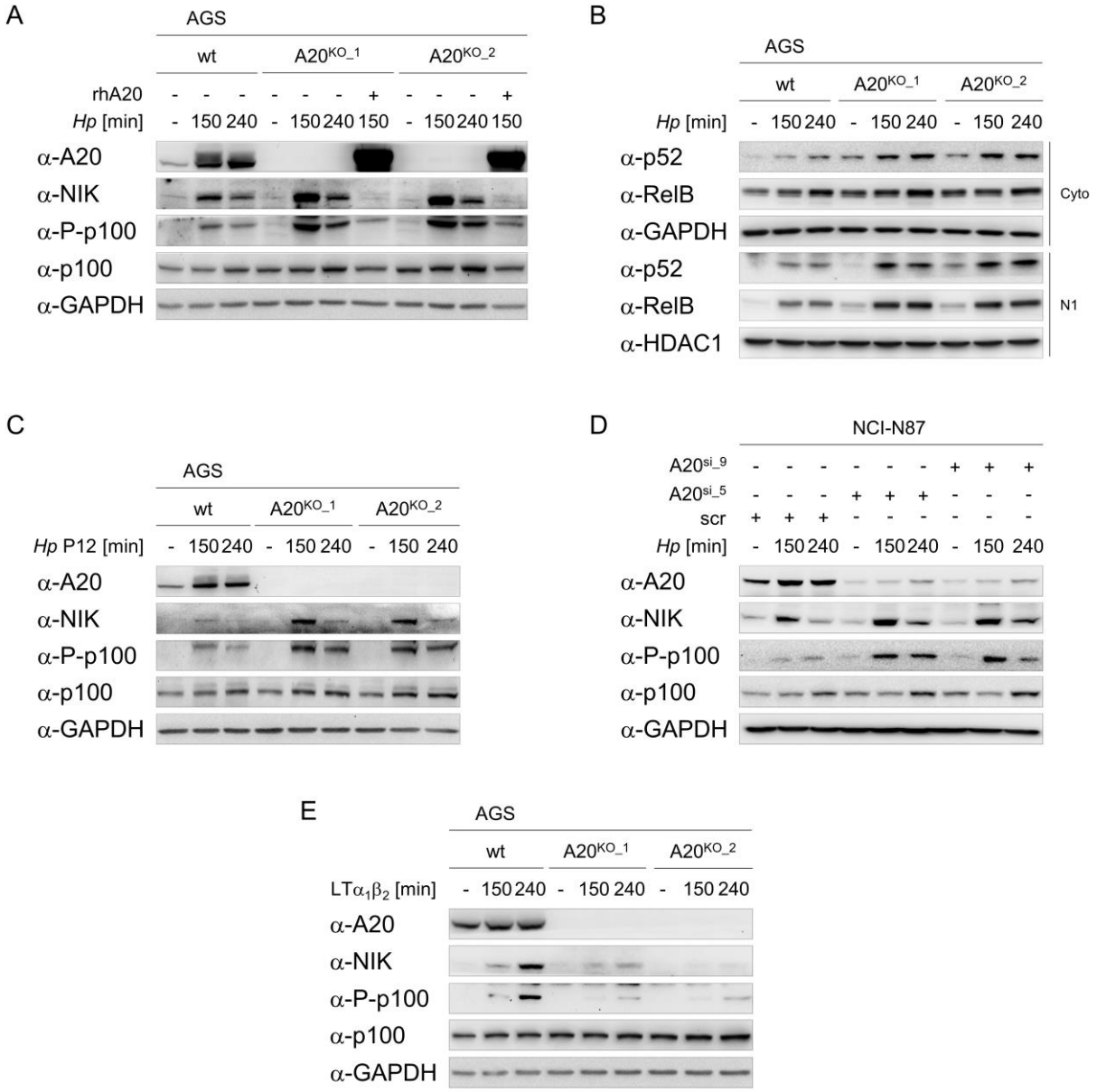

Figure 11. A20 is involved in the negative regulation of *H. pylori*-induced alternative NF-κB activation.
(A) Parental (wt), A20^{KO_1} and A20^{KO_2} AGS cells were infected with *H. pylori*. A20^{KO_1} and A20^{KO_2} cells were transfected with 1 μg recombinant human A20 (rhA20) protein for 24 h prior to *H. pylori* infection.
(B) wt, A20^{KO_1} and A20^{KO_2} AGS cells were infected with *H. pylori*. Cytosolic extracts (Cyto) and soluble nuclear (N1) fractions were prepared.
(C) wt, A20^{KO_1} and A20^{KO_2} AGS cells were infected with *H. pylori* P12 wt strain.
(D) NCI-N87 cells were transfected with non-target-specific siRNA (scr) or siRNAs targeting A20 (A20^{si_5} or A20^{si_9}) for 48 h prior to infection with *H. pylori*.
(E) wt, A20^{KO_1} and A20^{KO_2} AGS cells were treated with 30 ng/ml LTα$_1$β$_2$.
The *H. pylori* P1 wt strain was used for infection (A, B and D). Total cell lysates (A, C, D and E) or cyto and N1 fractions (B) were analysed for the indicated proteins by IB and GAPDH was used to show equivalent protein loading. HDAC1 was used to show equivalent protein loading in N1 fractions. The IBs shown in each panel are generated from the same experiment. Data are representative of at least two independent experiments.

3.1.3 A20 interacts with NIK regulatory complex-bound TIFA in *H. pylori* infection

We have recently shown that TIFA is crucial for *H. pylori*-induced alternative NF-κB activation. Specifically, the binding of TIFA to the NIK regulatory complex (TRAF3/TRAF2/cIAP1) supports the proteasome-dependent transient turnover of cIAP1 and the ensuing accumulation of NIK (Maubach et al., 2021). Thus, we asked whether A20 functions at this juncture in the alternative NF-κB signalling pathway. Intriguingly, in a TRAF2 immunoprecipitation (IP), we found at early time points after *H. pylori* infection a stronger association of TIFA with TRAF2 in A20^{KO} cells, which correlated with decreasing amounts of cIAP1 (Figure 12A). Notably, an inducible recruitment of TIFA and A20 into the TRAF2 immunoprecipitates was triggered upon *H. pylori* infection but not in response to LT$\alpha_1\beta_2$ treatment (Figure 12B). In addition, in TIFA-knockout cells, no A20 was co-immunoprecipitated with TRAF2 (Figure 12B). These observations are consistent with our previous findings that the association of TIFA with the NIK regulatory complex is specific for *H. pylori* infection (Maubach et al., 2021) and suggest that the interaction of A20 with the NIK regulatory complex depends on TIFA.

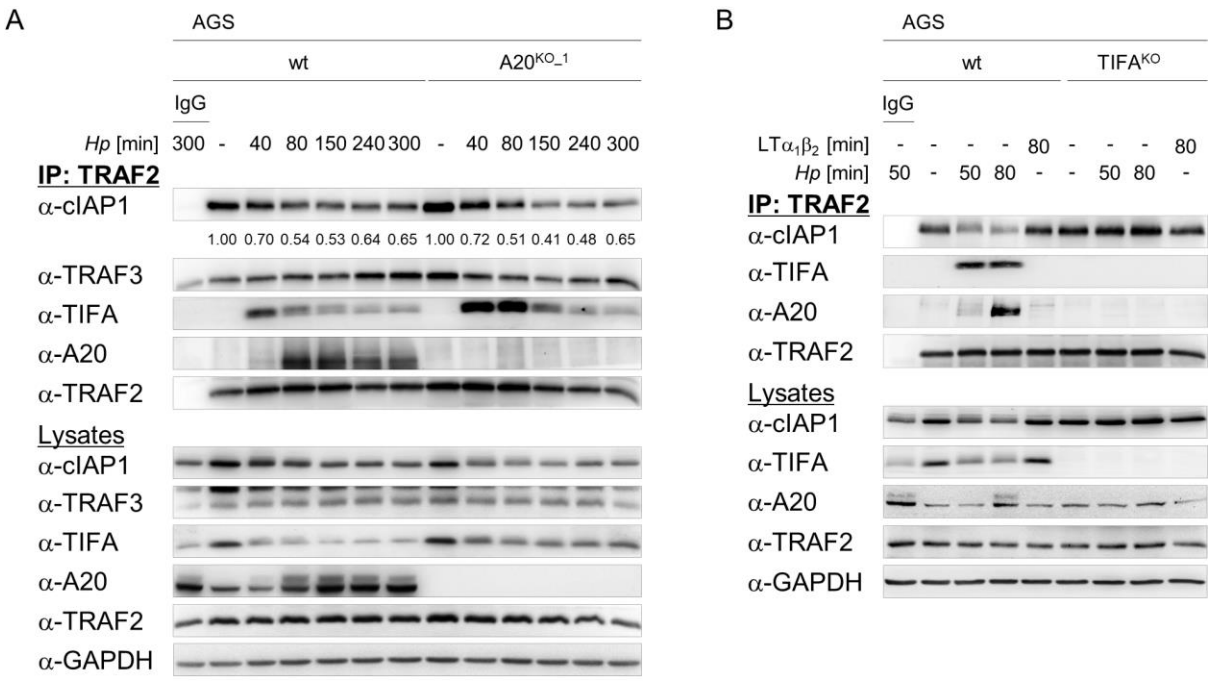

Figure 12. TIFA is required for the interaction of A20 with the NIK regulatory complex in *H. pylori* infection.
(A) Parental (wt) and A20^{KO}_1 AGS cells were infected with *H. pylori*. Total cell lysates were harvested and an IP was performed using an antibody against TRAF2 or isotype-matched IgG (IgG). The numbers indicate the band intensities of cIAP1 (normalised to the respective band intensities of TRAF2) of *H. pylori*-infected samples relative to uninfected control (set to 1).
(B) wt and TIFA^{KO} AGS cells were infected with *H. pylori* or treated with 30 ng/ml LT$\alpha_1\beta_2$. Total cell lysates were subjected to IP using an antibody against TRAF2 or isotype-matched IgG (IgG).
The IBs shown in each panel are generated from the same experiment. Data are representative of at least two independent experiments.

To narrow down the direct interaction partner of A20 in the NIK regulatory complex, we performed siRNA-mediated depletion of TRAF2, cIAP1 or TRAF3 followed by a TIFA IP. Strikingly, knockdown of TRAF2, cIAP1 or TRAF3 did not prevent the binding of A20 to TIFA in response to *H. pylori* infection (Figures 13A and 13B). When we incubated recombinant human A20 and TIFA proteins together *in vitro*, we could immunoprecipitate the A20 protein in a TIFA IP (Figure 13C) and vice versa (Figure 13D). These results led us to speculate that this interaction is of relevance to the function of A20 in the suppression of TIFA-dependent alternative NF-κB activity. To test this hypothesis, we infected $A20^{KO}$ cells and performed a TIFA IP. Immunoblot analyses of the TIFA-immunoprecipitates revealed the association of components of the NIK regulatory complex with TIFA (Figure 13E, lanes 2-4). However, when we incubated the IP samples (beads with TIFA-immunoprecipitates) with recombinant human A20 protein for one hour prior to immunoblot analyses of the TIFA-immunoprecipitates, we observed a reduction in the abundance of TIFA-associated cIAP1, TRAF2 and TRAF3 (Figure 13E, lanes 5-7). Thus, our results demonstrate that upon *H. pylori* infection, A20 binds to TIFA within the NIK regulatory complex that in turn leads to the displacement of TIFA.

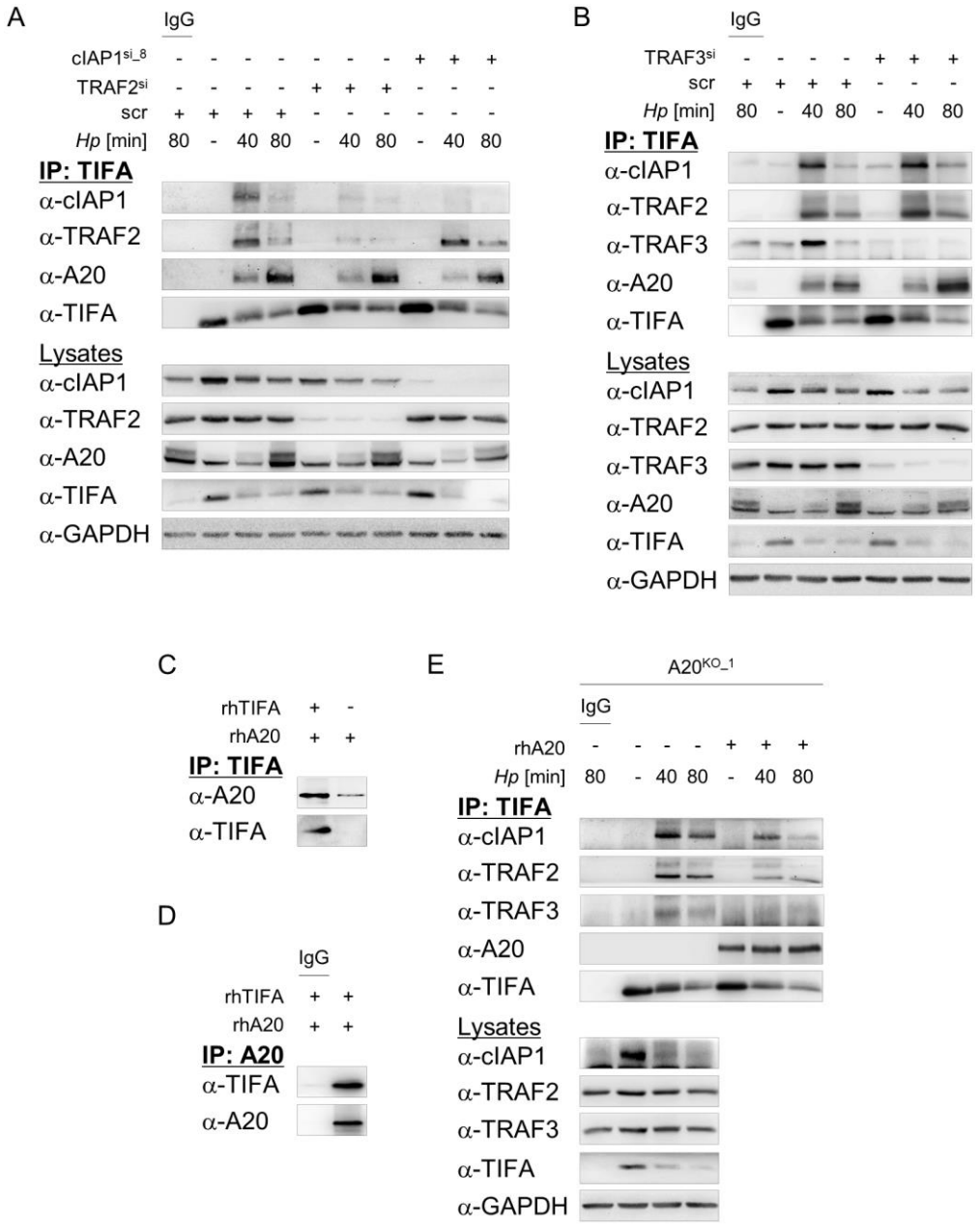

Figure 13. A20 interacts with NIK regulatory complex-bound TIFA in *H. pylori* infection.
(A) AGS cells were transfected with non-target-specific siRNA (scr) or siRNAs targeting TRAF2 ($TRAF2^{si}$) or cIAP1 ($cIAP1^{si\_8}$) for 48 h prior to infection with *H. pylori*. Total cell lysates were used for IP with an antibody against TIFA or isotype-matched IgG.
(B) AGS was transfected with non-target-specific siRNA (scr) or siRNAs targeting TRAF3 ($TRAF3^{si}$) for 48 h prior to infection with *H. pylori*. Total cell lysates were used for IP with an antibody against TIFA or isotype-matched IgG.
(C) Following incubation of recombinant human A20 and TIFA proteins *in vitro*, IP was performed using an antibody against TIFA.
(D) as in (C) but IP was performed using an antibody against A20 or isotype-matched IgG.
(E) $A20^{KO\_1}$ AGS cells were infected with *H. pylori* and IP was performed as in (A). IB analyses were performed with TIFA-immunoprecipitates without and with 1 h incubation with 100 ng recombinant human A20 protein prior to elution of immunoprecipitates.
The *H. pylori* P1 wt strain was used for infection (A, B and E). The IBs shown in each panel are generated from the same experiment. Data are representative of at least two independent experiments.

3.1.4 Alternative NF-κB signalling promotes the expression of anti-apoptotic genes during *H. pylori* infection

Classical and alternative NF-κB signalling regulate distinct as well as overlapping target genes involved in many cellular processes including cell survival (de Oliveira et al., 2016). To analyse the impact of *H. pylori*-induced alternative NF-κB on cell survival, we first carried out quantitative real-time PCR to analyse the transcription of anti-apoptotic genes, *BCL2L11* (BIM), *BCL2* (BCL-2), *BCL2A1* (BCL2A1), *CFLAR* (cFLIP), *BIRC2* (cIAP1), *BIRC3* (cIAP2) and *BIRC5* (survivin), known to be regulated by NF-κB. Infection by *H. pylori* led to a striking albeit transient up-regulation of *BIRC2*, *BIRC3* and *BCL2A1* (Figure 14A). In response to *H. pylori* infection, RelB-depleted cells showed a lower expression of these three genes, suggesting that they are regulated at least in part by alternative NF-κB (Figure 14B). Further, we examined whether the inhibitory effect of A20 on the alternative NF-κB pathway could have an impact on the expression of these three anti-apoptotic genes. Upon *H. pylori* infection, the up-regulation of *BIRC2*, *BIRC3* and *BCL2A1* was further increased in $A20^{KO}$ cells compared to wt cells (Figure 14B). This is most likely due to the missing inhibitory effect of A20 on not only the alternative but also the classical NF-κB signalling pathway. Importantly, RelB-depleted $A20^{KO}$ cells (compromised in alternative NF-κB) showed attenuated up-regulation of these anti-apoptotic genes compared to $A20^{KO}$ cells (Figure 14B). This diminished up-regulation represents the contribution of alternative NF-κB to the expression of these anti-apoptotic genes.

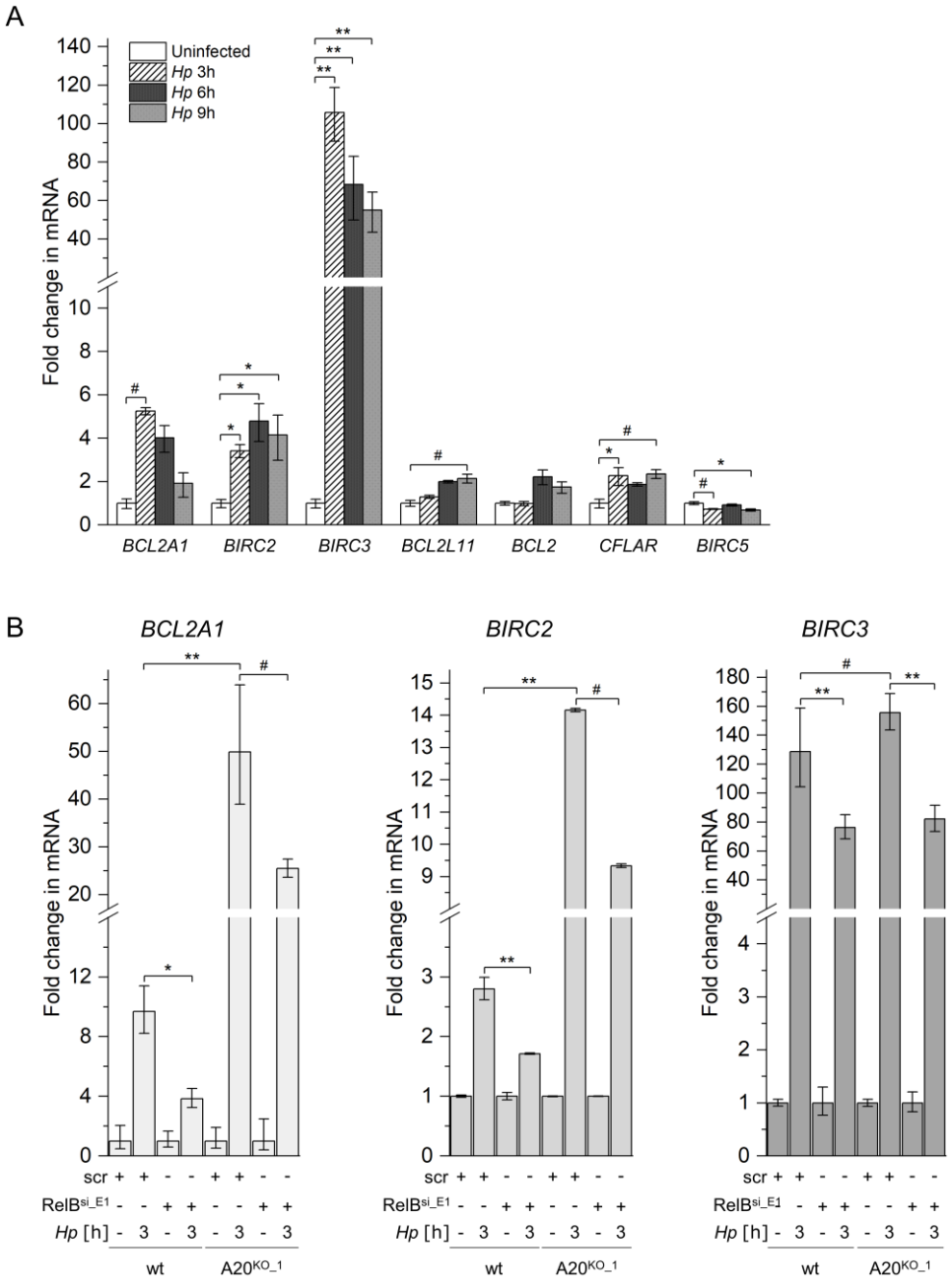

Figure 14. A20 inhibits specific alternative NF-κB-regulated anti-apoptotic genes in *H. pylori* infection.
(A) Total RNA was isolated after *H. pylori* infection of AGS cells. Changes in the expression of the indicated transcripts were analysed by quantitative real-time PCR.
(B) Parental (wt) and A20^{KO_1} AGS cells were transfected with non-target-specific siRNA (scr) or siRNA targeting RelB (RelB^{si_E1}) for 48 h prior to infection by *H. pylori* for 3 h. Total RNA was isolated and analysed by quantitative real-time PCR.
The *H. pylori* P1 wt strain was used for infection. Data are normalised to the *RPL13A* housekeeping gene and expressed as fold change in mRNA expression relative to uninfected cells. Triplicate determinations of each experiment was performed. Error bars denote means ± SD of at least two independent experiments. # $p < 0.05$, * $p < 0.01$ and ** $p < 0.001$.

We proceeded to determine apoptotic cell death by flow cytometric analysis of cells stained with annexin V-FITC and propidium iodide (PI). After *H. pylori* infection, we observed an increase in the percentage of apoptotic cells in control and RelB-depleted cells compared to their uninfected counterparts, 9.6 % to 20.2 % and 14.4 % to 27.0 %, respectively (Figure 15A), indicating that cells with reduced expression of RelB were even more sensitive to *H. pylori*-induced apoptosis. Taken together, our data imply that A20 undermines cell survival to a certain extent because of its inhibitory effect on alternative and classical NF-κB-dependent regulation of anti-apoptotic genes.

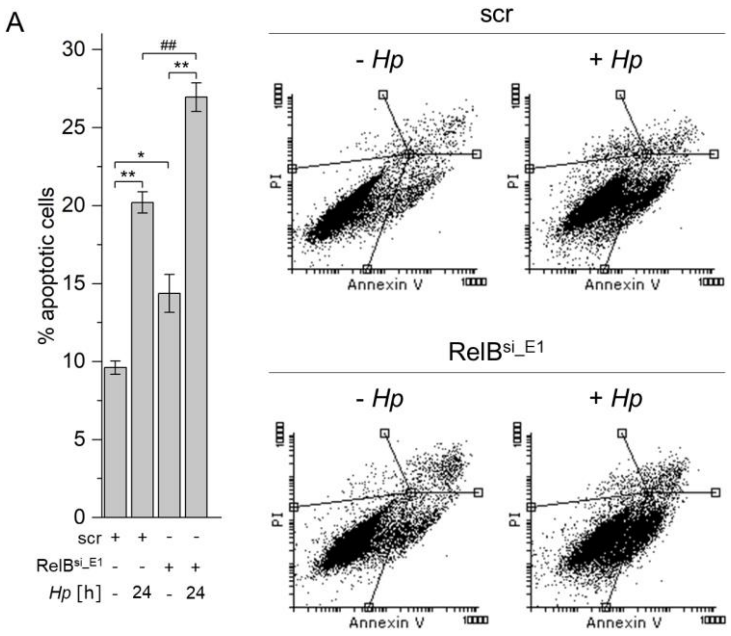

Figure 15. Alternative NF-κB signalling contributes to cell survival in *H. pylori* infection.
(A) AGS cells were transfected with non-target-specific siRNA (scr) or siRNA targeting RelB ($RelB^{si\_E1}$) for 48 h. After *H. pylori* infection for 24 h, cells were harvested and stained with annexin V-FITC/PI, followed by analysis using flow cytometry. A graph showing data from three independent experiments is depicted (means ± SD). ## $p < 0.005$, * $p < 0.01$ and ** $p < 0.001$. Representative dot plots are shown for each treatment.

3.1.5 Summary

In summary, we demonstrate that A20 participates in the negative regulation of alternative NF-κB signalling and expression of specific anti-apoptotic genes during *H. pylori* infection (Figure 16). Infection with *H. pylori* leads to NF-κB-dependent up-regulation of A20 expression. A20 interacts with TIFA within the TIFA/NIK regulatory complex, which in turn destabilises the interaction of TIFA with the complex. This restores the stability of cIAP1 in the complex and this TIFA-free NIK regulatory complex recovers the ability to mediate the proteasomal degradation of NIK, leading to the shutdown of alternative NF-κB signalling.

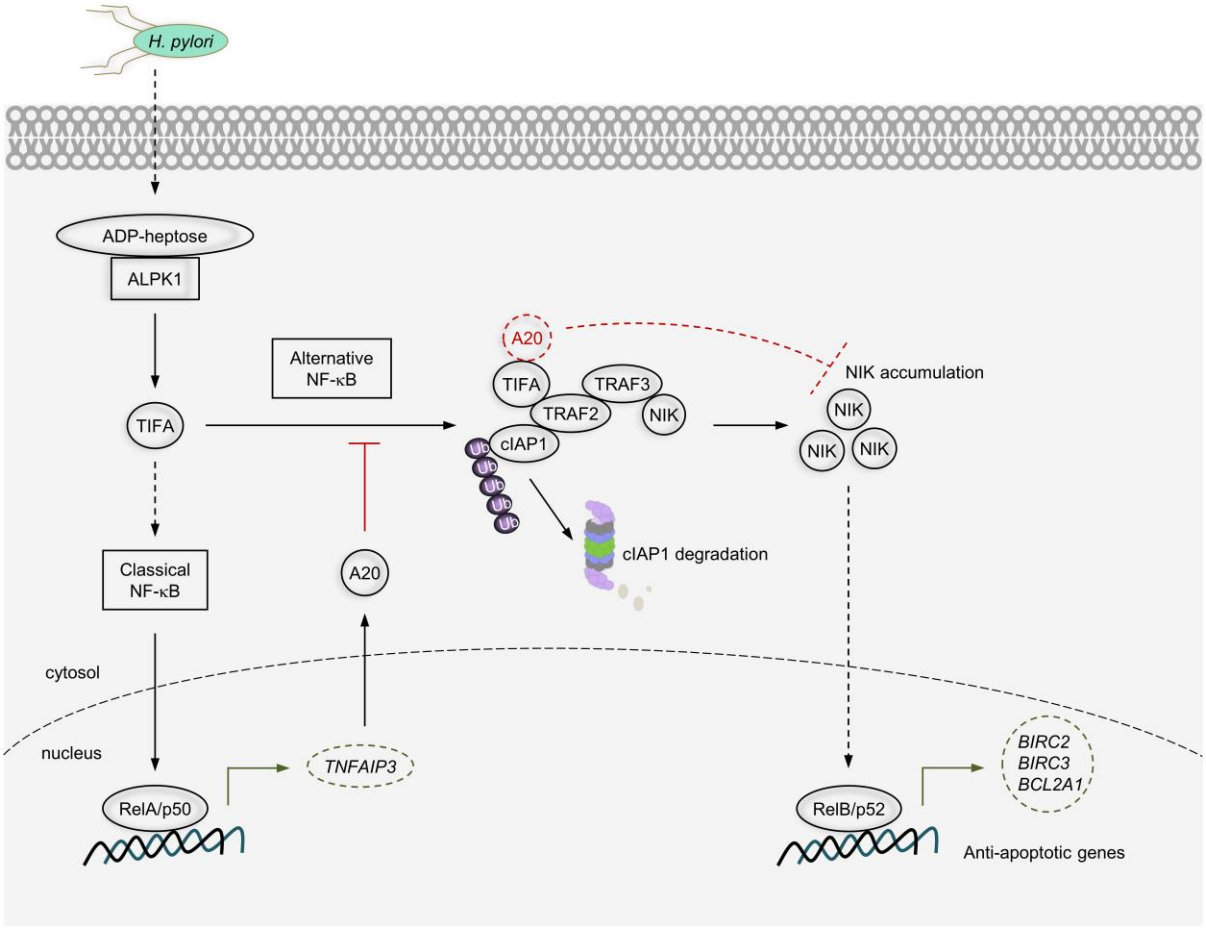

Figure 16. A proposed model for the role of A20 in the negative regulation of alternative NF-κB activation in *H. pylori* infection.

3.2 Function of A20 in *H. pylori*-induced caspase-8-dependent apoptotic cell death in gastric epithelial cells

3.2.1 *H. pylori* triggers the processing of caspases-8 and -3 leading to apoptotic cell death

In AGS cells, infection by *H. pylori* and treatment with CD95L triggered the processing of caspases-8 and -3, contrary to TNF, IL-1β and $LT\alpha_1\beta_2$ stimulations (Figure 17A), as indicated by the detection of active (cleaved) caspases-8 and -3. In another gastric carcinoma epithelial cell line MKN-45, infection by *H. pylori* also triggered the processing of caspases-8 and -3 (Figure 17B). Further, we examined apoptotic cell death using annexin V-FITC/PI staining followed by flow cytometric analysis. Herein, we showed that *H. pylori* infection induces apoptotic cell death of AGS as well as MKN-45 cells, thus excluding cell line-specific effects (Figure 17C).

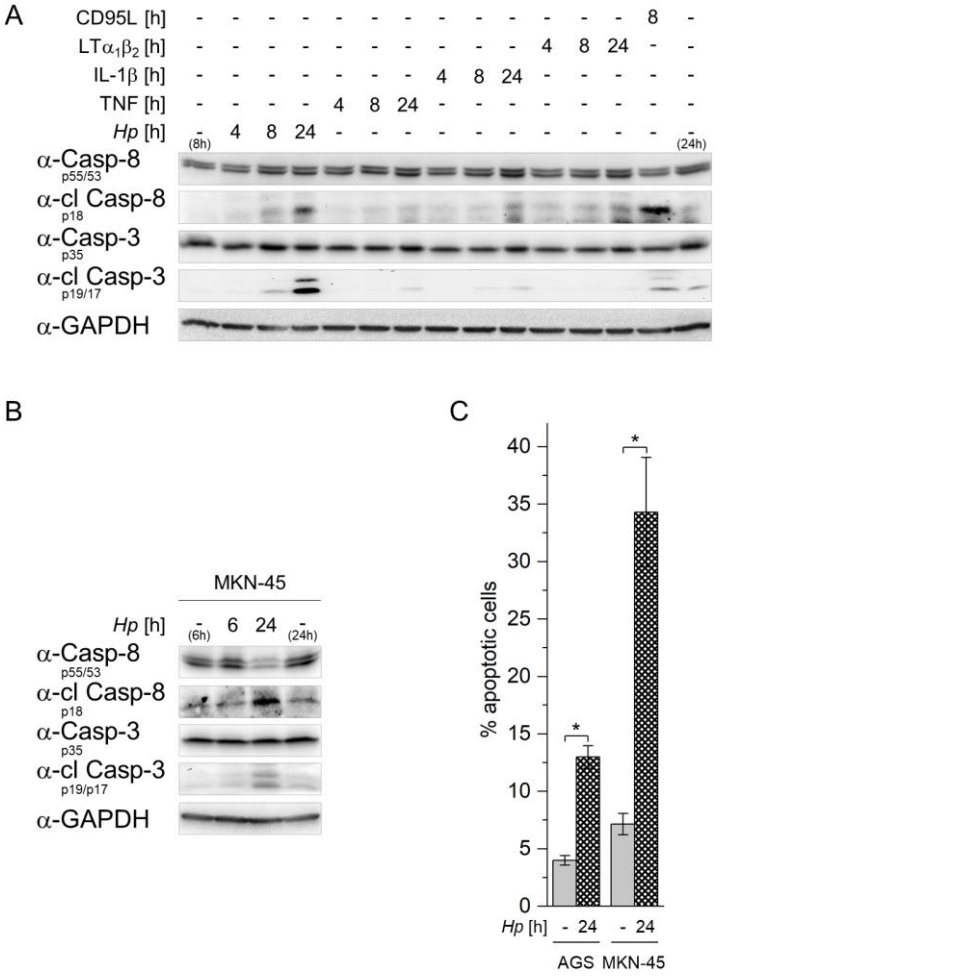

Figure 17. *H. pylori* infection induces apoptotic cell death of gastric epithelial cells.
(A) AGS cells were infected with *H. pylori* or treated with 10 ng/ml TNF, 10 ng/ml IL-1β, 20 ng/ml LTα1β2 or 250 ng/ml CD95L.
(B) MKN-45 cells were infected with *H. pylori*.
(C) AGS or MKN-45 cells were infected with *H. pylori* for 24 h and analysed by imaging flow cytometry after annexin V-FITC/PI staining. Percent apoptotic cells represents the sum of annexin V-FITC-positive and double positive (annexin V-FITC/PI) cells. The values are presented as means ± SD (n = three independent experiments), * $p < 0.005$.
The *H. pylori* P1 wt strain was used for infection. (A and B) Total cell lysates were analysed for the processing of caspases-8 and -3 by IB. GAPDH was used as protein loading control. The IBs shown in each panel are generated from the same experiment. Data are representative of at least two independent experiments.

3.2.2 A20 suppresses the processing of caspases-8 and -3 in *H. pylori* infection

A20 has been described to promote or impede apoptosis in a context-specific manner (Priem et al., 2020). Therefore, the impact of A20 on *H. pylori*-elicited processing of caspases-8 and -3 was investigated. Upon *H. pylori* infection, $A20^{KO}$ cells showed more prominent processing of caspases-8 and -3 compared to parental AGS cells (Figure 18A). When wt A20 was overexpressed in the $A20^{KO}$ cells, infection by *H. pylori* resulted in less cleaved caspases-8 and -3 (Figure 18B), strongly implying that, in part, A20 engages in the regulation of the processing of caspases-8 and -3 in *H. pylori* infection.

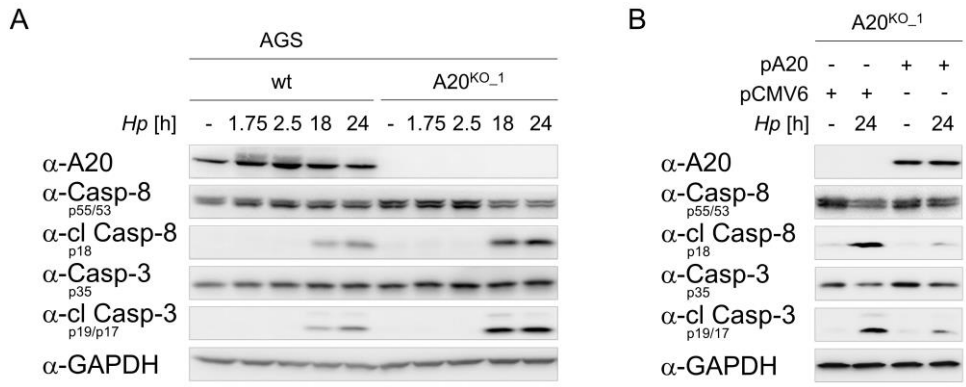

Figure 18. A20 impedes the processing of caspases-8 and -3 in *H. pylori* infection.
(A) Parental (wt) and A20^{KO_1} AGS cells were infected with *H. pylori*.
(B) A20^{KO_1} cells were transfected with either pCMV6 (as empty vector control) or wt A20 (pA20) plasmids 24 h prior to *H. pylori* infection for a further 24 h.
The *H. pylori* P1 wt strain was used for infection. Total cell lysates were analysed for the processing of caspases-8 and -3 by IB and GAPDH was used as protein loading control. The IBs shown in each panel are generated from the same experiment. Data are representative of at least two independent experiments.

3.2.3 A20 regulates the processing of caspase-8 in *H. pylori* infection

We next assessed whether A20 interferes with the activation of caspase-8 to regulate *H. pylori*-induced apoptotic signalling, as has been shown for TRAIL stimulation (Jin et al., 2009). First, we showed that addition of the caspase-8-specific inhibitor Z-IETD-FMK blocked the generation of cleaved caspases-8 and -3 in parental as well as A20^{KO} AGS cells upon *H. pylori* infection (Figure 19A), indicating that the activity of caspase-8 mediates *H. pylori*-induced processing of caspases-8 and -3. Accordingly, imaging flow cytometric analysis of cells stained with annexin V-FITC/PI showed a decrease in the percentage of apoptotic cells in parental (15 % to 9 % apoptotic cells) and A20^{KO} AGS cells (22 % to 10 % apoptotic cells) upon inhibition of the activity of caspase-8 (Figures 19B and 19C). Herein, Z-IETD-FMK had a stronger impact on the apoptotic cell death induced in A20^{KO} cells compared to parental AGS cells (parental 38% reduction versus A20^{KO} 52% reduction). Thus, our results implicate A20 in the negative regulation of the caspase-8-dependent apoptotic cell death in *H. pylori* infection.

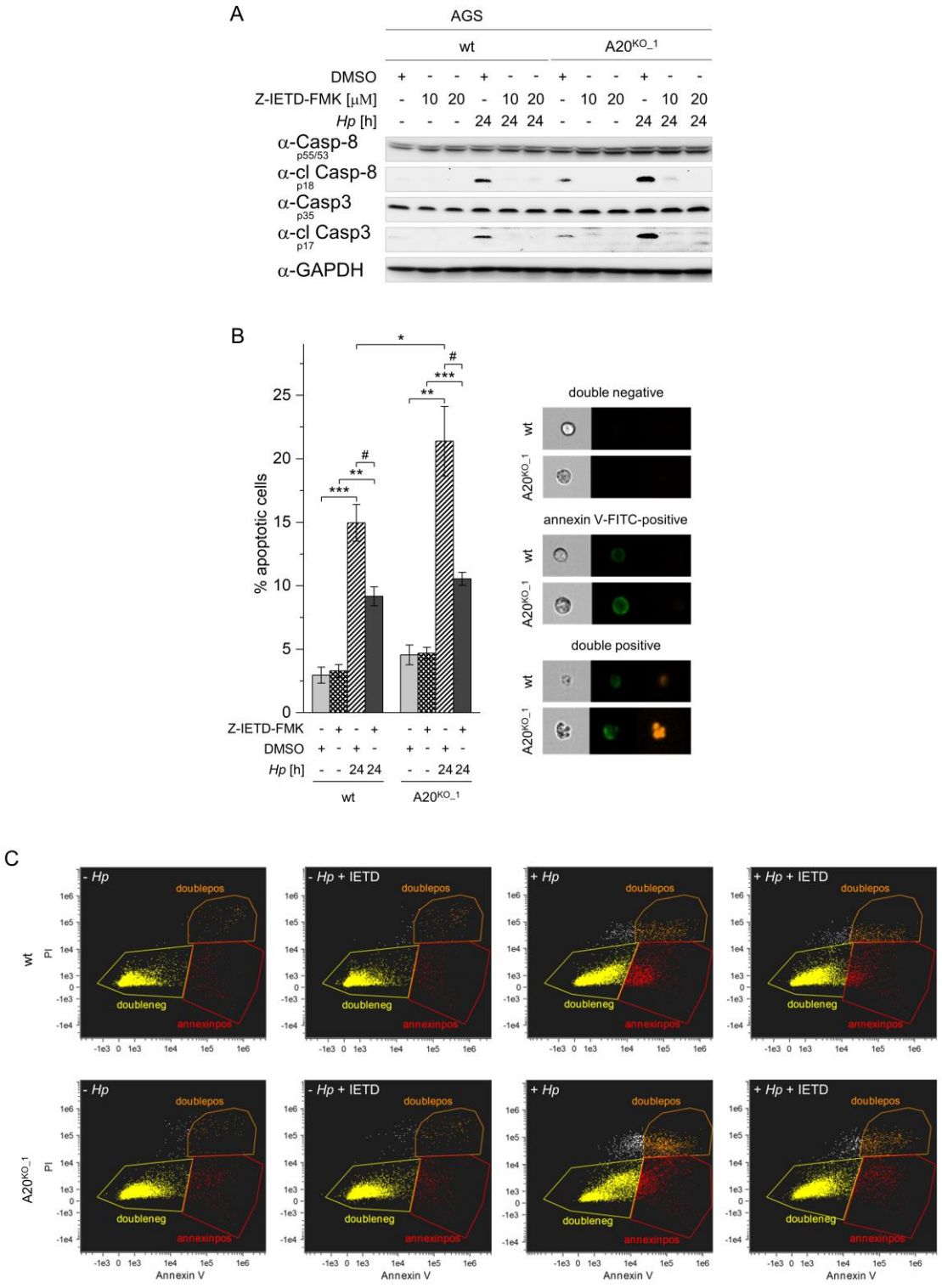

Figure 19. A20 negatively regulates caspase-8-dependent apoptotic cell death in *H. pylori* infection.
(A) Parental (wt) and A20^{KO_1} AGS cells were pre-treated with 10 μM or 20 μM Z-IETD-FMK for 15 min followed by infection with *H. pylori* P1 wt strain for 24 h. Cell lysates were analysed for the processing of caspases-8 and -3 by IB. GAPDH was used as protein loading control. The IBs shown in the panel are generated from the same experiment. Data are representative of at least two independent experiments.
(B) wt and A20^{KO_1} AGS cells were pre-treated with 20 μM Z-IETD-FMK for 15 min followed by infection with *H. pylori* P1 wt strain for 24 h. Cells were stained by annexin V-FITC and PI, followed by analysis using imaging flow cytometry. Percent apoptotic cells represents the sum of annexin V-FITC-positive and double positive (annexin V-FITC/PI) cells. The values are presented as means ± SD (n = three independent experiments), $^{\#}p < 0.01$, * $p < 0.05$, ** $p < 0.005$, *** $p < 0.0005$. Representative images for the cellular staining are shown.
(C) Representative dot plots for the cellular staining are shown.

3.2.4 Cul3-mediated polyubiquitinylation of caspase-8 supports its activation leading to apoptotic cell death in *H. pylori* infection

Recently, it was described that during extrinsic apoptotic signalling, the Cul3-based E3 ubiquitin ligase-mediated K63-linked polyubiquitinylation of caspase-8 supported its full activation and processing (Jin et al., 2009). In AGS cells infected with *H. pylori*, Cul3 IP revealed an interaction with caspase-8 (data not shown). To address the role of Cul3 in this context, AGS cells were depleted of Cul3 by means of siRNA transfection using two different siRNAs. For examining the ubiquitinylation status of endogenous caspase-8, a caspase-8 IP was performed using cell lysates harvested under denaturing conditions to exclude co-IP of associated ubiquitinylated protein. We observed that the K63-linked polyubiquitinylation of caspase-8 was absent in Cul3-depleted cells after *H. pylori* infection (Figures 20A and 20B). In addition, Cul3-knockdown cells were less apoptotic in comparison to control cells after *H. pylori* infection as assessed by imaging flow cytometry (Figure 20C). Our results suggest that Cul3 is involved in the K63-linked polyubiquitinylation of caspase-8, which is associated with the induction of apoptotic cell death by *H. pylori*.

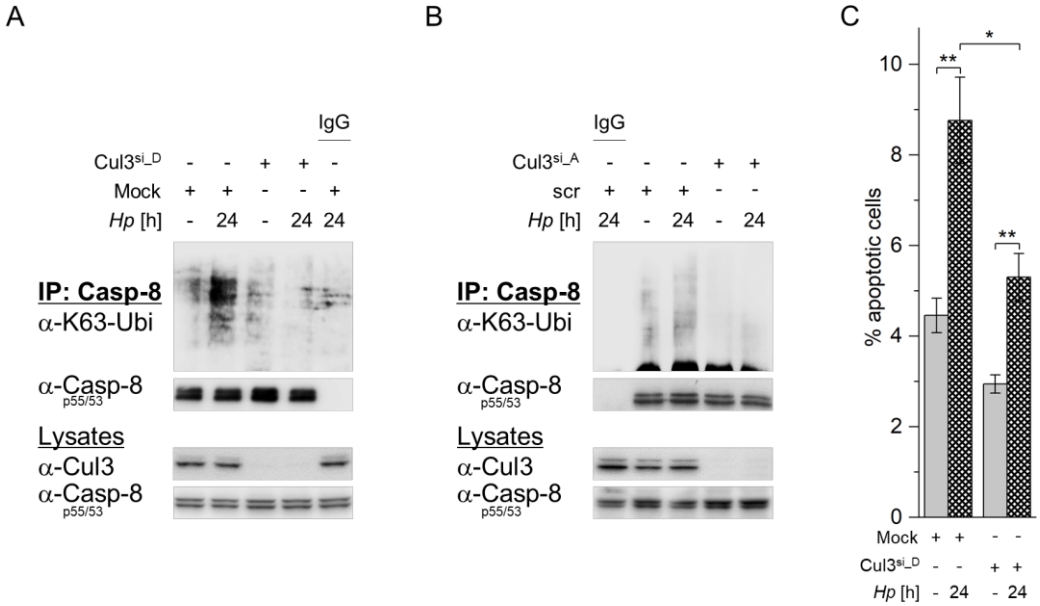

Figure 20. Cul3-mediated K63-linked polyubiquitinylation of caspase-8 is associated with the induction of apoptotic cell death by *H. pylori*.

(A) AGS cells were transfected with 20 nM siRNA targeted to Cul3 ($Cul3^{si\_D}$) or with transfection reagent only (Mock) for 48 h prior to infection with *H. pylori* for 24 h.

(B) AGS cells were transfected with 20 nM siRNA targeted to Cul3 ($Cul3^{si\_A}$) or non-target-specific siRNA (scr) for 48 h prior to infection with *H. pylori* for 24 h.

(C) AGS cells were transfected with 20 nM siRNA targeted to Cul3 ($Cul3^{si\_D}$) or with transfection reagent only (Mock) for 48 h prior to infection with *H. pylori* for 24 h. The impact of Cul3 depletion on apoptotic cell death was evaluated using annexin V-FITC/PI staining followed by imaging flow cytometry. Percent apoptotic cells represents the sum of annexin V-FITC-positive and double positive (annexin V-FITC/PI) cells. The values are presented as means ± SD (n = three independent experiments), * $p < 0.01$, ** $p < 0.005$.

The *H. pylori* P1 wt strain was used for infection. (A and B) Cell lysates were prepared under denaturing conditions and subjected to IP with a caspase-8 or isotype-matched (IgG) antibody. IB was performed to assess the K63-linked ubiquitinylation status of caspase-8. The IBs shown in individual panels are generated from the same experiment. Data are representative of at least two independent experiments.

3.2.5 The DUB activity of A20 counteracts efficient caspase-8 activation by removal of K63-linked polyubiquitin in *H. pylori* infection

As a start to explore the function of A20 in the regulation of caspase-8 activation in *H. pylori*-infected cells, a caspase-8 IP was performed showing an inducible interaction between A20 and caspase-8 upon *H. pylori* infection (Figure 21A).

In the presence of *H. pylori*, we observed an increase in the K63-linked polyubiquitinylation of endogenous caspase-8, an effect which was even more pronounced in $A20^{KO}$ cells (Figure 21B). Notably, the apparent decrease in the endogenous caspase-8 polyubiquitinylation from 9 h to 24 h post infection corresponded to an increase in the signal of cleaved caspase-8 (Figure 21B). This observation led us to hypothesise that the decrease in the signal of the K63-linked polyubiquitinylation detected is due to the processing of ubiquitinylated caspase-8 to its active fragment, thus reducing the pool of ubiquitinylated caspase-8. This hypothesis was supported when we detected an increase in the K63-linked polyubiquitinylation of caspase-8 in infected cells co-incubated with the caspase-8-specific inhibitor Z-IETD-FMK (Figure 21C). Collectively, these results indicate that A20 plays a role in regulating the deubiquitinylation of endogenous caspase-8 during *H. pylori* infection.

To test whether the DUB activity of A20 is involved in this process, we transiently transfected wt A20 (pA20) or A20 mutant defective in the DUB activity (pC103A) into $A20^{KO}$ cells followed by caspase-8 IP under denaturing conditions. Overexpression of the A20 mutant defective in the ZnF4 region that mediates substrate ubiquitinylation (pC624A/C627A) was also included in these experiments as a negative control. Infection with *H. pylori* led to a stark increase in the K63-linked polyubiquitinylation of caspase-8 in control $A20^{KO}$ cells (transfected with empty vector) as well as $A20^{KO}$ cells overexpressing the A20 DUB mutant (Figure 21D). On the other hand, only marginal polyubiquitinylation of caspase-8 was observed in $A20^{KO}$ cells reconstituted with the A20 ZnF4 mutant or wt A20 (Figure 21D). These results indicate that the DUB activity of A20 is important for the deubiquitinylation of caspase-8.

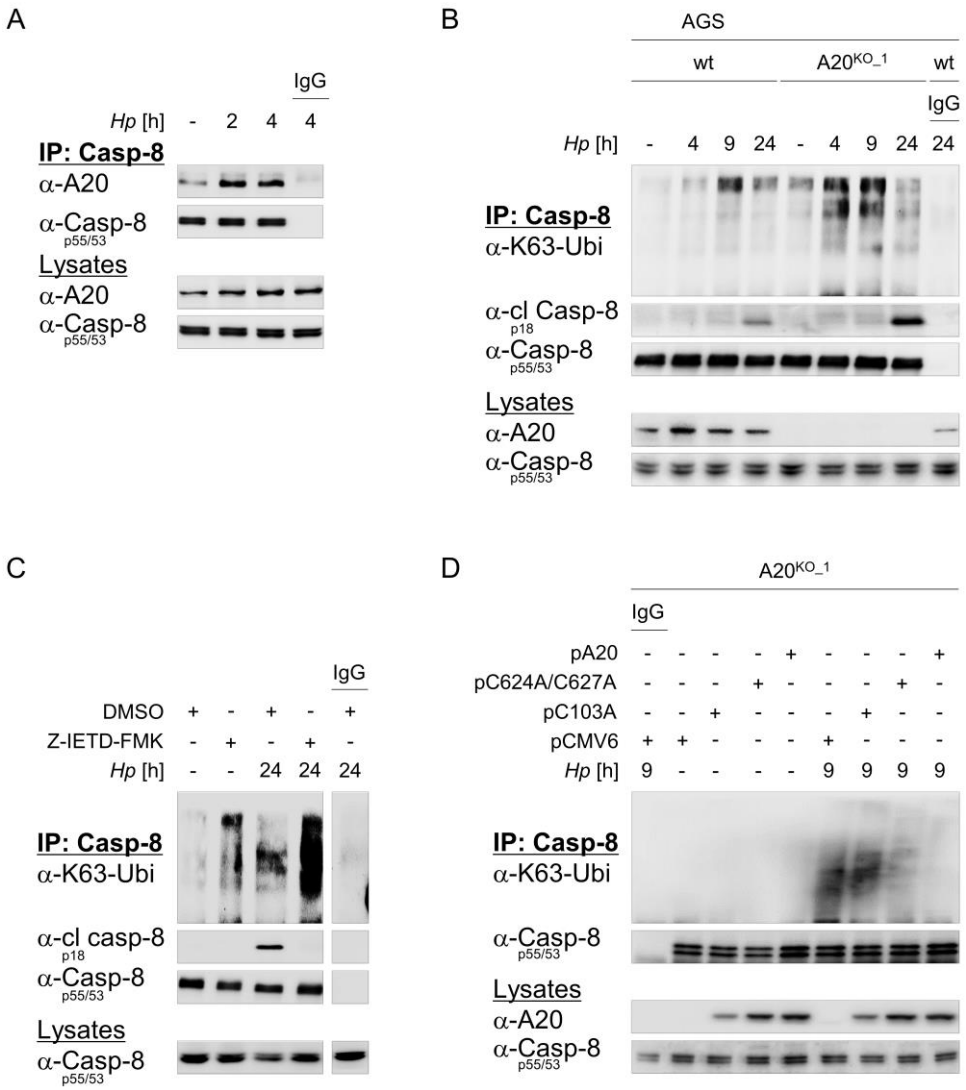

Figure 21. The DUB activity of A20 is important for the deubiquitinylation of caspase-8 in *H. pylor*i infection.
(A) AGS cells were infected with *H. pylori*. Cell lysates were used for IP with a caspase-8 or isotype-matched (IgG) antibody and analysed by IB for the indicated proteins.
(B) Parental (wt) and A20^{KO_1} AGS cells were infected with *H. py€i*.
(C) AGS cells were pre-treated with 10 μM Z-IETD-FMK for 15 min followed by *H. pylori* infection for 24 h.
(D) A20^{KO_1} cells were transfected with the following plasmids: pCMV6 (empty vector control); pC103A (A20 DUB mutant); pC624A/C627A (A20 mutant defective in the ZnF4 region that mediates substrate ubiquitinylation); or pA20 (wt A20) for 24 h prior to infection with *H. pylori*.
The *H. pylori* P1 wt strain was used for infection. Cell lysates were prepared under denaturing conditions and subjected to IP with a caspase-8 or isotype-matched (IgG) antibody, followed by analysis by IB for endogenous K63-linked polyubiquitin (B-D). The IBs shown in individual panels are generated from the same experiment. Data are representative of at least two independent experiments.

3.2.6 The scaffold protein p62 promotes the interaction between A20 and caspase-8 in *H. pylori* infection

The binding of accessory proteins to A20 helps it to achieve adequate ubiquitin-editing function towards the target proteins (Das et al., 2018). Therefore, to elucidate further the mechanism underlying the regulation of caspase-8 activation by A20, we investigated whether accessory proteins participate in this process. In this regard, we were interested in the p62 protein for two reasons. First, p62 has been described to be a ubiquitin-binding protein serving as a scaffold or molecular bridge (Geetha and Wooten, 2002). Second, in accordance with this described function, p62 was found to mediate the aggregation of ubiquitinylated caspase-8 (Jin et al., 2009). Infection by *H. pylori* led to the up-regulation of p62 (Figure 22A). In cells treated with an IKK inhibitor prior to *H. pylori* infection, however, the expression of p62 remained largely unchanged (Figure 22A). These results imply an NF-κB-dependent regulation of p62, in agreement with other reports (Ling et al., 2012; Song et al., 2017).

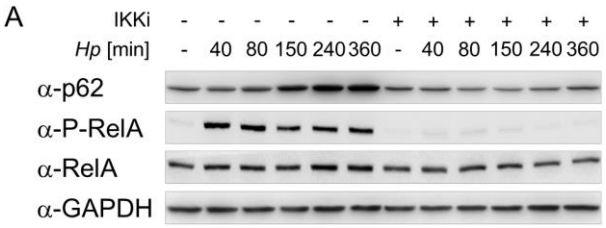

Figure 22. The expression of p62 is NF-κB-dependent in *H. pylori* infection.
(A) AGS cells were infected with *H. pylori* P1 wt strain for the indicated times in the absence of IKKi or after 30 min pre-incubation with 10 μM IKKi. IB was performed and GAPDH was used as a reference for protein loading. The IBs shown are generated from the same experiment. Data are representative of at least two independent experiments.

In the search for a possible link between p62, A20 and caspase-8, we performed first IP analyses of A20. An inducible interaction of both caspase-8 and p62 with A20 was observed after *H. pylori* infection (Figure 23A). Silencing of caspase-8 with two different siRNAs did not affect the interaction between p62 and A20 (Figures 23B and 23C). Next, we evaluated whether p62 is required for the interaction between A20 and caspase-8. For this purpose, IP analyses of caspase-8 were performed using AGS cells, which were transfected with p62-targeting siRNAs to reduce its expression. An inducible interaction of caspase-8 with both A20 and p62 was observed following infection with *H. pylori*, and the depletion of p62 diminishes the association of A20 with caspase-8 (Figures 23D and 23E). Altogether, these observations suggest that p62 functions as an adaptor protein between A20 and caspase-8.

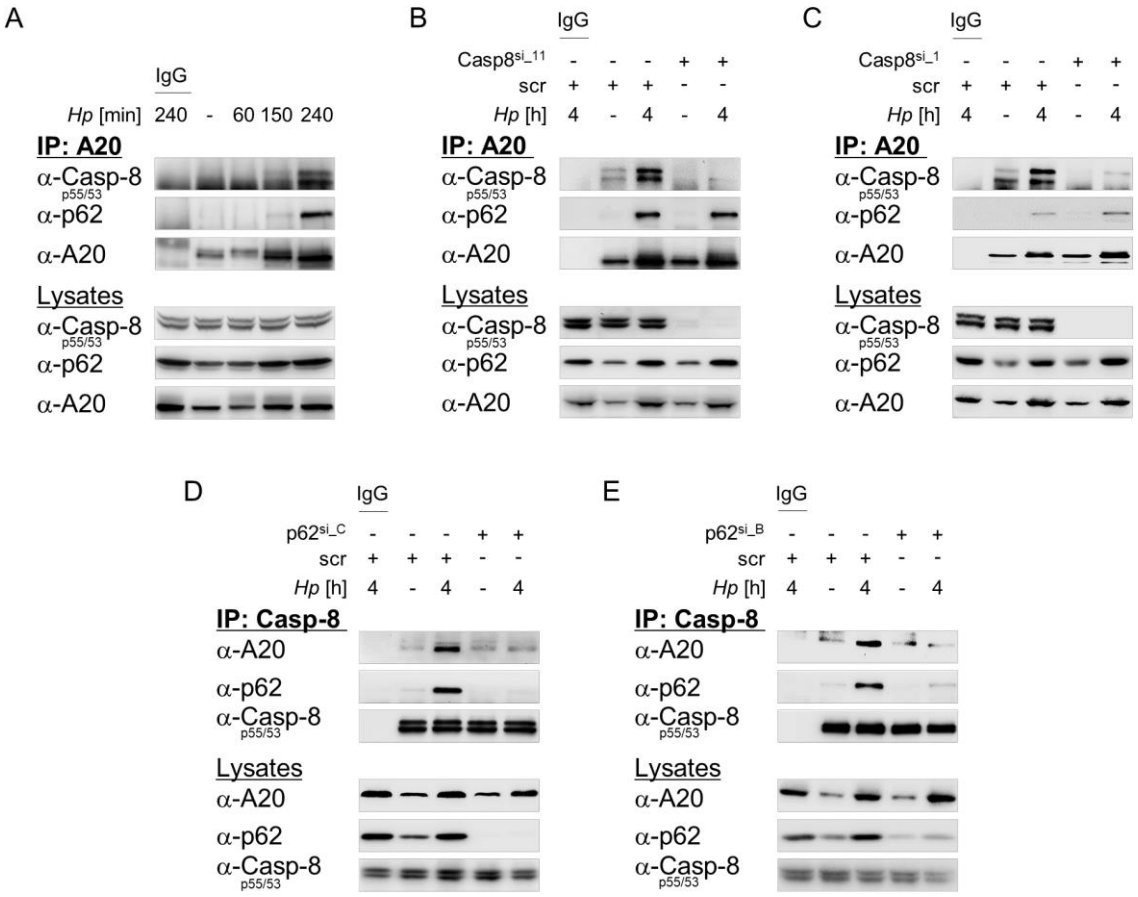

Figure 23. p62 promotes the interaction between A20 and caspase-8 in *H. pylori* infection.
(A) AGS cells were infected with *H. pylori* for 4 h. Cell lysates were used for IP with an A20 or isotype-matched (IgG) antibody and analysed by IB for the indicated proteins.
(B) AGS cells were transfected with 20 nM siRNA targeted to caspase-8 ($Casp8^{si\_11)}$) or 20 nM non-target-specific siRNA (scr) for 48 h prior to infection with *H. pylori*. Cell lysates were used for IP with an A20 or isotype-matched (IgG) antibody and analyse€y IB.
(C) AGS cells were transfected with 20 nM siRNA targeted to caspase-8 ($Casp8^{si\_1)}$) or 20 nM non-target-specific siRNA (scr) for 48 h prior to infection with *H. pylori*. Cell lysates were used for IP with an A20 or isotype-matched (IgG) antibody and analysed by IB.
(D) AGS cells were transfected with 10 nM siRNA targeted to p62 ($p62^{si\_C}$) or 10 nM non-target-specific siRNA (scr) for 48 h prior to infection with *H. pylori*. Cell lysates were used for IP with a caspase-8 or isotype-matched (IgG) antibody and anal€d by IB.
(E) AGS cells were transfected with 10 nM siRNA targeted to p62 ($p62^{si\_B}$) or 10 nM non-target-specific siRNA (scr) for 48 h prior to infection with *H. pylori*. Cell lysates were used for IP with a caspase-8 or isotype-matched (IgG) antibody and analysed by IB.
The *H. pylori* P1 wt strain was used for infection. The IBs shown in individual panels are generated from the same experiment. Data are representative of at least two independent experiments.

3.2.7 p62 supports the deubiquitinylation of caspase-8 by A20 in *H. pylori* infection

We further explored whether p62 would contribute to A20-mediated deubiquitinylation of caspase-8. Indeed, silencing of p62 led to a significant increase in the *H. pylori*-induced K63-linked ubiquitinylation of caspase-8 (Figures 24A and 24B). In line with this, the processing of caspases-8 and -3 was also greatly enhanced in p62-depleted cells infected with *H. pylori* (Figure 24C). Cumulatively, our observations suggest that p62 is important for the efficient interaction of A20 with caspase-8 to support the removal of K63-linked polyubiquitin from caspase-8 during *H. pylori* infection.

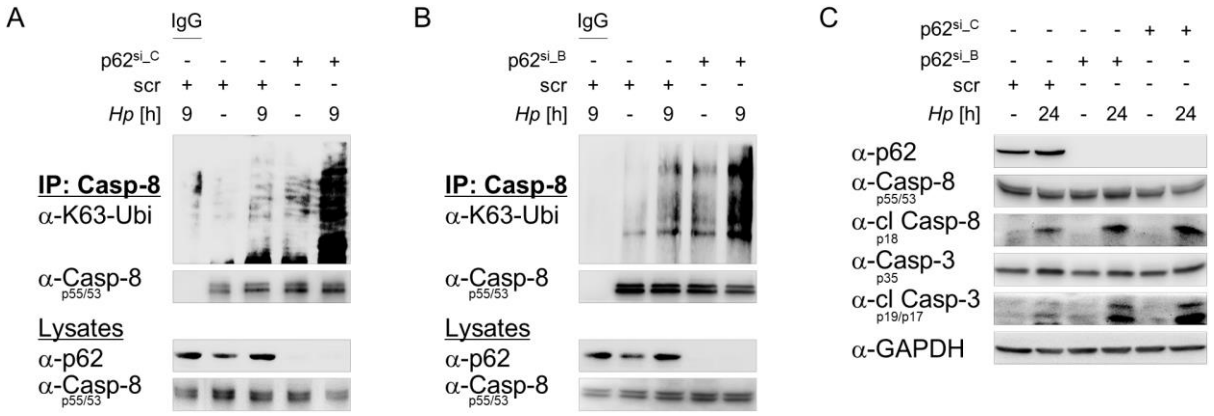

Figure 24. p62 supports the effective deubiquitinylation of caspase-8 leading to its attenuated processing in *H. pylori* infection.
(A) AGS cells were transfected with 10 nM siRNA targeted to p62 ($p62^{si\_C}$) or 10 nM non-target-specific siRNA (scr) for 48 h prior to infection with *H. pylori* for 9 h.
(B) AGS cells were transfected with 10 nM siRNA targeted to p62 ($p62^{si\_B}$) or 10 nM non-target-specific siRNA (scr) for 48 h prior to infection with *H. pylori* for 9 h.
(C) AGS cells were transfected with two different siRNAs targeted to p62 (10nM, $p62^{si\_B}$ or $p62^{si\_C}$) or 10 nM non-target-specific siRNA (scr) for 48 h prior to infection with *H. pylori* for 24 h. The effect of p62 depletion on the processing of caspases-8 and -3 was analysed by IB. The expression of GAPDH was used as a reference for protein loading.
The *H. pylori* P1 wt strain was used for infection. Cell lysates were prepared under denaturing conditions and subjected to IP with a caspase-8 or isotype-matched (IgG) antibody, followed by analysis by IB for endogenous K63-linked polyubiquitin (A and B). The IBs shown in individual panels are generated from the same experiment. Data are representative of at least two independent experiments.

3.2.8 Summary

In brief, we provide evidence that the NF-κB-regulated and *de novo* synthesised A20 participates in the negative regulation of caspase-8-dependent apoptotic cell death during *H. pylori* infection (Figure 25). The DUB activity of A20 counteracts the Cul3-mediated K63-linked ubiquitinylation of caspase-8, therefore restricting the activation of caspase-8. Infection with *H. pylori* also leads to the NF-κB-dependent up-regulation of p62, which ameliorates the interaction between A20 and caspase-8.

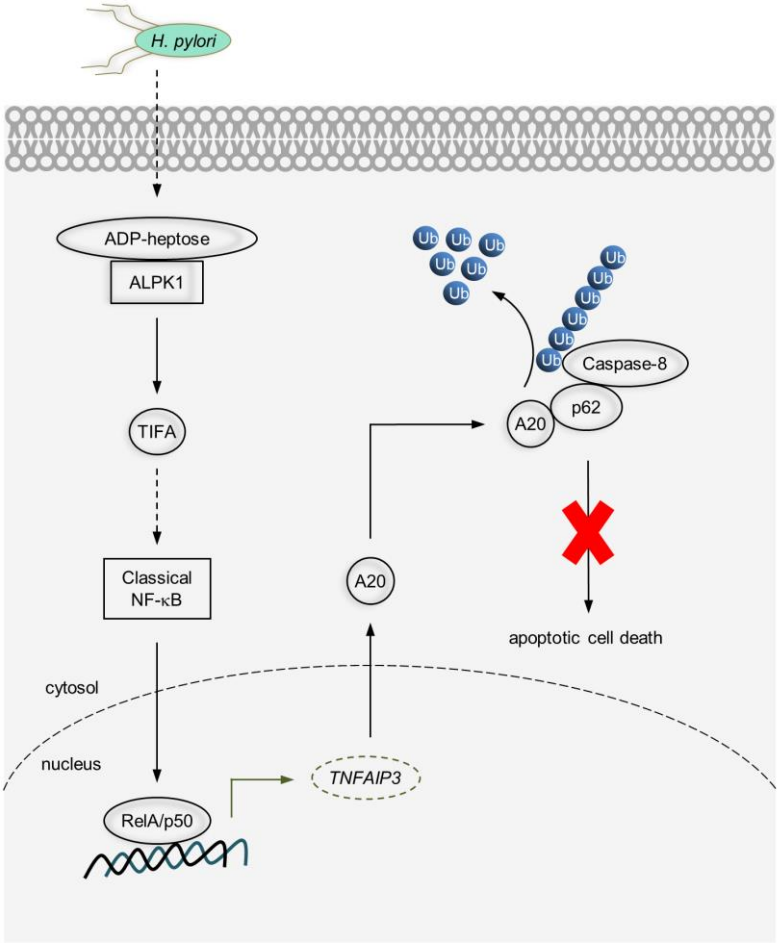

Figure 25. A proposed model for the role of A20 in the negative regulation of caspase-8-dependent apoptotic cell death in *H. pylori* infection.

4. Discussion

Based on our observations, we could envision a scenario where A20 controls the host innate response to *H. pylori* infection as follows. In *H. pylori* infection, A20 suppresses classical and alternative NF-κB-regulated anti-apoptotic genes, and thereby promotes apoptotic cell death. On the other side, A20 inhibits the activation of caspase-8, a process that is supported by the functional complex of caspase-8/p62/A20, thereby counteracting *H. pylori*-induced caspase-8-dependent apoptotic cell death.

Role of A20 in *H. pylori*-induced alternative NF-κB pathway

Our study implicates A20 in the negative regulation of alternative NF-κB activation during *H. pylori* infection. This is intriguing because it is contrary to an earlier study by Yamaguchi and colleagues (2013) which reported that A20 was involved, independent of its catalytic activities, in the activation of LTβR, Fn14, and RANK-mediated alternative NF-κB in mouse embryonic fibroblasts and a breast cancer epithelial cell line (MDA-MB-231) by treatments with 500 ng/ml $LT\alpha_1\beta_2$ or agonistic anti-LTβR antibody, 100 ng/ml tumour necrosis factor-like weak inducer of apoptosis and 100 ng/ml RANK ligand, respectively. These authors reported that in ligand – receptor-mediated activation of alternative NF-κB, the binding of A20 to cIAP1 results in the disruption of the interaction between TRAF2 and TRAF3. This in principle leads to the disintegration of the NIK regulatory complex so that NIK could accumulate and activate alternative NF-κB signalling. We are cautious in the interpretation of the data by Yamaguchi and colleagues (2013) due to some discrepancies in their observations. For instance, the direct binding of A20 to cIAP1 was shown by overexpressing A20 and cIAP1 proteins in HEK293T cells followed by an IP using tandem affinity purification-tagged NIK in the absence of any stimulus, suggesting that accumulation of A20 alone would already lead to alternative NF-κB activation. However, despite the high concentrations of ligands used (mentioned above), the authors did not consistently show the induction of A20 expression, although alternative NF-κB activation was triggered. At this point, it should be mentioned that in a previous publication, we have postulated an involvement of the LTβR in *H. pylori*-induced alternative NF-κB based on LTβR knockdown experiments and corroborated by data showing the recruitment of NIK to endogenous LTβR in co-IP experiments (Feige et al., 2018). However, the exact role of the LTβR in contributing to the activation of alternative NF-κB in *H. pylori* infection remains elusive. Here, an internalisation of the LTβR as described by Ganeff and colleagues (2011) could be a way where the receptor is involved. The cytoplasmic binding of TRAF2/3 to the internalised LTβR might contribute to the liberation of NIK from the NIK regulatory complex (Sanjo et al., 2010) after cIAP1 is unable to further ubiquitinylate NIK (Maubach et al., 2021). In the course of this study and our recent observations (Maubach et

al., 2021), we showed that involvement of the ADP-heptose – ALPK1 – TIFA signalling module is the feature that distinguishes the activation of alternative NF-κB in *H. pylori* infection from ligand – receptor-mediated signalling. Consistently, we show in the current study that A20 requires TIFA to fulfil its inhibitory function on *H. pylori*-induced alternative NF-κB signalling. Therefore, the *H. pylori*-dependent binding of TIFA to the NIK regulatory complex might mask the binding site of A20 on cIAP1, which in turn drives the response of NF-κB-induced A20 towards a different binding partner, and this could also explain the distinct functions of A20 reported here and by Yamaguchi *et al*. (2013).

Considering the studies showing the binding of A20 to TRAF2 (Song et al., 1996) and the binding of TRAF2 to TIFA (Kanamori et al., 2002), we expected TRAF2 to be the adaptor molecule that brings together A20 and the TIFA – NIK regulatory complex. Surprisingly, our data indicated that TRAF2 is dispensable for this interaction. Instead, we have demonstrated *in vitro* that a direct interaction between A20 and TIFA is possible. The A20 proteins form dimers, which can self-associate to form higher-order oligomers (Lu et al., 2013). Since TIFA dimers also undergo self-oligomerisation (Weng et al., 2015), it is conceivable that under physiological conditions, A20 and TIFA proteins associate through oligomeric interactions. Also speculative would be that TIFA binds to A20 and induces the oligomerisation of A20, reminiscent of the inducible oligomerisation of TRAF6 upon binding to TIFA (Ea et al., 2004), that in turn expedite the displacement of the NIK regulatory complex from TIFA to halt alternative NF-κB activation.

Most knowledge of the alternative NF-κB pathway has been garnered in connection with lymphoid organogenesis and functions of other immune cells such as B cells and dendritic cells (Sun, 2012). However, receptors that trigger the alternative NF-κB pathway including LTβR, Fn14 and RANK are also expressed in non-immune cells such as fibroblasts, endothelial and epithelial cells (Lau et al., 2014; Madge et al., 2008; Mikami et al., 2014). Whether the alternative NF-κB pathway in non-immune cells has a function in cell survival has not been clearly investigated. Quantitative real-time PCR analyses revealed that alternative NF-κB activity contributes to up-regulation of the survival genes *BIRC2*, *BIRC3* and *BCL2A1* in gastric epithelial cells infected with *H. pylori*. Furthermore, we found a positive correlation between the absence of RelB and the increase in apoptotic epithelial cells upon *H. pylori* infection, suggesting that alternative NF-κB activity is pro-survival in gastric epithelial cells. Supporting this notion is an earlier study showing that LTβR-driven alternative NF-κB signalling has a protective role in intestinal epithelial cells by inducing the production of IL-23 to promote cell survival (Macho-Fernandez et al., 2015). The LTβR-dependent induction of the alternative NF-κB pathway in intestinal epithelial cells was also shown to lead to the recruitment of neutrophils via the secretion of C-X-C motif chemokine ligand 1 (CXCL1) and

CXCL2 (Wang et al., 2010). Therefore, it would be interesting to address the molecular cross-talk between the pro-survival function of alternative NF-κB and its other function in facilitating the recruitment of immune cells during *H. pylori* infection to extend our understanding of immunopathogenic responses.

Role of A20 in *H. pylori*-induced caspase-8-dependent apoptotic cell death

Our data also shed light on the role of NF-κB-induced A20 in limiting the activation of caspase-8, a protein that is directly involved in the induction of the apoptotic signalling pathway, during *H. pylori* infection. In addition to A20, previous studies have reported that cIAP2 as well as dopamine and cyclic adenosine monophosphate-regulated phosphoprotein (DARPP-32), both of which are up-regulated by NF-κB, also prevent apoptosis in *H. pylori* infection (Yanai et al., 2003; Zhu et al., 2017). These examples collectively imply that, besides using its own virulence factors to actively manipulate host signalling pathways to its own advantage (Sgouras et al., 2019), *H. pylori* could also benefit from the NF-κB-dependent up-regulation of anti-apoptotic proteins to establish successful colonisation.

Our findings show that the DUB activity of A20 is involved in the depolymerisation of the K63-linked polyubiquitin chains from caspase-8. This leads to a reduction in the processing of caspase-8 to its active form and subsequent apoptotic signalling. Conversely, an earlier published study suggested that in human T-cell leukaemia virus type I (HTLV-I)-infected T-cell lines, A20 inhibits cell death by interacting separately with caspase-8 and FADD, and thus blocks the activation of caspase-8 by preventing its recruitment to FADD (Saitoh et al., 2016). It is important to note that mechanistically, there are differences in the apoptosis induction between our model system and that of Saitoh and colleagues (2016). We infected gastric epithelial cells with *H. pylori* to trigger extrinsic apoptotic pathway, whereas in the report by Saitoh and colleagues (2016), the HTLV-I-infected T-cell lines they utilised underwent autonomous apoptosis upon depletion of A20. To the best of our knowledge, it has never been clearly shown how apoptosis could be induced in HTLV-I-infected T-cell lines. On the contrary, these cells are strongly resistant to pro-apoptotic stimuli (Hasegawa et al., 2005; Kishi et al., 1997), although there were studies suggesting that reactive oxygen species and NF-κB activity might be involved in the regulation of apoptosis in these cells (Mori et al., 2002; Takahashi et al., 2013).

Caspase-8 is the apical protease participating in the death receptor-mediated signal transduction cascade leading to apoptotic cell death. We showed caspase-8-mediated apoptosis in *H. pylori* infection. Herein, however, neither we nor existing studies have identified the death receptor(s) involved. In most cases, TNF induces caspase-8-mediated apoptosis when NF-κB-induced anti-apoptotic genes expression is down-regulated or when cIAP1/2 proteins are degraded (Wang et al., 2008). Both phenomena were also observed by us in

H. pylori-infected gastric epithelial cells. Therefore, we cannot rule out that TNFR1 might play a role by way of the NF-κB-induced up-regulation of TNF in a paracrine loop upon *H. pylori* infection, which is possible given that a robust increase in the TNF mRNA level was detected in *H. pylori*-infected gastric epithelial cells (Sakitani et al., 2012). As a side note, it should be mentioned that the induction of other apoptosis-associated ligands upon *H. pylori* infection (Martin et al., 2004) is also conceivable. In TNFR1 signalling, the ZnF7 ubiquitin-binding domain of A20 binds to the linear ubiquitin chains in the plasma membrane-bound complex I (comprising TNFR1, TRADD, RIPK1, TRAF2, and cIAP1), resulting in the stabilisation of this complex and inhibition of TNFR1-mediated cell death (Draber et al., 2015). For this reason, we cannot exclude a contribution of A20's ZnF7 domain in the regulation of apoptotic cell death during *H. pylori* infection.

An earlier study by Jin and colleagues (2009) showed that p62 promotes apoptotic cell death induction in TRAIL-stimulated cells by associating with ubiquitinylated caspase-8 to mediate its aggregation and subsequent effective processing to trigger the apoptotic pathway. They also implied that A20 binds directly to caspase-8 and reverses the ubiquitinylation of caspase-8, although the former has not been explicitly confirmed in their data (Jin et al., 2009). Our study does not rule out that p62 supports the effective processing and concomitant activation of caspase-8; it does, however, reveal that there is more than meets the eye to the role of p62. We showed that p62 protects against cell death induction upon *H. pylori* infection by functioning as an adaptor protein between caspase-8 and A20 to support the A20-dependent deubiquitinylation of K63-linked caspase-8. This idea is supported by reports from other groups showing the distinct feature of A20 to recruit adaptor molecules to fulfil its function (Parvatiyar et al., 2010; Shembade et al., 2009). Whether other A20's adaptor molecules like the A20-binding inhibitor of NF-κB activation proteins (Gao et al., 2011), which have been implicated in the regulation of cell survival (Kattah et al., 2018), are also involved during *H. pylori* infection remains to be elucidated. Together, our study and the study by Jin and colleagues (2009) emphasise that p62 could directly influence cell death signalling by regulating the activation of a key initiator caspase. However, depending on its mechanism of action that affects the balance between the ubiquitinylation and deubiquitinylation of caspase-8, p62 may exert paradoxical function in regulating apoptotic cell death induction in different model systems. Another point worth ruminating is, although TRAIL application has been reported to activate the NF-κB pathway (Varfolomeev et al., 2005), it would be interesting to see if this leads to the up-regulation of p62, as is the case in our *H. pylori* model. Perhaps protein abundance is one of the determinants of the function of p62.

In conclusion, our study highlights the complexity of the interplay between NF-κB and apoptosis in *H. pylori* infection due to the involvement of A20 that has distinct functions in the

regulation of each of these processes, with implications for the fate of the infected cells. Although cell death is undoubtedly an important component of host defence, it could also be viewed as a double-edge sword as is the case for *H. pylori* infection because while it is beneficial as a source of nutrients, disintegration of the host cells also diminishes the colonisation niche of the bacterium. Future studies that focus on elucidating how these opposing functions of A20 are regulated (spatiotemporal considerations and possible involvement of other participating molecules) could reveal ways to better appraise the benefits for *H. pylori* and broaden our understanding on how these might contribute to cellular transformation and gastric cancer. Conceptualising mathematical model(s) followed by subsequent experimental validations could provide the stepping stone to these studies, as exemplified in the recent study of the impact on NF-κB dynamics due to its regulation by A20 (Mothes et al., 2020). Moreover, investigations of other host factors that are also involved in both the NF-κB and apoptotic pathways, like TRAF2 and TRAF6, will be key to a comprehensive understanding of the elaborate picture that is the regulation of host responses towards *H. pylori* infection, which is a paradigm for persistent pathogen infections, and open windows of opportunity for intervention to contain the infection.

5. Materials and Methods

5.1 Materials

5.1.1 General lab consumables

The following laboratory consumables were used routinely: nitril gloves (B. Braun); sterile serological pipettes (1 ml, 25 ml and 50 ml, TPP); sterile serological pipettes (5 ml and 10 ml, Corning); non-sterile serological pipettes (10 ml, VWR); polypropylene tubes (15 ml and 50 ml, Greiner Bio-One); microtubes (0.75 ml, 1.5 ml and 2 ml, Sarstedt); PCR tubes (0.2 ml, Biozym Scientific); curvettes (1.6 ml, Sarstedt); pipette tips (10 µl, 200 µl and 1000 µl, Eppendorf); sterile filtered pipette tips (10 µl, 100 µl, 200 µl and 1000 µl, Sorenson Bioscience); sterile filtered pipette tips (20 µl, Biozym Scientific); gel loading tips (1-200 µl, Sorenson Bioscience); polyvinylidene fluoride (PVDF) membrane (0.45 µm, Millipore); Whatman filter papers (0.34 µm, GE Healthcare); cell scrapers (TPP); sterile filters (0.22 µm, Millipore); syringes (1 ml and 60 ml, B. Braun); and needles (26G x 1/2", B. Braun).

5.1.2 Materials for cell culture

Plastic materials used for cell culture were as follows: cell culture flasks (T175, T75 and T25, Greiner Bio-One); culture dishes (d = 100 mm and 60 mm, Greiner Bio-One); tissue culture plates (6-well and 96-well, Greiner Bio-One); and internally threaded cryotubes for storage of cells in liquid nitrogen (Carl Roth).

Table 1. Mediums and solutions for cell culture

Name	Company	Catalogue number
RPMI-1640 + glutamine	Gibco®	11875093
Opti-MEM™, GlutaMAX™		51985034
Fetal calf serum		10500064
Trypsin		25200072
Dulbecco's PBS with magnesium and calcium ($DPBS^{+/+}$)		14040091
Dulbecco's PBS without magnesium and calcium (DPBS)		14190094
Trypan blue stain 0.4 %	Invitrogen	T10282

Trypan blue was kept at room temperature. Fetal calf serum and trypsin were stored at -20°C. The rest were stored at 4°C.

5.1.2.1 Cell lines

Table 2. Overview of cell lines used

Name	Description	Ordering information
AGS	Human gastric epithelial adenocarcinoma cell line	ATCC, CRL-1739
MKN-45	Human gastric epithelial adenocarcinoma cell line	DSMZ, ACC 409
NCI-N87	Human gastric epithelial adenocarcinoma cell line	ATCC, CRL-5822
HKC-8	Human renal adenovirus 12-SV40-transformed epithelial cell line	RRID:CVCL Y910

5.1.3 Chemicals and reagents

The molecular formulas are given for chemicals that are components of buffers and solutions (Table 7) where applicable.

Table 3. List of chemicals and reagents

Name	Company	Catalogue number
2-mercaptoethanol	Sigma-Aldrich	63689
4-Aminobenzoic acid sodium salt	Sigma-Aldrich	A6928
4-(2-aminoethyl)benzenesulfonyl fluoride hydrochloride (AEBSF)	AppliChem	A1421.0001
Acrylamide 4K solution (30 %) mix 29:1	AppliChem	A0951.1000
Adenine	Sigma-Aldrich	A9795
Ammonium peroxodisulphate (APS)	AppliChem	A2941.0100
Bacto™ Proteose Peptone No. 3	BD Biosciences	211693
Blotting grade dry milk	Bio-Rad	1706404
b-Nicotinamide adenine dinucleotide hydrate	Sigma-Aldrich	N1511
Chemiluminescent HRP substrate	Millipore	WBKLS0500
Chloramphenicol	Sigma-Aldrich	C0378
Dextrose	Sigma-Aldrich	D9434
di-Potassium hydrogen phosphate anhydrous (K_2HPO_4)	Roth	P749.2
Effectene transfection reagent	Qiagen	301427
Ethylenediaminetetraacetic acid disodium salt dihydrate (EDTA)	Sigma-Aldrich	E5134
GC agar base	ThermoFisher Scientific	CM0367
Glycerol	Carl Roth	3783.1
Glycerol 2-phosphate disodium salt hydrate ($C_3H_7Na_2O_6P.xH_2O$)	Sigma-Aldrich	G9422
Glycine	AppliChem	A1067.5000
Guanine hydrochloride	Sigma-Aldrich	51030
Horse serum	Biowest	S0910-500
Hydrochloric acid 37 % (HCl)	Chemsolute	836.1000
IKK inhibitor VII	Calbiochem	401486
Iron (III) nitrate nonahydrate	Sigma-Aldrich	44949
L-arginine monohydrochloride	Sigma-Aldrich	A6969
L-cysteine hydrochloride monohydrate	Sigma-Aldrich	C6852
L-glutamine	Sigma-Aldrich	G9273
Magnesium chloride ($MgCl_2$)	Carl Roth	A537.1
Methanol	J.T. Baker	8045
MG-132	Selleckchem	S2619

Table 3. List of chemicals and reagents (continuation)

Name	Company	Catalogue number
NP-40 Alternative	Calbiochem	492016
Nystatin	Sigma-Aldrich	N6261
Pierce Protein A/G magnetic beads	Thermo Scientific	88803
Protease inhibitors mix	Roche	48047900
Protein marker for SDS-PAGE	New England BioLabs	7719 and 7712
Puromycin	Sigma-Aldrich	P8833
Sodium chloride (NaCl)	Carl Roth	3957.2
Sodium dodecyl sulfate (SDS)	AppliChem	A1112.1000
Sodium fluoride (NaF)	Sigma-Aldrich	S7920
Sodium hydroxide (NaOH)	Carl Roth	6771.1
Sodium molybdate (Na_2MoO_4)	Sigma-Aldrich	331058
Sodium orthovanadate (Na_3VO_3)	Sigma-Aldrich	S6508
Sodium pyrophosphate decahydrate ($Na_4P_2O_7.10H_2O$)	Sigma-Aldrich	221368
Tetramethylethylenediamine (TEMED)	Carl Roth	2367.1
Thiamine hydrochloride	Sigma-Aldrich	T1270
Thiamine pyrophosphate	Sigma-Aldrich	C8754
Trimethoprim	Sigma-Aldrich	T7883
Tris	Carl Roth	5429.2
Triton X-100	Sigma-Aldrich	X100
Tween® 20	Carl Roth	9127.2
Uracil	Sigma-Aldrich	U1128
Vancomycin	AppliChem	A1839.1000
Vitamin B12	Sigma-Aldrich	V2876
Z-IETD-FMK	Tonbo Biosciences	TNB-1004-M001

Table 4. Plasmids and recombinant proteins

Name	Company	Catalogue number
A20/TNFAIP3 Double Nickase Plasmid (h)	Santa Cruz Biotechnology	sc-400447-NIC
Control Double Nickase Plasmid	Santa Cruz Biotechnology	sc-437281
pCMV6-Entry Mammalian Expression Vector	OriGene	PS100001
Plasmid expressing FLAG-tagged A20	OriGene	RC221337
Recombinant human A20	BPS Bioscience	80408
Recombinant human TIFA	Novus Biologicals	NBP1-99103-50ug

Table 5. Recombinant cytokines

Name	Company	Catalogue number
Recombinant human CD95L	Enzo Life Sciences	ALX-522-020-C005
Recombinant human IL-1β	PeproTech	200-01B
Recombinant human $LT\alpha_1\beta_2$	R&D Systems	8884-LY-025
Recombinant human TNF	PeproTech	300-01A

Table 6. Kits

Name	Company	Catalogue number
Annexin-V Apoptosis Detection kit	MabTag	AnxF100PI
METAFECTENE® SI^+ kit	Biontex Laboratories	T100-1.0
jetPRIME kit	VWR	101000015
Lipofectamine® CRISPRMAX transfection reagent kit	Invitrogen	CMAX00015
NucleoSpin® RNAII kit	Macherey-Nagel	740955.250
Pierce™ BCA protein assay kit	ThermoFisher Scientific	23225
QuickChange II XL site-directed mutagenesis kit	Agilent	200521
RevertAid First Strand cDNA Synthesis kit	ThermoFisher Scientific	K1622
RT^2 First Strand kit	Qiagen	330404
SensiMix™ SYBR® Hi-ROX kit	Meridian Bioscience	QT605-05

5.1.4 Buffers and solutions

All buffers and solutions were constituted using Milli-Q grade water.

Table 7. List of buffers

Name	Components	Use
Lysis buffer (Modified RIPA) pH 7.5	50 mM Tris-HCl pH 7.5, 150 mM NaCl, 2 mM EDTA, 10 mM K_2HPO_4, 10 % Glycerol[2], 1 % Triton X-100[2], 0.5 % NP-40[2], 10 mM $Na_4P_2O_7.10H_2O$[4], Phosphatase inhibitors mix[1,4], Protease inhibitors mix[4]	Total cell lysate preparation
Buffer A pH 7.9	20 mM Tris-HCl pH 7.9, 10 mM NaCl, 1.5 mM $MgCl_2$, 10 mM K_2HPO_4, 10 % Glycerol[2], 10 mM $Na_4P_2O_7.10H_2O$ [4], Phosphatase inhibitors mix[1,4], Protease inhibitors mix[4]	Cytosolic fraction
Buffer C pH 7.9	20 mM Tris-HCl pH 7.5, 420 mM NaCl, 1.5 mM $MgCl_2$, 10 mM K_2HPO_4, 10 % Glycerol[2], 10 mM $Na_4P_2O_7.10H_2O$ [4], Phosphatase inhibitors mix[1,4], Protease inhibitors mix[4]	Soluble nuclear fraction, N1
IP buffer pH 7.5	50 mM Tris-HCl pH 7.5, 150 mM NaCl, 1 mM $MgCl_2$, 10 mM K_2HPO_4, 1 % Triton X-100[2], 10 mM $Na_4P_2O_7.10H_2O$ [4], Phosphatase inhibitors mix[1,4], Protease inhibitors mix[4]	Total cell lysate preparation for IP
Denaturing IP buffer pH 7.5	30 mM Tris-HCl pH 7.5, 150 mM NaCl, 1 mM $MgCl_2$, 1 mM $CaCl_2$, 10 mM K_2HPO_4, 1 % Triton X-100[2], 1 % SDS[3], 10 mM $Na_4P_2O_7.10H_2O$ [4], Phosphatase inhibitors mix[1,4], Protease inhibitors mix[4]	Total cell lysate preparation for denaturing IP
Resolving gel buffer (4X) pH 8.8	1.5 M Tris-HCl pH 8.8, 0.04 % SDS[3]	SDS-PAGE
Stacking gel buffer (4X) pH 6.8	0.5 M Tris-HCl pH 6.8, 0.04 % SDS[3]	SDS-PAGE
Reducing sample buffer (5X) pH 6.8	250 mM Tris-HCl pH 6.8, 10 % SDS[3], 25 % Glycerol[2], 0.1 % bromophenol blue[3], 10 % mercaptoethanol[2,4]	SDS-PAGE
Electrophoresis buffer	25 mM Tris, 192 mM Glycine, 0.1 % SDS[3]	SDS-PAGE
Transfer buffer	25 mM Tris, 192 mM Glycine, 10 % Methanol[2,4]	IB
Washing buffer (TBS-T) pH 7.4	20 mM Tris, 137 mM NaCl, 0.1 % Tween 20[2,4]	IB

[1] Phosphatase inhibitors mix consists of 1 mM AEBSF, 20 mM $C_3H_7Na_2O_6P.xH_2O$, 20 mM NaF, 1 mM Na_2MoO_4, 1 mM Na_3VO_3. Each phosphatase inhibitor was stored as stock solution at -20 °C. Concentrations shown reflect final concentration in the buffer used.
[2] (v/v). [3] (w/v). [4] added directly before use.

Table 8. Solutions for preparing polyacrylamide resolving and stacking gels

Components	Resolving gels			Stacking gel
	6 %	10 %	15 %	3 %
Milli-Q grade water (ml)	5.29	3.96	2.29	6.29
4X Resolving gel buffer pH 8.8 (ml)	2.5	2.5	2.5	-
4X Stacking gel buffer pH 6.8 (ml)	-	-	-	2.5
10 % SDS (ml)	0.1	0.1	0.1	0.1
Acrylamide 4K solution (30 %) mix 29:1 (ml)	2	3.33	5	1
10 % APS* (ml)	0.1	0.1	0.1	0.1
TEMED* (ml)	0.01	0.01	0.01	0.01
Total volume (ml)	10	10	10	10

The volume of solutions is enough for casting two and four 1 mm-thick resolving and stacking gels, respectively. 10-well or 15-well combs of 1 mm thickness were used.

*APS and TEMED were added last to the solution(s), mixed and poured immediately into the gel casting module.

5.1.5 Antibodies

Table 9. List of antibodies

Name	Host	Company	Catalogue Number	Dilution used
α-A20	Rabbit	Cell Signaling Technology	5630	1:1000[3,4]
α-A20	Mouse	Imgenex	IMG-161A	1:2000[5]
α-A20[1]	Mouse	Santa Cruz Biotechnology	sc-166692	1:1000
α-CagA	Mouse	Austral Biologicals	HPM-5001-5	1:1000
α-Caspase 3	Rabbit	Cell Signaling Technology	9662	1:2000
α-Caspase 8	Mouse	Cell Signaling Technology	9746	1:2000[3]
α-Caspase 8[2]	Goat	Santa Cruz Biotechnology	sc-6136	-
α-Caspase 8[2]	Mouse	Santa Cruz Biotechnology	sc-56070	-
α-cIAP1	Rabbit	Cell Signaling Technology	7065	1:2000[3]
α-Cleaved Caspase 3	Rabbit	Cell Signaling Technology	9661	1:2000
α-Cullin-3	Mouse	BD Biosciences	611848	1:2000
α-Flagellin	Mouse	Acris Antibodies	AM00865PU-N	1:500
α-GAPDH	Mouse	Millipore	MAB374	1:10000
α-HDAC1	Rabbit	Santa Cruz Biotechnology	sc-7872	1:1000
α-IKKα	Rabbit	Cell Signaling Technology	2682	1:1000[3]
α-IKKβ	Rabbit	Cell Signaling Technology	8943	1:1000[3]
α-IKKγ, NEMO	Mouse	Santa Cruz Biotechnology	sc-8032	1:1000
α-IκBα	Rabbit	Cell Signaling Technology	4812	1:1000[3]
α-Lys63-Ubiquitin	Mouse	BioLegend	932202	1:1000
α-Lys63-Ubiquitin	Rabbit	Millipore	05-1308	1:1000
α-NIK	Rabbit	Cell Signaling Technology	4994	1:3000[3]
α-NF-κB p65	Mouse	Santa Cruz Biotechnology	sc-8008	1:1000
α-NF-κB2 p100/52	Rabbit	Cell Signaling Technology	4882	1:1000[3]

For IB, antibodies were diluted in 5 % (w/v) blotting grade dry milk in TBS-T unless otherwise stated.
[1] also used for IP. [2] for IP only. [3] diluted in 5 % (w/v) BSA in TBS-T. [4] used for analysis in IB after TRAF2 IP.
[5] used for analysis in IB after A20 IP.

Table 9. List of antibodies (continuation)

Name	Host	Company	Catalogue Number	Dilution used
α-p62	Mouse	MBL	M162-3	1:2000
α-Phospho-IκBα (Ser32/36)	Rabbit	Cell Signaling Technology	9246	1:2000
α-Phospho-IKKα/β (Ser176/180)	Rabbit	Cell Signaling Technology	2697	1:1000[3]
α-Phospho-NF-κB, P-p65 (Ser536)	Rabbit	Cell Signaling Technology	3031	1:2000[3]
α-Phospho-NF-κB2, P-p100 (Ser866/870)	Rabbit	Cell Signaling Technology	4810	1:1000[3]
α-RelA	Mouse	Santa Cruz Biotechnology	sc-81622	1:1000
α-RelB	Rabbit	Santa Cruz Biotechnology	sc-226	1:2000
α-TIFA	Rabbit	Cell Signaling Technology	61358	1:1000[3]
α-TRAF2[1]	Mouse	Santa Cruz Biotechnology	sc-876	1:1000
α-TRAF3	Rabbit	Cell Signaling Technology	4729	1:1000[3]
α-TRAF3[1]	Rabbit	Invitrogen	700121	1:5000

For IB, antibodies were diluted in 5 % (w/v) blotting grade dry milk in TBS-T unless otherwise stated.
[1] also used for IP. [2] for IP only. [3] diluted in 5 % (w/v) BSA in TBS-T. [4] used for analysis in IB after TRAF2 IP. [5] used for analysis in IB after A20 IP.

Table 10. HRP-conjugated secondary antibodies for IB

Name	Company	Catalogue Number
α-mouse IgG ($F(ab')_2$ fragment)-HRP	Jackson ImmunoResearch Laboratories Inc.	715-036-151
α-mouse IgG (light chain-specific)-HRP		115-035-174
α-rabbit IgG ($F(ab')_2$ fragment)-HRP		711-036-152
α-rabbit IgG (light chain-specific)-HRP		211-032-171

All antibodies were used at a dilution of 1:6000 in 5 % (w/v) blotting grade dry milk in TBS-T.

Table 11. Isotype-specific antibodies for IgG control in IP

Name	Company	Catalogue Number
α-mouse IgG	Millipore	12-371
α-rabbit IgG		12-370

5.1.6 siRNAs

Table 12. Commercially purchased siRNAs

Name	Final concentration used	Company	Catalogue number
AllStars negative control siRNA	Equimolar to specific siRNA used in the same experiment	Qiagen	SI03650318
$A20^{si\_5}$	40 nM	Dharmacon	J-009919-05-0005
$A20^{si\_9}$	40 nM	Qiagen	SI05018601
$Casp8^{si\_11}$	20 nM	Qiagen	SI02661946
$cIAP1^{si\_8}$	30 nM	Qiagen	SI02654442
TRAF2	30 nM	Santa Cruz Biotechnology	sc-29509
TRAF3	30 nM	Santa Cruz Biotechnology	sc-29510

Table 13. Customised siRNAs

Name	Final concentration used	Sequence (5'→3')	Reference
$Casp8^{si\_1}$	20 nM	GGAGCUGCUCUUCCGAAUU	Afshar et al., 2006
$Cul3^{si\_A}$	20 nM	GAGAAGAUGUACUAAAUUCdTdT	Maddika and Chen, 2009
$Cul3^{si\_D}$	20 nM	GAGAUCAAGUUGUACGUUAdTdT	Maddika and Chen, 2009
$p62^{si\_B}$	10 nM	GGACCCAUCUGUCUUCAAAdTdT	Lim et al., 2017
$p62^{si\_C}$	10 nM	GCAUUGAAGUUGAUAUCGAdTdT	Pankiv et al., 2007
$RelB^{si\_E1}$	20 nM	GACUGCACCGACGGCAUCUdTdT	Brandl et al., 2010

All customised siRNAs were from Eurofins Genomics and were based on the sequence information in the cited reference.

5.1.7 Instruments

Instruments used for routine work are listed in Table 14. Instruments for specific work are accounted for in the appropriate sub-sections.

Table 14. Instruments used in routine laboratory work

Name	Company
-20 °C Freezer	Liebherr
-80 °C Freezer (HFU320BV)	Thermo Scientific
Bio-Rad Mini-PROTEAN® Electrophoresis System	Bio-Rad
Cell Counter Countess™ II	ThermoFisher Scientific
Centrifuge 5415R	Eppendorf
Centrifuge Heraeus Fresco 17	Thermo Scientific
Chemo Cam Luminescent Image Analysis System	INTAS
Inverted Microscope Wilovert S	Hund Wetzlar
Megafuge 2.0R	Heraeus Instruments
Mixing Block MB-102	Bioer
pH Meter	Mettler Toledo
Pipet Aid accu-jet® pro	Brand
Precision Weighing Balance XB 120A	Precisa
Refrigerators	Liebherr
See-saw Rocker SSL4 (rocking platform)	Stuart
Techne Dri-Block Heater DB.3	Techne
Tube Rotator (for IP)	Windaus Labortechnik

5.2 Methods

5.2.1 Cell culture

5.2.1.1 Cultivation and maintenance of cell lines

Mediums and solutions required for cell culture were pre-warmed in a 37 °C incubator (Thermo Electron Corporation) before use. Cell culture was performed in a sterile environment under a laminar flow hood (SAVVY SL, Lamsystems). Cells were routinely cultivated in cell culture flasks at 37 °C in a 5 % CO_2 humidified incubator (CB 220, Binder). AGS, NCI-N87 and HKC-8 cells were routinely cultivated in RPMI-1640 medium supplemented with glutamine and 10 % FCS. MKN-45 cells were routinely cultivated in RPMI-1640 medium supplemented with glutamine and 20 % FCS.

For the detachment of adherent cells using trypsin, adherent cells were washed once with DPBS and incubated with an appropriate volume of 0.05 % Trypsin-EDTA (the entire cell monolayer should be covered) for 10 min at 37 °C. This reaction was stopped by adding cell culture medium supplemented with glutamine and 10 % FCS (double the volume of trypsin added). Cells were collected by centrifugation at 600 x g for 4 min. For cell counting, cells were resuspended in fresh cell culture medium. Ten microlitres of the cell suspension was mixed with 10 µl trypan blue stain before application to the cell counting chamber slide (Invitrogen).

5.2.1.2 Freezing and thawing of cell lines

For long term storage, cells were grown to a confluency of ~80 % in a T75 cell culture flask. Cells were detached using trypsin and collected by centrifugation. The cell pellet was resuspended in freezing medium (90 % FCS and 10 % DMSO) and aliquoted into cryotubes for storage at -80 °C for at least 3 h before transferring to a liquid nitrogen tank. For thawing of cells, frozen stocks were thawed in a 37 °C water bath and transferred to 5 ml of pre-warmed culture medium. Cells were collected by centrifugation and cultivated as described in section 5.2.1.1.

5.2.1.3 Cultivation of cells for experiments

Cells were seeded at a density of 3.5 x 10^5 per 60mm culture dish or 1.4 x 10^6 per 100 mm culture dish for *H. pylori* infection (MOI 100), TNF (10 ng/ml), IL-1β (10 ng/ml), LT$\alpha_1\beta_2$ (20 ng/ml unless otherwise specified) or CD95L (250 nM) treatment. Cell culture medium was changed to fresh RPMI-1640 containing 0.2 % FCS or 10 % FCS (for apoptosis study by either flow cytometry or apoptotic markers analyses in IBs) 18 - 24 h prior to *H. pylori* infection or treatment of the cells. Where required, cells were pre-incubated with Z-IETD-FMK (10 μM or 20 μM) or IKK inhibitor VII (10 μM) for 15 min prior to *H. pylori* infection. For experiments involving MG-132, MG-132 (10 μM) was added to the cells 30 min after infection.

5.2.2 Handling of *H. pylori* strains

5.2.2.1 Preparation of agar plates

The agar plates were prepared as follows. Bacto™ Proteose Peptone No. 3 (15 g/l) und GC agar base (36 g/l) were dissolved in Milli-Q grade water and autoclaved. After cooling the agar to around 55 °C in a water bath, the following compounds were added: 10 % (v/v) horse serum; 1 μg/ml (v/v) nystatin; 5 μg/ml (v/v) trimethoprim; and 1 % (v/v) vitamin mix containing 0.5 M dextrose, 68 mM L-glutamine, 165 mM L-cysteine hydrochloride monohydrate, 217 μM thiamine pyrophosphate, 50 μM iron (III) nitrate, 890 nM thiamine hydrochloride, 95 μM 4-aminobenzoic acid, 380 μM b-nicotinamide adenine dinucleotide, 7.4 μM vitamin B12, 4.6 μM L-cystine dihydrochloride, 7.4 mM adenine, 160 μM guanine hydrochloride, 142 μM L-arginine monohydrochloride and 4.5 mM uracil. Sterile filtered vancomycin (10 μg/ml) was added to the agar plates for the cultivation of *H. pylori* wt P1 and wt P12 strains. Sterile filtered vancomycin (10 μg/ml) and chloramphenicol (6 μg/ml) were added to the agar plates for the cultivation of isogenic Δ*cagA* (CagA-deficient), *virB7* (T4SS-deficient) and ΔHP0857 (defective in LPS synthesis) P1 strains. The agar was poured into petri dishes. The agar plates were allowed to cool and solidify at room temperature (RT) overnight followed by storage at 4 °C.

5.2.2.2 Preparation of *H. pylori* culture for infection

The preparation of *H. pylori* culture for an infection experiment as follows had to commence four to five days before the day of the experiment itself.

An agar plate was allowed to reach room temperature under a laminar flow hood (Herasafe, Thermo Scientific). A small clump of *H. pylori* was removed from the frozen stock using a sterile inoculation loop and streaked onto the agar plate. The agar plate was incubated upside down (agar facing downwards) in anaerobic jars (ThermoFisher Scientific) containing Oxoid™ CampyGen™ gas packs (ThermoFisher Scientific) to create a microaerophilic atmosphere. The jars were placed in a 37 °C incubator (Heratherm IGS400, Thermo Scientific) for 48 h to 72 h to allow for patch growth of the bacteria on the agar plate. A sterile cotton-tipped applicator (Goodwood Medical Care Ltd) was used to remove bacteria from the plate followed by resuspension in 1 ml $DPBS^{+/+}$. One hundred microlitres of the bacterial suspension was pipetted onto a fresh agar plate, spread evenly using a sterilised spreader and cultivated for 48 h before use for experiments.

On the day of experiment, a sterile cotton-tipped applicator was used to remove bacteria from the plate followed by resuspension in 5 ml to 10 ml $DPBS^{+/+}$. The bacterial suspension was diluted 10-fold and 20-fold using $DPBS^{+/+}$. The optical densities of both dilutions were measured at a wavelength of 550 nm (OD_{550}) using a spectrophotometer (Ultrospec 3100 pro, Biochrom). The concentrations of the diluted bacterial suspensions at the corresponding OD_{550} measured were read directly from a standard *H. pylori*'s growth curve, plotted as number of bacterial cells/ml versus OD_{550} on a semi-log graph, multiplied by the respective dilution factors. The original concentration of the bacterial suspension is regarded as the average of the two values obtained.

5.2.3 Transfection of siRNAs, plasmids and recombinant proteins

Twenty-four hours prior to siRNA transfections, cells were seeded at a density of 1.5×10^5 per 60 mm or 0.5×10^6 per 100 mm culture dish. Transfection was performed using the jetPRIME kit or METAFECTENE® SI^+ kit according to the manufacturer's protocol. Cell culture medium was changed to fresh RPMI-1640 containing 10 % FCS prior to transfection. For plasmid transfections, cells were seeded at a density of 1.4×10^6 per 100 mm dish 24 h prior to transfection. The amount of plasmid used per 100 mm dish was 2 µg. Plasmid transfection was performed using the Effectene transfection reagent according to the suggested protocol from the manufacturer for the 100 mm dish format. The siRNAs and plasmids were transfected into the cells for 24 h and 6 h, respectively, before the cell culture medium was changed to fresh RPMI-1640 medium containing 0.2 % FCS or 10 % FCS (for experiments in Figure 15 and section 3.2) followed by further incubation for 18 h to 24 h. Mock control referred to cells treated with only the transfection reagent.

Transfection of recombinant human A20 protein was performed using reagents from the Lipofectamine® CRISPRMAX transfection reagent kit. Twenty-four hours prior to protein transfection, cells were seeded at a density of 6 x 10^5 per 60 mm culture dish. The cell culture medium was changed to fresh RPMI-1640 medium supplemented with 0.2 % FCS prior to transfection. One microgram recombinant protein was combined with 5 µl Cas9 PLUS™ reagent in 500 µl Opti-MEM and incubated at RT for 5 min. Six microliters of CRISPRMAX transfection reagent diluted in 500 µl Opti-MEM was combined with the diluted Cas9 PLUS™ reagent/recombinant protein solution and incubated at RT for 20 min before adding drop-wise to the cells in the dishes. After 16-20 h, the cells were infected with *H. pylori*.

5.2.4 Preparation of total cell lysates and subcellular fractionation for SDS-PAGE and immunoblotting

Cells were washed two times with ice-cold DPBS. Cells were scraped in lysis buffer (80-100 µl for 60 mm culture dish) and incubated on ice for 15 min. Total cell lysates were obtained after centrifugation at 13000 rpm for 10 min at 4 °C.

For subcellular fractionation, cells were washed two times and scraped in ice-cold DPBS (500 µl for 100 mm culture dish). Cell pellet was obtained after centrifugation at 600 x g for 4 min and resuspended in 300 µl buffer A. The cell suspension was incubated for 10 min on ice. Thereafter, 3 µl 12.5 % NP-40 was added to the cell suspension followed by incubation for another 5 min on ice with incidental vortexing. The nuclei were separated from the cytosolic supernatant by centrifugation at 2000 x g for 10 min at 4 °C. The cytosolic supernatant was centrifuged again at 13000 x g for 10 min at 4 °C to obtain a cleared cytosolic fraction. The nuclear pellet was washed once by resuspension in 300 µl buffer A followed by centrifugation at 2000 x g for 10 min at 4 °C. The nuclear pellet was resuspended in 50 µl buffer C and incubated on ice for 40 min with occasional vortexing. After centrifugation at 13000 x g for 10 min at 4 °C, the supernantant containing soluble nuclear proteins (N1 fraction) was transferred to a clean microtube.

Protein concentration was estimated using the Pierce™ BCA protein assay kit. After quantification of protein concentration, 5X reducing sample buffer was added to 20-100 µg cell lysates followed by incubation at 95 °C for 10 min to denature the proteins. Equal amounts of protein were separated in 6 %, 10 % or 15 % SDS-polyacrylamide gels and transferred onto PVDF membranes. The subsequent handling of membranes involved incubation on a rocking platform. The membranes were incubated for 1 h at RT in blocking solution and with the primary antibodies overnight at 4 °C. The membranes were washed thrice in TBS-T and incubated with the appropriate HRP-conjugated secondary antibody for 1 h at RT, followed by three washes in TBS-T. The membranes were developed using a chemiluminescent substrate

and the band pattern was visualised using the Chemo Cam Luminescent Image Analysis System.

5.2.5 Immunoprecipitation

Cells were washed two times with ice-cold DPBS, scraped in IP buffer (500 µl for 100 mm culture dish) and sheared by passing several times through a 26G x 1/2" needle attached to a 1 ml syringe. Cell lysates were obtained after centrifugation at 13000 rpm for 10 min at 4 °C. One to two milligrams cell lysate was incubated with 1-2 µg IP antibody or isotype-specific IgG at 4 °C overnight on a rotator (7 rpm). Precipitation of protein complexes was achieved by adding protein A/G magnetic beads and incubated for 1 h at 4 °C on a rotator (7 rpm). The beads were washed three times in IP buffer and twice in DPBS. Elution of beads was achieved by incubation with 2X reducing sample buffer for 20 min at RT. Eluate was transferred to a clean tube and heated for 10 min at 95 °C. For analysis, equal amounts of eluate were separated in SDS-PAGE and immunoblotting was performed as described in section 5.2.4.

For the preparation of cell lysates for IP under denaturing conditions, cells were lysed in denaturing IP buffer and sheared by passing several times through a 26G x 1/2" needle attached to a 1 ml syringe. The cell suspensions were heated at 95 °C for 15 min followed by centrifugation at 13000 rpm for 15 min. Cell lysates were diluted 1:10 in denaturing IP buffer without SDS before IP.

For the experiments in Figure 13, panels C and D, 50 ng recombinant human A20 and TIFA proteins, respectively, were combined in 500 µl DPBS, and incubated for 1 h. IP was performed by incubation with 1 µl α-TIFA or 1 µg α-A20 antibody for 1 h. Both incubation steps were carried out at 4 °C on a rotator (7 rpm). Subsequent steps from precipitation of protein complexes to elution were the same as described in the first paragraph of this section.

For the experiments in Figure 13, panel E, after the last washing step of the beads with immunoprecipitates, these were resuspended in 500 µl DPBS and divided into two (250 µl) aliquots. Elution of immunoprecipitates was performed for one aliquot. One hundred nanograms recombinant human A20 protein was added to the other aliquot and rotated at 7 rpm for 1 h at 4 °C. The beads with immunoprecipitates were washed two times in lysis buffer followed by elution of immunoprecipitates.

5.2.6 Site-directed mutagenesis

Silencing of the DUB activity or mutation in the ZnF4 region of A20 was achieved using the QuickChange II XL site-directed mutagenesis kit according to the manufacturer's protocol and the FLAG-tagged A20-expressing plasmid as template. Primers were designed to replace C103 or C624/C627 by alanine to mutate the DUB activity and the region in ZnF4 that mediates substrate ubiquitinylation, respectively. The primers used were

C103A 5'-GAACGGTGACGGCAATGCCCTCATGCATGCCAC-3' and C624A/C627A 5'-GACTCCAGAAAACAAGGGCTTTGCCACACTGGCTTTCATCGAGTACA GAGAAAA-3'. Successful mutation was verified by sequencing.

5.2.7 Generation of knock-out AGS cell lines using CRISPR/Cas9

For experiments in section 3.1, the knockout of A20 in AGS cells was performed using reagents from IDT as follows: Alt-R® CRISPR-Cas9 crRNA Hs.Cas9.TNFAIP3.1.AB 5'-AACCATGCACCGATACACAC TGG -3'; Alt-R® CRISPR-Cas9 tracrRNA ATTO™ 550 (1075927); Alt-R® S.p. HiFi Cas9 Nuclease V3 (1081060); and nuclease-free duplex buffer. Reagents from the Lipofectamine® CRISPRMAX transfection reagent kit were used for transfection. Equimolar (1 μM) of crRNA and tracrRNA were mixed in 100 μl nuclease-free duplex buffer, heated at 95 °C for 5 min and cooled to RT to produce gRNA. To form the ribonucleoprotein (RNP) complex, the gRNA (1 μM, 1.5 μl) was combined with Cas9 (1 μM, 1.5 μl) and Cas9 PLUS™ reagent (0.6 μl) in 21.4 μl Opti-MEM medium, and incubated for 5 min at RT. The RNP (total volume 25 μl) was combined with 1.2 μl CRISPRMAX transfection reagent in 23.8 μl Opti-MEM and incubated for another 20 min at RT. The transfection mixture was added to a well in a 96-well tissue culture plate followed by the addition of 40000 AGS cells. After 24 h incubation, the cells were detached using trypsin and monoclonal cell lines were generated using the limiting dilution method. Control AGS cells used have undergone the same CRISPR/Cas9 procedure but were not successful for the depletion of A20.

For experiments in section 3.2, cells were seeded at a density of 0.2 x 10^5 per well in a 6-well tissue culture plate. The next day, 1 μg of the A20/TNFAIP3 double nickase plasmid or the control double nickase plasmid was combined with 2 μl JetPrime transfection reagent in 300 μl JetPrime buffer. This transfection mixture was mixed gently by pipetting up and down once, followed by incubation for 20 min at RT. The transfection mixture was added to the cells in a well in the 6-well culture plate. After 24 h incubation, the medium was changed to selection medium containing 0.5 μg/ml Puromycin. After 10 days in selection medium, monoclonal cell lines were generated using the limiting dilution method.

The TIFA-knockout AGS cell line was generated and provided by my colleague Dr. G. Maubach (Maubach et al., 2021).

5.2.8 Flow cytometry

Cells were harvested using trypsin and stained using the Annexin-V Apoptosis Detection kit according to the manufacturer's protocol. A gating for viable single cells based on forward and side scatter was performed, and 1 x 10^4 cells were counted. All samples were recorded in the respective channels and compensation was performed before analysis. For the quantification

of cell death, annexin V-FITC-positive and double positive (annexin V-FITC- plus PI-stained) cells were added together to give the percentage of apoptotic cells.
For section 4.1.4, analysis of cells after annexin V-FITC/PI staining was performed using the CyFlow® Space flow cytometer (Sysmex Partec) and quantified using the Flowing Software (version 2.5.1).
For section 4.2.3, analysis of cells after annexin V-FITC/PI staining was performed using the Amnis® FlowSight® Imaging flow cytometer (Merck) and the IDEAS software (version 6.0).

5.2.9 Quantitative real-time polymerase chain reaction

Total RNA was isolated using the NucleoSpin® RNAII kit according to the manufacturer's protocol. The total RNA was reverse transcribed into complementary DNA (cDNA) using the RT^2 First Strand kit or the RevertAid First Strand cDNA Synthesis kit and the C1000 Touch™ thermal cycler (Bio-Rad). Quantitative real-time polymerase chain reaction (PCR) was performed with the Taqman® gene expression assay primers (Applied Biosystems) for A20 (Hs00234713_m1) and GAPDH (Hs03929097_g1) was used for normalisation. Alternatively, quantitative real-time PCR was performed using the primer sets targeted against *BCL2L11*, *BCL2*, *BIRC2*, *BCL2A1*, *CFLAR*, *BIRC3*, *BIRC5* and *RPL13A* (endogenous control gene for normalisation) provided in the Human Apoptosis Primer Library masterplate (RealTimePrimers, HPA-1) and the SensiMix™ SYBR® Hi-ROX kit. Amplification was performed using the StepOnePlus™ Real-Time PCR system (Applied Biosystems). The Comparative C_T Method ($\Delta\Delta C_T$) was used to quantify relative changes of the target mRNA. Data were expressed as fold change in target mRNA.

5.2.10 Densitometric analysis

The densitometric quantification of cIAP1 band intensities in figure 12A was performed using the ImageJ software according to Schneider and colleagues (2012). For normalisation purpose, the values of the cIAP1 band intensities were divided by the values of the respective TRAF2 band intensities. The numbers indicate the normalised band intensities of cIAP1 in *H. pylori*-infected samples relative to uninfected control.

5.2.11 Statistical analysis

All quantitative data were analysed using OriginPro (versions 2015 or 2020b) and are presented as means ± SD. Time-dependent changes during quantitative real-time PCR studies (Figure 14A) were tested for significance using one-way ANOVA and Bonferroni's post-hoc test. All other quantitative data were tested for significance using two-sample Student's t-test. A p value of < 0.05 was regarded as statistical significant.

Reference List

Afshar, G., Jelluma, N., Yang, X., Basila, D., Arvold, N.D., Karlsson, A., Yount, G.L., Dansen, T.B., Koller, E., and Haas-Kogan, D.A. (2006). Radiation-induced caspase-8 mediates p53-independent apoptosis in glioma cells. Cancer Res *66*, 4223-4232. 10.1158/0008-5472.CAN-05-1283.

Alzahrani, S., Lina, T.T., Gonzalez, J., Pinchuk, I.V., Beswick, E.J., and Reyes, V.E. (2014). Effect of Helicobacter pylori on gastric epithelial cells. World J Gastroenterol *20*, 12767-12780. 10.3748/wjg.v20.i36.12767.

Andersen-Nissen, E., Smith, K.D., Strobe, K.L., Barrett, S.L., Cookson, B.T., Logan, S.M., and Aderem, A. (2005). Evasion of Toll-like receptor 5 by flagellated bacteria. Proc Natl Acad Sci U S A *102*, 9247-9252. 10.1073/pnas.0502040102.

Asrat, S., Davis, K.M., and Isberg, R.R. (2015). Modulation of the host innate immune and inflammatory response by translocated bacterial proteins. Cell Microbiol *17*, 785-795. 10.1111/cmi.12445.

Backert, S., and Tegtmeyer, N. (2017). Type IV secretion and signal transduction of Helicobacter pylori CagA through interactions with host cell receptors. Toxins (Basel) *9*. 115. 10.3390/toxins9040115.

Backert, S., Tegtmeyer, N., and Fischer, W. (2015). Composition, structure and function of the Helicobacter pylori cag pathogenicity island encoded type IV secretion system. Future Microbiol *10*, 955-965. 10.2217/fmb.15.32.

Bellail, A.C., Olson, J.J., Yang, X., Chen, Z.J., and Hao, C. (2012). A20 ubiquitin ligase-mediated polyubiquitination of RIP1 inhibits caspase-8 cleavage and TRAIL-induced apoptosis in glioblastoma. Cancer Discov *2*, 140-155. 10.1158/2159-8290.CD-11-0172.

Bertrand, M.J., Milutinovic, S., Dickson, K.M., Ho, W.C., Boudreault, A., Durkin, J., Gillard, J.W., Jaquith, J.B., Morris, S.J., and Barker, P.A. (2008). cIAP1 and cIAP2 facilitate cancer cell survival by functioning as E3 ligases that promote RIP1 ubiquitination. Mol Cell *30*, 689-700. 10.1016/j.molcel.2008.05.014.

Boatright, K.M., Renatus, M., Scott, F.L., Sperandio, S., Shin, H., Pedersen, I.M., Ricci, J.E., Edris, W.A., Sutherlin, D.P., Green, D.R., and Salvesen, G.S. (2003). A unified model for apical caspase activation. Mol Cell *11*, 529-541. 10.1016/s1097-2765(03)00051-0.

Boone, D.L., Turer, E.E., Lee, E.G., Ahmad, R.C., Wheeler, M.T., Tsui, C., Hurley, P., Chien, M., Chai, S., Hitotsumatsu, O., et al. (2004). The ubiquitin-modifying enzyme A20 is required for termination of Toll-like receptor responses. Nat Immunol *5*, 1052-1060. 10.1038/ni1110.

Brandl, M., Seidler, B., Haller, F., Adamski, J., Schmid, R.M., Saur, D., and Schneider, G. (2010). IKKα controls canonical TGFβ-SMAD signaling to regulate genes expressing SNAIL and SLUG during EMT in panc1 cells. J Cell Sci *123*, 4231-4239. 10.1242/jcs.071100.

Bren, G. D., Solan, N. J., Miyoshi, H., Pennington, K. N., Pobst, L. J., and Paya, C. V. (2001). Transcription of the RelB gene is regulated by NF-kappaB. Oncogene *20*, 7722-7733. 10.1038/sj.onc.1204868.

Burkitt, M.D., Duckworth, C.A., Williams, J.M., and Pritchard, D.M. (2017). Helicobacter pylori-induced gastric pathology: Insights from in vivo and ex vivo models. Dis Model Mech *10*, 89-104. 10.1242/dmm.027649.

Buß, M., Tegtmeyer, N., Schnieder, J., Dong, X., Li, J., Springer, T.A., Backert, S., and Niemann, H.H. (2019). Specific high affinity interaction of Helicobacter pylori CagL with integrin α. FEBS J *286*, 3980-3997. 10.1111/febs.14962.

Chang, D.W., Xing, Z., Capacio, V.L., Peter, M.E., and Yang, X. (2003). Interdimer processing mechanism of procaspase-8 activation. EMBO J *22*, 4132-4142. 10.1093/emboj/cdg414.

Chang, W.L., Yeh, Y.C., and Sheu, B.S. (2018). The impacts of H. pylori virulence factors on the development of gastroduodenal diseases. J Biomed Sci *25*, 68. 10.1186/s12929-018-0466-9.

Chmiela, M., Miszczyk, E., and Rudnicka, K. (2014). Structural modifications of Helicobacter pylori lipopolysaccharide: an idea for how to live in peace. World J Gastroenterol *20*, 9882-9897. 10.3748/wjg.v20.i29.9882.

Costa, T.R.D., Harb, L., Khara, P., Zeng, L., Hu, B., and Christie, P.J. (2021). Type IV secretion systems: Advances in structure, function, and activation. Mol Microbiol *115*, 436-452. 10.1111/mmi.14670.

Daniel, S., Arvelo, M.B., Patel, V.I., Longo, C.R., Shrikhande, G., Shukri, T., Mahiou, J., Sun, D.W., Mottley, C., Grey, S.T., and Ferran, C. (2004). A20 protects endothelial cells from TNF-, Fas-, and NK-mediated cell death by inhibiting caspase 8 activation. Blood *104*, 2376-2384. 10.1182/blood-2003-02-0635.

Das, T., Chen, Z., Hendriks, R.W., and Kool, M. (2018). A20/Tumor Necrosis Factor α-Induced Protein 3 in immune cells controls development of autoinflammation and autoimmunity: Lessons from mouse models. Front Immunol *9*, 104. 10.3389/fimmu.2018.00104.

de Oliveira, K.A., Kaergel, E., Heinig, M., Fontaine, J.F., Patone, G., Muro, E.M., Mathas, S., Hummel, M., Andrade-Navarro, M.A., Hübner, N., and Scheidereit, C. (2016). A roadmap of constitutive NF-κB activity in Hodgkin lymphoma: Dominant roles of p50 and p52 revealed by genome-wide analyses. Genome Med *8*, 28. 10.1186/s13073-016-0280-5.

de Wit, H., Dokter, W. H., Koopmans, S. B., Lummen, C., van der Leij, M., Smit, J. W., and Vellenga, E. (1998). Regulation of p100 (NFKB2) expression in human monocytes in response to inflammatory mediators and lymphokines. Leukemia *12*, 363-370. 10.1038/sj.leu.2400950.

Dixit, V.M., Green, S., Sarma, V., Holzman, L.B., Wolf, F.W., O'Rourke, K., Ward, P.A., Prochownik, E.V., and Marks, R.M. (1990). Tumor necrosis factor-alpha induction of novel gene products in human endothelial cells including a macrophage-specific chemotaxin. J Biol Chem *265*, 2973-2978.

Dorstyn, L., Akey, C.W., and Kumar, S. (2018). New insights into apoptosome structure and function. Cell Death Differ *25*, 1194-1208. 10.1038/s41418-017-0025-z.

Draber, P., Kupka, S., Reichert, M., Draberova, H., Lafont, E., de Miguel, D., Spilgies, L., Surinova, S., Taraborrelli, L., Hartwig, T., et al. (2015). LUBAC-recruited CYLD and A20 regulate gene activation and cell death by exerting opposing effects on linear ubiquitin in signaling complexes. Cell Rep *13*, 2258-2272. 10.1016/j.celrep.2015.11.009.

Díaz, P., Valenzuela Valderrama, M., Bravo, J., and Quest, A.F.G. (2018). Helicobacter pylori and gastric cancer: Adaptive cellular mechanisms involved in disease progression. Front Microbiol *9*, 5. 10.3389/fmicb.2018.00005.

Düwel, M., Welteke, V., Oeckinghaus, A., Baens, M., Kloo, B., Ferch, U., Darnay, B.G., Ruland, J., Marynen, P., and Krappmann, D. (2009). A20 negatively regulates T cell receptor signaling to NF-κB by cleaving Malt1 ubiquitin chains. J Immunol *182*, 7718-7728. 10.4049/jimmunol.0803313.

Ea, C.K., Sun, L., Inoue, J., and Chen, Z.J. (2004). TIFA activates IκB kinase (IKK) by promoting oligomerization and ubiquitination of TRAF6. Proc Natl Acad Sci U S A *101*, 15318-15323. 10.1073/pnas.0404132101.

Feige, M.H., Vieth, M., Sokolova, O., Täger, C., and Naumann, M. (2018). Helicobacter pylori induces direct activation of the lymphotoxin beta receptor and non-canonical nuclear factor-kappa B signaling. Biochim Biophys Acta *1865*, 545-550. 10.1016/j.bbamcr.2018.01.006.

Fischer, W. (2011). Assembly and molecular mode of action of the Helicobacter pylori Cag type IV secretion apparatus. FEBS J *278*, 1203-1212. 10.1111/j.1742-4658.2011.08036.x.

Frick-Cheng, A.E., Pyburn, T.M., Voss, B.J., McDonald, W.H., Ohi, M.D., and Cover, T.L. (2016). Molecular and structural analysis of the Helicobacter pylori cag type IV secretion system core complex. MBio *7*, e02001-02015. 10.1128/mBio.02001-15.

Galluzzi, L., Vitale, I., Aaronson, S.A., Abrams, J.M., Adam, D., Agostinis, P., Alnemri, E.S., Altucci, L., Amelio, I., Andrews, D.W., et al. (2018). Molecular mechanisms of cell death: Recommendations of the Nomenclature Committee on Cell Death 2018. Cell Death Differ *25*, 486-541. 10.1038/s41418-017-0012-4.

Ganeff, C., Remouchamps, C., Boutaffala, L., Benezech, C., Galopin, G., Vandepaer, S., Bouillenne, F., Ormenese, S., Chariot, A., Schneider, P., Caamaño, J., Piette, J., and Dejardin, E. (2011). Induction of the alternative NF-κB pathway by lymphotoxin αβ (LTαβ) relies on internalization of LTβ receptor. Mol Cell Biol *31*, 4319-4334. 10.1128/MCB.05033-11.

Gao, L., Coope, H., Grant, S., Ma, A., Ley, S.C., and Harhaj, E.W. (2011). ABIN1 protein cooperates with TAX1BP1 and A20 proteins to inhibit antiviral signaling. J. Biol. Chem. *286*, 36592-36602. 10.1074/jbc.M111.283762.

Garcia-Carbonell, R., Wong, J., Kim, J.Y., Close, L.A., Boland, B.S., Wong, T.L., Harris, P.A., Ho, S.B., Das, S., Ernst, P.B., et al. (2018). Elevated A20 promotes TNF-induced and RIPK1-dependent intestinal epithelial cell death. Proc Natl Acad Sci U S A *115*, E9192-E9200. 10.1073/pnas.1810584115.

Geetha, T., and Wooten, M.W. (2002). Structure and functional properties of the ubiquitin binding protein p62. FEBS Lett *512*, 19-24. 10.1016/s0014-5793(02)02286-x.

Goh, K.L., Chan, W.K., Shiota, S., and Yamaoka, Y. (2011). Epidemiology of Helicobacter pylori infection and public health implications. Helicobacter *16 Suppl 1*, 1-9. 10.1111/j.1523-5378.2011.00874.x.

Gonzalez-Rivera, C., Bhatty, M., and Christie, P. J. (2016). Mechanism and function of type IV secretion during infection of the human host. Microbiol Spectr *4*, 10.1128/microbiolspec.VMBF-0024-2015.

Gonzalvez, F., Schug, Z. T., Houtkooper, R. H., MacKenzie, E. D., Brooks, D. G., Wanders, R. J., Petit, P. X., Vaz, F. M., and Gottlieb, E. (2008). Cardiolipin provides an essential activating platform for caspase-8 on mitochondria. J Cell Biol *183*, 681-696. 10.1083/jcb.200803129.

Hasegawa, H., Yamada, Y., Harasawa, H., Tsuji, T., Murata, K., Sugahara, K., Tsuruda, K., Ikeda, S., Imaizumi, Y., Tomonaga, M., Masuda, M., Takasu, N., and Kamihira, S. (2005). Sensitivity of adult T-cell leukaemia lymphoma cells to tumour necrosis factor-related apoptosis-inducing ligand. Br J Haematol *128*, 253-265. 10.1111/j.1365-2141.2004.05289.x.
Hatakeyama, M. (2008). SagA of CagA in Helicobacter pylori pathogenesis. Curr Opin Microbiol *11*, 30-37. 10.1016/j.mib.2007.12.003.

Hayden, M.S., and Ghosh, S. (2012). NF-κB, the first quarter-century: Remarkable progress and outstanding questions. Genes Dev *26*, 203-234. 10.1101/gad.183434.111.

Heusch, M., Lin, L., Geleziunas, R., and Greene, W. C. (1999). The generation of nfkb2 p52: mechanism and efficiency. Oncogene *18*, 6201-6208. 10.1038/sj.onc.1203022.

Higashi, H., Yokoyama, K., Fujii, Y., Ren, S., Yuasa, H., Saadat, I., Murata-Kamiya, N., Azuma, T., and Hatakeyama, M. (2005). EPIYA motif is a membrane-targeting signal of Helicobacter pylori virulence factor CagA in mammalian cells. J Biol Chem *280*, 23130-23137. 10.1074/jbc.M503583200.

Hohlfeld, S., Pattis, I., Püls, J., Plano, G. V., Haas, R., and Fischer, W. (2006). A C-terminal translocation signal is necessary, but not sufficient for type IV secretion of the Helicobacter pylori CagA protein. Mol Microbiol *59*, 1624-1637. 10.1111/j.1365-2958.2006.05050.x.

Hu, H., and Sun, S.C. (2016). Ubiquitin signaling in immune responses. Cell Res *26*, 457-483. 10.1038/cr.2016.40.

Hutti, J.E., Turk, B.E., Asara, J.M., Ma, A., Cantley, L.C., and Abbott, D.W. (2007). IκB kinase β phosphorylates the K63 deubiquitinase A20 to cause feedback inhibition of the NF-κB pathway. Mol Cell Biol *27*, 7451-7461. 10.1128/MCB.01101-07.

Isomoto, H., Miyazaki, M., Mizuta, Y., Takeshima, F., Murase, K., Inoue, K., Yamasaki, K., Murata, I., Koji, T., and Kohno, S. (2000). Expression of nuclear factor-κB in Helicobacter pylori-infected gastric mucosa detected with southwestern histochemistry. Scand J Gastroenterol *35*, 247-254. 10.1080/003655200750024092.

Jiménez-Soto, L.F., Kutter, S., Sewald, X., Ertl, C., Weiss, E., Kapp, U., Rohde, M., Pirch, T., Jung, K., Retta, S.F., et al. (2009). Helicobacter pylori type IV secretion apparatus exploits β1 integrin in a novel RGD-independent manner. PLoS Pathog *5*, e1000684. 10.1371/journal.ppat.1000684.

Jin, Z., Li, Y., Pitti, R., Lawrence, D., Pham, V.C., Lill, J.R., and Ashkenazi, A. (2009). Cullin3-based polyubiquitination and p62-dependent aggregation of caspase-8 mediate extrinsic apoptosis signaling. Cell *137*, 721-735. 10.1016/j.cell.2009.03.015.

Jones, N.L., and Sherman, P.M. (1999). Helicobacter pylori-epithelial cell interactions: From adhesion to apoptosis. Can J Gastroenterol *13*, 563-566. doi: 10.1155/1999/848346.

Julien, O., and Wells, J.A. (2017). Caspases and their substrates. Cell Death Differ *24*, 1380-1389. 10.1038/cdd.2017.44.

Kalisperati, P., Spanou, E., Pateras, I.S., Korkolopoulou, P., Varvarigou, A., Karavokyros, I., Gorgoulis, V.G., Vlachoyiannopoulos, P.G., and Sougioultzis, S. (2017). Inflammation, DNA damage, Helicobacter pylori and gastric tumorigenesis. Front Genet *8*, 20. 10.3389/fgene.2017.00020.

Kanamori, M., Suzuki, H., Saito, R., Muramatsu, M., and Hayashizaki, Y. (2002). T2BP, a novel TRAF2 binding protein, can activate NF-κB and AP-1 without TNF stimulation. Biochem Biophys Res Commun *290*, 1108-1113. 10.1006/bbrc.2001.6315.

Kaplan-Türköz, B., Jiménez-Soto, L.F., Dian, C., Ertl, C., Remaut, H., Louche, A., Tosi, T., Haas, R., and Terradot, L. (2012). Structural insights into Helicobacter pylori oncoprotein CagA interaction with β1 integrin. Proc Natl Acad Sci U S A *109*, 14640-14645. 10.1073/pnas.1206098109.

Kattah, M.G., Shao, L., Rosli, Y.Y., Shimizu, H., Whang, M.I., Advincula, R., Achacoso, P., Shah, S., Duong, B.H., Onizawa, M., et al. (2018). A20 and ABIN-1 synergistically preserve intestinal epithelial cell survival. J Exp Med *215*, 1839-1852. 10.1084/jem.20180198.

Keates, S., Hitti, Y.S., Upton, M., and Kelly, C.P. (1997). Helicobacter pylori infection activates NF-κB in gastric epithelial cells. Gastroenterology *113*, 1099-1109. 10.1053/gast.1997.v113.pm9322504.

Kishi, S., Saijyo, S., Arai, M., Karasawa, S., Ueda, S., Kannagi, M., Iwakura, Y., Fujii, M., and Yonehara, S. (1997). Resistance to Fas-mediated apoptosis of peripheral T cells in human T lymphocyte virus type I (HTLV-I) transgenic mice with autoimmune arthropathy. J Exp Med *186*, 57-64. 10.1084/jem.186.1.57.

Kool, M., van Loo, G., Waelput, W., De Prijck, S., Muskens, F., Sze, M., van Praet, J., Branco-Madeira, F., Janssens, S., Reizis, B., et al. (2011). The ubiquitin-editing protein A20 prevents dendritic cell activation, recognition of apoptotic cells, and systemic autoimmunity. Immunity *35*, 82-96. 10.1016/j.immuni.2011.05.013.

Kuck, D., Kolmerer, B., Iking-Konert, C., Krammer, P.H., Stremmel, W., and Rudi, J. (2001). Vacuolating cytotoxin of Helicobacter pylori induces apoptosis in the human gastric epithelial cell line AGS. Infect Immun *69*, 5080-5087. 10.1128/iai.69.8.5080-5087.2001.

Kwok, T., Zabler, D., Urman, S., Rohde, M., Hartig, R., Wessler, S., Misselwitz, R., Berger, J., Sewald, N., Koenig, W., and Backert, S. (2007). Helicobacter exploits integrin for type IV secretion and kinase activation. Nature *449*, 862-866. 10.1038/nature06187.

Lai, T.Y., Wu, S.D., Tsai, M.H., Chuang, E.Y., Chuang, L.L., Hsu, L.C., and Lai, L.C. (2013). Transcription of Tnfaip3 is regulated by NF-κB and p38 via C/EBPβ in activated macrophages. PLoS ONE *8*, e73153. 10.1371/journal.pone.0073153.

Lau, T.S., Chung, T.K., Cheung, T.H., Chan, L.K., Cheung, L.W., Yim, S.F., Siu, N.S., Lo, K.W., Yu, M.M., Kulbe, H., et al. (2014). Cancer cell-derived lymphotoxin mediates reciprocal tumour-stromal interactions in human ovarian cancer by inducing CXCL11 in fibroblasts. J Pathol *232*, 43-56. 10.1002/path.4258.

Lavrik, I., Krueger, A., Schmitz, I., Baumann, S., Weyd, H., Krammer, P.H., and Kirchhoff, S. (2003). The active caspase-8 heterotetramer is formed at the CD95 DISC. Cell Death Differ *10*, 144-145. 10.1038/sj.cdd.4401156.

Lettl, C., Haas, R., and Fischer, W. (2021). Kinetics of CagA type IV secretion by Helicobacter pylori and the requirement for substrate unfolding. Mol Microbiol *116*, 794-807. 10.1111/mmi.14772.

Li, H., Zhu, H., Xu, C.J., and Yuan, J. (1998). Cleavage of BID by caspase 8 mediates the mitochondrial damage in the Fas pathway of apoptosis. Cell *94*, 491-501. 10.1016/s0092-8674(00)81590-1.

Lim, M.C.C., Maubach, G., Sokolova, O., Feige, M.H., Diezko, R., Buchbinder, J., Backert, S., Schlüter, D., Lavrik, I.N., and Naumann, M. (2017). Pathogen-induced ubiquitin-editing enzyme A20 bifunctionally shuts off NF-κB and caspase-8-dependent apoptotic cell death. Cell Death Differ *24*, 1621-1631. 10.1038/cdd.2017.89.

Ling, J., Kang, Y., Zhao, R., Xia, Q., Lee, D.F., Chang, Z., Li, J., Peng, B., Fleming, J.B., Wang, H., et al. (2012). KrasG12D-induced IKK2/β/NF-κB activation by IL-1α and p62 feedforward loops is required for development of pancreatic ductal adenocarcinoma. Cancer Cell *21*, 105-120. 10.1016/j.ccr.2011.12.006.

Lu, T.T., Onizawa, M., Hammer, G.E., Turer, E.E., Yin, Q., Damko, E., Agelidis, A., Shifrin, N., Advincula, R., Barrera, J., et al. (2013). Dimerization and ubiquitin mediated recruitment of A20, a complex deubiquitinating enzyme. Immunity *38*, 896-905. 10.1016/j.immuni.2013.03.008.

Luo, X., Budihardjo, I., Zou, H., Slaughter, C., and Wang, X. (1998). Bid, a Bcl2 interacting protein, mediates cytochrome c release from mitochondria in response to activation of cell surface death receptors. Cell *94*, 481-490. 10.1016/s0092-8674(00)81589-5.

Macho-Fernandez, E., Koroleva, E.P., Spencer, C.M., Tighe, M., Torrado, E., Cooper, A.M., Fu, Y.X., and Tumanov, A.V. (2015). Lymphotoxin beta receptor signaling limits mucosal damage through driving IL-23 production by epithelial cells. Mucosal Immunol *8*, 403-413. 10.1038/mi.2014.78.

Maddika, S., and Chen, J. (2009). Protein kinase DYRK2 is a scaffold that facilitates assembly of an E3 ligase. Nat Cell Biol *11*, 409-419. 10.1038/ncb1848.

Madge, L.A., Kluger, M.S., Orange, J.S., and May, M.J. (2008). Lymphotoxin-α1β2 and LIGHT induce classical and noncanonical NF-κB-dependent proinflammatory gene expression in vascular endothelial cells. The Journal of Immunology *180*, 3467-3477. 10.4049/jimmunol.180.5.3467.

Makarova, K.S., Aravind, L., and Koonin, E.V. (2000). A novel superfamily of predicted cysteine proteases from eukaryotes, viruses and Chlamydia pneumoniae. Trends Biochem Sci *25*, 50-52. 10.1016/s0968-0004(99)01530-3.

Makarova, K.S., Koonin, E.V., and Albers, S.V. (2016). Diversity and evolution of type IV pili systems in archaea. Front Microbiol *7*, 667. 10.3389/fmicb.2016.00667.

Martens, A., Priem, D., Hoste, E., Vetters, J., Rennen, S., Catrysse, L., Voet, S., Deelen, L., Sze, M., Vikkula, H., et al. (2020). Two distinct ubiquitin-binding motifs in A20 mediate its anti-inflammatory and cell-protective activities. Nat Immunol *21*, 381-387. 10.1038/s41590-020-0621-9.

Martens, A., and van Loo, G. (2020). A20 at the crossroads of cell death, inflammation, and autoimmunity. Cold Spring Harb Perspect Biol *12*, a036418. 10.1101/cshperspect.a036418.

Martin, J.H., Potthoff, A., Ledig, S., Cornberg, M., Jandl, O., Manns, M.P., Kubicka, S., Flemming, P., Athmann, C., Beil, W., and Wagner, S. (2004). Effect of H. pylori on the expression of TRAIL, FasL and their receptor subtypes in human gastric epithelial cells and their role in apoptosis. Helicobacter *9*, 371-386. 10.1111/j.1083-4389.2004.00269.x.

Mathes, E., O'Dea, E. L., Hoffmann, A., and Ghosh, G. (2008). NF-κB dictates the degradation pathway of IκBα. EMBO J *27*, 1357-1367. 10.1038/emboj.2008.73.

Maubach, G., Lim, M.C.C., Sokolova, O., Backert, S., Meyer, T.F., and Naumann, M. (2021). TIFA has dual functions in Helicobacter pylori-induced classical and alternative NF-κB pathways. EMBO Rep *22*, e52878. 10.15252/embr.202152878.

Mejías-Luque, R., Zöller, J., Anderl, F., Loew-Gil, E., Vieth, M., Adler, T., Engler, D.B., Urban, S., Browning, J.L., Müller, A., et al. (2016). Lymphotoxin β receptor signalling executes Helicobacter pylori-driven gastric inflammation in a T4SS-dependent manner. Gut *66*, 1369-1381. 10.1136/gutjnl-2015-310783.

Mikami, Y., Matsuzaki, H., Horie, M., Noguchi, S., Jo, T., Narumoto, O., Kohyama, T., Takizawa, H., Nagase, T., and Yamauchi, Y. (2014). Lymphotoxin β receptor signaling induces IL-8 production in human bronchial epithelial cells. PLoS ONE *9*, e114791. 10.1371/journal.pone.0114791.

Milhas, D., Cuvillier, O., Therville, N., Clavé, P., Thomsen, M., Levade, T., Benoist, H., and Ségui, B. (2005). Caspase-10 triggers Bid cleavage and caspase cascade activation in FasL-induced apoptosis. J Biol Chem *280*, 19836-19842. 10.1074/jbc.M414358200.

Mori, N., Yamada, Y., Ikeda, S., Yamasaki, Y., Tsukasaki, K., Tanaka, Y., Tomonaga, M., Yamamoto, N., and Fujii, M. (2002). Bay 11-7082 inhibits transcription factor NF-κB and induces apoptosis of HTLV-I-infected T-cell lines and primary adult T-cell leukemia cells. Blood *100*, 1828-1834. 10.1182/blood-2002-01-0151.

Moss, S.F., Sordillo, E.M., Abdalla, A.M., Makarov, V., Hanzely, Z., Perez-Perez, G.I., Blaser, M.J., and Holt, P.R. (2001). Increased gastric epithelial cell apoptosis associated with colonization with CagA + Helicobacter pylori strains. Cancer Res *61*, 1406-1411.

Mothes, J., Ipenberg, I., Arslan, S., Benary, U., Scheidereit, C., and Wolf, J. (2020). A quantitative modular modeling approach reveals the effects of different A20 feedback implementations for the NF-κB signaling dynamics. Front Physiol *11*, 896. 10.3389/fphys.2020.00896.

Mullaney, E., Brown, P.A., Smith, S.M., Botting, C.H., Yamaoka, Y.Y., Terres, A.M., Kelleher, D.P., and Windle, H.J. (2009). Proteomic and functional characterization of the outer membrane vesicles from the gastric pathogen Helicobacter pylori. Proteomics Clin Appl *3*, 785-796. 10.1002/prca.200800192.

Murata-Kamiya, N., Kikuchi, K., Hayashi, T., Higashi, H., and Hatakeyama, M. (2010). Helicobacter pylori exploits host membrane phosphatidylserine for delivery, localization, and pathophysiological action of the CagA oncoprotein. Cell Host Microbe *7*, 399-411. 10.1016/j.chom.2010.04.005.

Naumann, M., Sokolova, O., Tegtmeyer, N., and Backert, S. (2017). Helicobacter pylori: A paradigm pathogen for subverting host cell signal transmission. Trends Microbiol *25*, 316-328. 10.1016/j.tim.2016.12.004.

Noto, J.M., and Peek, R.M. (2012). The Helicobacter pylori cag pathogenicity island. Methods Mol Biol *921*, 41-50. 10.1007/978-1-62703-005-2_7.

O' Reilly, E., Tirincsi, A., Logue, S.E., and Szegezdi, E. (2016). The Janus face of death receptor signaling during tumor immunoediting. Front Immunol *7*, 446. 10.3389/fimmu.2016.00446.

Ohmae, T., Hirata, Y., Maeda, S., Shibata, W., Yanai, A., Ogura, K., Yoshida, H., Kawabe, T., and Omata, M. (2005). Helicobacter pylori activates NF-κB via the alternative pathway in B lymphocytes. J Immunol *175*, 7162-7169. 10.4049/jimmunol.175.11.7162.

Oldani, A., Cormont, M., Hofman, V., Chiozzi, V., Oregioni, O., Canonici, A., Sciullo, A., Sommi, P., Fabbri, A., Ricci, V., and Boquet, P. (2009). Helicobacter pylori counteracts the apoptotic action of its VacA toxin by injecting the CagA protein into gastric epithelial cells. PLoS Pathog *5*, e1000603. 10.1371/journal.ppat.1000603.

Olofsson, A., Nygård Skalman, L., Obi, I., Lundmark, R., and Arnqvist, A. (2014). Uptake of Helicobacter pylori vesicles is facilitated by clathrin-dependent and clathrin-independent endocytic pathways. MBio *5*, e00979-14. 10.1128/mBio.00979-14.

Opipari, A.W., Boguski, M.S., and Dixit, V.M. (1990). The A20 cDNA induced by tumor necrosis factor α encodes a novel type of zinc finger protein. J Biol Chem *265*, 14705-14708.

Pankiv, S., Clausen, T.H., Lamark, T., Brech, A., Bruun, J.A., Outzen, H., Øvervatn, A., Bjørkøy, G., and Johansen, T. (2007). p62/SQSTM1 binds directly to Atg8/LC3 to facilitate degradation of ubiquitinated protein aggregates by autophagy. J Biol Chem *282*, 24131-24145. 10.1074/jbc.M702824200.

Park, J.Y., Forman, D., Waskito, L.A., Yamaoka, Y., and Crabtree, J.E. (2018). Epidemiology of Helicobacter pylori and CagA-positive infections and global variations in gastric cancer. Toxins (Basel) *10*. 10.3390/toxins10040163.

Parvatiyar, K., Barber, G.N., and Harhaj, E.W. (2010). TAX1BP1 and A20 inhibit antiviral signaling by targeting TBK1-IKKi kinases. J. Biol. Chem. *285*, 14999-15009. 10.1074/jbc.M110.109819.

Pfannkuch, L., Hurwitz, R., Traulsen, J., Sigulla, J., Poeschke, M., Matzner, L., Kosma, P., Schmid, M., and Meyer, T.F. (2019). ADP heptose, a novel pathogen-associated molecular pattern identified in Helicobacter pylori. FASEB J *33*, 9087-9099. 10.1096/fj.201802555R.

Priem, D., van Loo, G., and Bertrand, M.J.M. (2020). A20 and Cell Death-driven Inflammation. Trends Immunol *41*, 421-435. 10.1016/j.it.2020.03.001.

Razani, B., Whang, M.I., Kim, F.S., Nakamura, M.C., Sun, X., Advincula, R., Turnbaugh, J.A., Pendse, M., Tanbun, P., Achacoso, P., et al. (2020). Non-catalytic ubiquitin binding by A20 prevents psoriatic arthritis-like disease and inflammation. Nat Immunol *21*, 422-433. 10.1038/s41590-020-0634-4.

Rohde, M., Püls, J., Buhrdorf, R., Fischer, W., and Haas, R. (2003). A novel sheathed surface organelle of the Helicobacter pylori cag type IV secretion system. Mol Microbiol *49*, 219-234. 10.1046/j.1365-2958.2003.03549.x.

Rudi, J., Kuck, D., Strand, S., von Herbay, A., Mariani, S.M., Krammer, P.H., Galle, P.R., and Stremmel, W. (1998). Involvement of the CD95 (APO-1/Fas) receptor and ligand system in Helicobacter pylori-induced gastric epithelial apoptosis. J Clin Investig *102*, 1506-1514. 10.1172/jci2808.

Saitoh, Y., Hamano, A., Mochida, K., Kakeya, A., Uno, M., Tsuruyama, E., Ichikawa, H., Tokunaga, F., Utsunomiya, A., Watanabe, T., and Yamaoka, S. (2016). A20 targets caspase-8 and FADD to protect HTLV-I-infected cells. Leukemia *30*, 716-727. 10.1038/leu.2015.267.

Sakitani, K., Hirata, Y., Hayakawa, Y., Serizawa, T., Nakata, W., Takahashi, R., Kinoshita, H., Sakamoto, K., Nakagawa, H., Akanuma, M., Yoshida, H., Maeda, S., and Koike, K. (2012). Role of interleukin-32 in Helicobacter pylori-induced gastric inflammation. Infect Immun *80*, 3795-3803. 10.1128/IAI.00637-12.

Sanjo, H., Zajonc, D.M., Braden, R., Norris, P.S., and Ware, C.F. (2010). Allosteric regulation of the ubiquitin:NIK and ubiquitin:TRAF3 E3 ligases by the lymphotoxin-β receptor. J Biol Chem *285*, 17148-17155. 10.1074/jbc.M110.105874.

Scaffidi, C., Fulda, S., Srinivasan, A., Friesen, C., Li, F., Tomaselli, K.J., Debatin, K.M., Krammer, P.H., and Peter, M.E. (1998). Two CD95 (APO-1/Fas) signaling pathways. EMBO J *17*, 1675-1687. 10.1093/emboj/17.6.1675.

Schindele, F. ;Weiss, E. ;Haas, R. ;Fischer, W. (2016). Quantitative analysis of CagA type IV secretion by Helicobacter pylori reveals substrate recognition and translocation requirements. Mol Microbiol *100*, 188-203. 10.1111/mmi.13309.

Schistosomes, liver flukes and Helicobacter pylori. IARC working group on the evaluation of carcinogenic risks to humans. Lyon, 7-14 June 1994. (1994). IARC Monogr Eval Carcinog Risks Hum *61*, 1-241.

Schneider, C. A., Rasband, W. S., and Eliceiri, K. W. (2012). NIH Image to ImageJ: 25 years of image analysis. Nat Methods *9*, 671-675. 10.1038/nmeth.2089.

Schug, Z.T., Gonzalvez, F., Houtkooper, R.H., Vaz, F.M., and Gottlieb, E. (2011). BID is cleaved by caspase-8 within a native complex on the mitochondrial membrane. Cell Death Differ *18*, 538-548. 10.1038/cdd.2010.135.

Schweitzer, K., Sokolova, O., Bozko, P.M., and Naumann, M. (2010). Helicobacter pylori induces NF-κB independent of CagA. EMBO Rep *11*, 10-11; author reply 11-12. 10.1038/embor.2009.263.

Scotiniotis, I.A., Rokkas, T., Furth, E.E., Rigas, B., and Shiff, S.J. (2000). Altered gastric epithelial cell kinetics in Helicobacter pylori-associated intestinal metaplasia: implications for gastric carcinogenesis. Int J Cancer *85*, 192-200.

Sgouras, D., Tegtmeyer, N., and Wessler, S. (2019). Activity and functional importance of Helicobacter pylori virulence factors. Adv Exp Med Biol *1149*, 35-56. 10.1007/5584_2019_358.

Shaffer, C.L., Gaddy, J.A., Loh, J.T., Johnson, E.M., Hill, S., Hennig, E.E., McClain, M.S., McDonald, W.H., and Cover, T.L. (2011). Helicobacter pylori exploits a unique repertoire of type IV secretion system components for pilus assembly at the bacteria-host cell interface. PLoS Pathog *7*, e1002237. 10.1371/journal.ppat.1002237.

Shamas-Din, A., Kale, J., Leber, B., and Andrews, D.W. (2013). Mechanisms of action of Bcl-2 family proteins. Cold Spring Harb Perspect Biol *5*, a008714. 10.1101/cshperspect.a008714.

Shembade, N., and Harhaj, E.W. (2012). Regulation of NF-κB signaling by the A20 deubiquitinase. Cell Mol Immunol *9*, 123-130. 10.1038/cmi.2011.59.

Shembade, N., Harhaj, N.S., Parvatiyar, K., Copeland, N.G., Jenkins, N.A., Matesic, L.E., and Harhaj, E.W. (2008). The E3 ligase Itch negatively regulates inflammatory signaling pathways by controlling the function of the ubiquitin-editing enzyme A20. Nat Immunol *9*, 254-262. 10.1038/ni1563.

Shembade, N., Ma, A., and Harhaj, E.W. (2010). Inhibition of NF-κB signaling by A20 through disruption of ubiquitin enzyme complexes. Science *327*, 1135-1139. 10.1126/science.1182364.

Shembade, N., Parvatiyar, K., Harhaj, N.S., and Harhaj, E.W. (2009). The ubiquitin-editing enzyme A20 requires RNF11 to downregulate NF-κB signalling. EMBO J. *28*, 513-522. 10.1038/emboj.2008.285.

Shibayama, K., Doi, Y., Shibata, N., Yagi, T., Nada, T., Iinuma, Y., and Arakawa, Y. (2001). Apoptotic signaling pathway activated by Helicobacter pylori infection and increase of apoptosis-inducing activity under serum-starved conditions. Infect Immun *69*, 3181-3189. 10.1128/iai.69.5.3181-3189.2001.

Shibayama, K., Kamachi, K., Nagata, N., Yagi, T., Nada, T., Doi, Y.H., Shibata, N., Yokoyama, K., Yamane, K., Kato, H., et al. (2003). A novel apoptosis-inducing protein from Helicobacter pylori. Mol Microbiol *47*, 443-451. 10.1046/j.1365-2958.2003.03305.x.

Shih, V.F., Tsui, R., Caldwell, A., and Hoffmann, A. (2011). A single NFκB system for both canonical and non-canonical signaling. Cell Res *21*, 86-102. 10.1038/cr.2010.161.

Shimoyama, A., Saeki, A., Tanimura, N., Tsutsui, H., Miyake, K., Suda, Y., Fujimoto, Y., and Fukase, K. (2011). Chemical synthesis of Helicobacter pylori lipopolysaccharide partial structures and their selective proinflammatory responses. Chemistry *17*, 14464-14474. 10.1002/chem.201003581.

Singh, R., Letai, A., and Sarosiek, K. (2019). Regulation of apoptosis in health and disease: the balancing act of BCL-2 family proteins. Nat Rev Mol Cell Biol *20*, 175-193. 10.1038/s41580-018-0089-8.

Sirard, J.C., Didierlaurent, A., Cayet, D., Sierro, F., and Rumbo, M. (2009). Toll-like receptor 5- and lymphotoxin β receptor-dependent epithelial Ccl20 expression involves the same NF-κB binding site but distinct NF-κB pathways and dynamics. Biochim Biophys Acta *1789*, 386-394. 10.1016/j.bbagrm.2009.03.001.

Skaug, B., Chen, J., Du, F., He, J., Ma, A., and Chen, Z.J. (2011). Direct, noncatalytic mechanism of IKK inhibition by A20. Mol Cell *44*, 559-571. 10.1016/j.molcel.2011.09.015.

Sokolova, O., Borgmann, M., Rieke, C., Schweitzer, K., Rothkötter, H.J., and Naumann, M. (2013). Helicobacter pylori induces type 4 secretion system-dependent, but CagA-independent activation of IκBs and NF-κB/RelA at early time points. Int J Med Microbiol *303*, 548-552. 10.1016/j.ijmm.2013.07.008.

Sokolova, O., Maubach, G., and Naumann, M. (2014). MEKK3 and TAK1 synergize to activate IKK complex in Helicobacter pylori infection. Biochim Biophys Acta *1843*, 715-724. 10.1016/j.bbamcr.2014.01.006.

Song, C., Mitter, S.K., Qi, X., Beli, E., Rao, H.V., Ding, J., Ip, C.S., Gu, H., Akin, D., Dunn, W.A., et al. (2017). Oxidative stress-mediated NFκB phosphorylation upregulates p62/SQSTM1 and promotes retinal pigmented epithelial cell survival through increased autophagy. PLoS One *12*, e0171940. 10.1371/journal.pone.0171940.

Song, H.Y., Rothe, M., and Goeddel, D.V. (1996). The tumor necrosis factor-inducible zinc finger protein A20 interacts with TRAF1/TRAF2 and inhibits NF-κB activation. Proc Natl Acad Sci U S A *93*, 6721-6725. 10.1073/pnas.93.13.6721.

Souza, D.P., Oka, G.U., Alvarez-Martinez, C.E., Bisson-Filho, A.W., Dunger, G., Hobeika, L., Cavalcante, N.S., Alegria, M.C., Barbosa, L.R., Salinas, R.K., et al. (2015). Bacterial killing via a type IV secretion system. Nat Commun *6*, 6453. 10.1038/ncomms7453.

Sprick, M.R., Rieser, E., Stahl, H., Grosse-Wilde, A., Weigand, M.A., and Walczak, H. (2002). Caspase-10 is recruited to and activated at the native TRAIL and CD95 death-inducing signalling complexes in a FADD-dependent manner but can not functionally substitute caspase-8. EMBO J *21*, 4520-4530. 10.1093/emboj/cdf441.

Sun, S.C. (2012). The noncanonical NF-κB pathway. Immunol Rev *246*, 125-140. 10.1111/j.1600-065X.2011.01088.x.

Sun, S.C. (2017). The non-canonical NF-κB pathway in immunity and inflammation. Nat Rev Immunol *17*, 545-558. 10.1038/nri.2017.52.

Takahashi, M., Higuchi, M., Makokha, G.N., Matsuki, H., Yoshita, M., Tanaka, Y., and Fujii, M. (2013). HTLV-1 Tax oncoprotein stimulates ROS production and apoptosis in T cells by interacting with USP10. Blood *122*, 715-725. 10.1182/blood-2013-03-493718.

Takahashi-Kanemitsu, A., Knight, C.T., and Hatakeyama, M. (2020). Molecular anatomy and pathogenic actions of Helicobacter pylori CagA that underpin gastric carcinogenesis. Cell Mol Immunol *17*, 50-63. 10.1038/s41423-019-0339-5.

Taniguchi, K., and Karin, M. (2018). NF-κB, inflammation, immunity and cancer: Coming of age. Nat Rev Immunol *18*, 309-324. 10.1038/nri.2017.142.

Tavares, R.M., Turer, E.E., Liu, C.L., Advincula, R., Scapini, P., Rhee, L., Barrera, J., Lowell, C.A., Utz, P.J., Malynn, B.A., and Ma, A. (2010). The ubiquitin modifying enzyme A20 restricts B cell survival and prevents autoimmunity. Immunity *33*, 181-191. 10.1016/j.immuni.2010.07.017.

Tsukanov, V.V., Shtygasheva, O.V., Vasyutin, A.V., Amel'chugova, O.S., Butorin, N.N., and Ageeva, E.S. (2015). Parameters of proliferation and apoptosis of epithelial cells in the gastric mucosa in indigenous and non-indigenous residents of Khakassia with Helicobacter pylori positive duodenal ulcer disease. Bull Exp Biol Med *158*, 431-433. 10.1007/s10517-015-2778-z.

Valenzuela, M., Bravo, D., Canales, J., Sanhueza, C., Díaz, N., Almarza, O., Toledo, H., and Quest, A.F. (2013). Helicobacter pylori-induced loss of survivin and gastric cell viability is attributable to secreted bacterial gamma-glutamyl transpeptidase activity. J Infect Dis *208*, 1131-1141. 10.1093/infdis/jit286.

Vallabhapurapu, S., Matsuzawa, A., Zhang, W., Tseng, P.H., Keats, J.J., Wang, H., Vignali, D.A., Bergsagel, P.L., and Karin, M. (2008). Nonredundant and complementary functions of TRAF2 and TRAF3 in a ubiquitination cascade that activates NIK-dependent alternative NF-κB signaling. Nat Immunol *9*, 1364-1370. 10.1038/ni.1678.

Varfolomeev, E., Maecker, H., Sharp, D., Lawrence, D., Renz, M., Vucic, D., and Ashkenazi, A. (2005). Molecular determinants of kinase pathway activation by Apo2 ligand/tumor necrosis factor-related apoptosis-inducing ligand. J Biol Chem *280*, 40599-40608. 10.1074/jbc.M509560200.

Vereecke, L., Beyaert, R., and van Loo, G. (2011). Genetic relationships between A20/TNFAIP3, chronic inflammation and autoimmune disease. Biochem Soc Trans *39*, 1086-1091. 10.1042/BST0391086.

Verstrepen, L., Verhelst, K., van Loo, G., Carpentier, I., Ley, S.C., and Beyaert, R. (2010). Expression, biological activities and mechanisms of action of A20 (TNFAIP3). Biochem Pharmacol *80*, 2009-2020. 10.1016/j.bcp.2010.06.044.

Virolle, C., Goldlust, K., Djermoun, S., Bigot, S., and Lesterlin, C. (2020). Plasmid transfer by conjugation in Gram-negative bacteria: From the cellular to the community level. Genes *11*, 1239. 10.3390/genes11111239.

Wang, J., Fan, X., Lindholm, C., Bennett, M., O'Connoll, J., Shanahan, F., Brooks, E.G., Reyes, V.E., and Ernst, P.B. (2000). Helicobacter pylori modulates lymphoepithelial cell interactions leading to epithelial cell damage through Fas/Fas ligand interactions. Infect Immun *68*, 4303-4311. 10.1128/iai.68.7.4303-4311.2000.

Wang, L., Du, F., and Wang, X. (2008). TNF-α induces two distinct caspase-8 activation pathways. Cell *133*, 693-703. 10.1016/j.cell.2008.03.036.

Wang, Y., Koroleva, E.P., Kruglov, A.A., Kuprash, D.V., Nedospasov, S.A., Fu, Y.X., and Tumanov, A.V. (2010). Lymphotoxin beta receptor signaling in intestinal epithelial cells orchestrates innate immune responses against mucosal bacterial infection. Immunity *32*, 403-413. 10.1016/j.immuni.2010.02.011.

Warren, J.R., and Marshall, B. (1983). Unidentified curved bacilli on gastric epithelium in active chronic gastritis. Lancet *1*, 1273-1275.

Watari, J., Chen, N., Amenta, P.S., Fukui, H., Oshima, T., Tomita, T., Miwa, H., Lim, K.J., and Das, K.M. (2014). Helicobacter pylori associated chronic gastritis, clinical syndromes, precancerous lesions, and pathogenesis of gastric cancer development. World J Gastroenterol *20*, 5461-5473. 10.3748/wjg.v20.i18.5461.

Weng, J.H., Hsieh, Y.C., Huang, C.C., Wei, T.Y., Lim, L.H., Chen, Y.H., Ho, M.R., Wang, I., Huang, K.F., Chen, C.J., and Tsai, M.D. (2015). Uncovering the mechanism of forkhead-associated domain-mediated TIFA oligomerization that plays a central role in immune responses. Biochemistry *54*, 6219-6229. 10.1021/acs.biochem.5b00500.

Wertz, I.E., Newton, K., Seshasayee, D., Kusam, S., Lam, C., Zhang, J., Popovych, N., Helgason, E., Schoeffler, A., Jeet, S., et al. (2015). Phosphorylation and linear ubiquitin direct A20 inhibition of inflammation. Nature *528*, 370-375. 10.1038/nature16165.

Wertz, I.E., O'Rourke, K.M., Zhou, H., Eby, M., Aravind, L., Seshagiri, S., Wu, P., Wiesmann, C., Baker, R., Boone, D.L., et al. (2004). De-ubiquitination and ubiquitin ligase domains of A20 downregulate NF-κB signalling. Nature *430*, 694-699. 10.1038/nature02794.

Won, M., Park, K.A., Byun, H.S., Sohn, K.C., Kim, Y.R., Jeon, J., Hong, J.H., Park, J., Seok, J.H., Kim, J.M., et al. (2010). Novel anti-apoptotic mechanism of A20 through targeting ASK1 to suppress TNF-induced JNK activation. Cell Death Differ *17*, 1830-1841. 10.1038/cdd.2010.47.

Xia, Y., Yamaoka, Y., Zhu, Q., Matha, I., and Gao, X. (2009a). A comprehensive sequence and disease correlation analyses for the C-terminal region of CagA protein of Helicobacter pylori. PLoS One *4*, e7736. 10.1371/journal.pone.0007736.

Xia, Z.P., Sun, L., Chen, X., Pineda, G., Jiang, X., Adhikari, A., Zeng, W., and Chen, Z.J. (2009b). Direct activation of protein kinases by unanchored polyubiquitin chains. Nature *461*, 114-119. 10.1038/nature08247.

Xiao, G., Fong, A., and Sun, S.C. (2004). Induction of p100 processing by NF-κB-inducing kinase involves docking IκB kinase α (IKKα) to p100 and IKKα-mediated phosphorylation. J Biol Chem *279*, 30099-30105. 10.1074/jbc.M401428200.

Xiao, G., Harhaj, E. W., and Sun, S. C. (2001). NF-κB-inducing kinase regulates the processing of NF-κB2 p100. Mol Cell *7*, 401-409. 10.1016/s1097-2765(01)00187-3.

Yamaguchi, N., Oyama, M., Kozuka-Hata, H., and Inoue, J. (2013). Involvement of A20 in the molecular switch that activates the non-canonical NF-κB pathway. Sci Rep *3*, 2568. 10.1038/srep02568.

Yamasaki, E., Wada, A., Kumatori, A., Nakagawa, I., Funao, J., Nakayama, M., Hisatsune, J., Kimura, M., Moss, J., and Hirayama, T. (2006). Helicobacter pylori vacuolating cytotoxin induces activation of the proapoptotic proteins Bax and Bak, leading to cytochrome c release and cell death, independent of vacuolation. J Biol Chem *281*, 11250-11259. 10.1074/jbc.M509404200.

Yanai, A., Hirata, Y., Mitsuno, Y., Maeda, S., Shibata, W., Akanuma, M., Yoshida, H., Kawabe, T., and Omata, M. (2003). Helicobacter pylori induces antiapoptosis through nuclear factor-κB Activation. J. Infect. Dis. *188*, 1741-1751. 10.1086/379629.

Yoshida, A., Isomoto, H., Hisatsune, J., Nakayama, M., Nakashima, Y., Matsushima, K., Mizuta, Y., Hayashi, T., Yamaoka, Y., Azuma, T., et al. (2009). Enhanced expression of CCL20 in human Helicobacter pylori-associated gastritis. Clin Immunol *130*, 290-297. 10.1016/j.clim.2008.09.016.

Zamani, M., Ebrahimtabar, F., Zamani, V., Miller, W.H., Alizadeh-Navaei, R., Shokri-Shirvani, J., and Derakhshan, M.H. (2018). Systematic review with meta-analysis: The worldwide prevalence of Helicobacter pylori infection. Aliment Pharmacol Ther *47*, 868-876. 10.1111/apt.14561.

Zarnegar, B.J., Wang, Y., Mahoney, D.J., Dempsey, P.W., Cheung, H.H., He, J., Shiba, T., Yang, X., Yeh, W.C., Mak, T.W., et al. (2008). Noncanonical NF-κB activation requires coordinated assembly of a regulatory complex of the adaptors cIAP1, cIAP2, TRAF2 and TRAF3 and the kinase NIK. Nat Immunol *9*, 1371-1378. 10.1038/ni.1676.

Zhang, Q., Lenardo, M. J., and Baltimore, D. (2017). 30 Years of NF-κB: A blossoming of relevance to human pathobiology. Cell *168*, 37-57. 10.1016/j.cell.2016.12.012.

Zhang, X.S., Tegtmeyer, N., Traube, L., Jindal, S., Perez-Perez, G., Sticht, H., Backert, S., and Blaser, M.J. (2015). A specific A/T polymorphism in Western tyrosine phosphorylation B-motifs regulates Helicobacter pylori CagA epithelial cell interactions. PLoS Pathog *11*, e1004621. 10.1371/journal.ppat.1004621.

Zhao, Q., Busch, B., Jiménez-Soto, L.F., Ishikawa-Ankerhold, H., Massberg, S., Terradot, L., Fischer, W., and Haas, R. (2018). Integrin but not CEACAM receptors are dispensable for Helicobacter pylori CagA translocation. PLoS Pathog *14*, e1007359. 10.1371/journal.ppat.1007359.

Zhou, P., She, Y., Dong, N., Li, P., He, H., Borio, A., Wu, Q., Lu, S., Ding, X., Cao, Y., et al. (2018). Alpha-kinase 1 is a cytosolic innate immune receptor for bacterial ADP-heptose. Nature *561*, 122-126. 10.1038/s41586-018-0433-3.

Zhu, S., Soutto, M., Chen, Z., Peng, D., Romero-Gallo, J., Krishna, U.S., Belkhiri, A., Washington, M.K., Peek, R., and El-Rifai, W. (2017). Helicobacter pylori-induced cell death is counteracted by NF-κB-mediated transcription of DARPP-32. Gut *66*, 761-762. 10.1136/gutjnl-2016-312141.

Zimmermann, S., Pfannkuch, L., Al-Zeer, M.A., Bartfeld, S., Koch, M., Liu, J., Rechner, C., Soerensen, M., Sokolova, O., Zamyatina, A., et al. (2017). ALPK1- and TIFA-dependent innate immune response triggered by the Helicobacter pylori type IV secretion system. Cell Rep *20*, 2384-2395. 10.1016/j.celrep.2017.08.039.

Ehrenerklärung

Ich versichere hiermit, dass ich die vorliegende Arbeit ohne unzulässige Hilfe Dritter und ohne Benutzung anderer als der angegebenen Hilfsmittel angefertigt habe; verwendete fremde und eigene Quellen sind als solche kenntlich gemacht.

Ich habe insbesondere nicht wissentlich:

- Ergebnisse erfunden oder widersprüchlich Ergebnisse verschwiegen,
- statistische Verfahren absichtlich missbraucht, um Daten in ungerechtfertigter Weise zu interpretieren,
- fremde Ergebnisse oder Veröffentlichungen plagiiert,
- fremde Forschungsergebnisse verzerrt wiedergegeben.

Mir ist bekannt, dass Verstöße gegen das Urheberrecht Unterlassungs- und Schadensersatzansprüche des Urhebers sowie eine strafrechtliche Ahndung durch die Strafverfolgungsbehörden begründen kann.

Ich erkläre mich damit einverstanden, dass die Arbeit ggf. mit Mitteln der elektronischen Datenverarbeitung auf Plagiate überprüft werden kann.

Die Arbeit wurde bisher weder im Inland noch im Ausland in gleicher oder ähnlicher Form als Dissertation eingereicht und ist als Ganzes auch noch nicht veröffentlicht.

Magdeburg, den 17.01.2022

Michelle Chin Chia Lim